Biofidelity Evaluation of THOR-05F in Rear-Facing Seating Configurations

Randolff L. Carpenter, Alexander Bendig, Hyunjung Kwon, Alena Hagedorn, Vikram Pradhan, Jason Stammen, Kevin Moorhouse, Yun-Seok Kang

Abstract Future Automated Driving System (ADS) vehicles may incorporate rear-facing seating configurations, presenting challenges for current safety systems and anthropomorphic test devices (ATDs) that were not originally designed to accommodate alternative crash scenarios. Evaluating an ATD's suitability in these non-traditional impact conditions requires comparison against post-mortem human subject (PMHS) response corridors in matched seating configurations. One crash mode that could arise from this is the high-speed rear-facing frontal impact (HSRFFI). While prior research has examined midsize male ATD biofidelity in HSRFFIs, comparable analyses for small-female ATDs remain unavailable. This study provides a preliminary evaluation of THOR-05F biofidelity in 56 km/h HSRFFI sled tests at 25° and 45° recline using All-Belts-to-Seat (ABTS) and Fixed D-Ring (FDR) seat designs. The biofidelity evaluation indicated better biofidelity at 45°, with excellent-to-marginal occupant response scores across both seats, and better seat loading scores in ABTS. However, differences in seatback loading, belt loading, pelvic angular kinematics, head restraint interaction did arise. Further, the ATD experienced sensor damage in FDR tests, and currently lacks the measurement capabilities and validated injury criteria necessary to capture the complex female PMHS injury mechanisms. Together these results indicate that modifications are needed before the THOR-05F is suitable for use in future HSRFFI testing.

Keywords Automated Driving System (ADS), Biofidelity, Biofidelity Ranking System (BRS), Rear-Facing Seats, THOR-05F.

I. INTRODUCTION

Advances in Automated Driving Systems (ADS) are anticipated to enable non-traditional vehicle interior layouts that promote comfort and social interaction [1-4]. As the task of driving is removed, occupants may no longer prefer standard, forward-facing seating postures typical of human-driven vehicles. Consumer surveys exploring these anticipated preferences have identified reclined seating and "face-to-face" arrangements (where front-row occupants face rearward and rear-row occupants face forward) as among the most preferred configurations, particularly for long-distance travel [1-3].

While variable seating options enhance the user experience, they introduce significant challenges for occupant protection, particularly because current restraint systems, anthropomorphic test devices (ATDs), and human body models (HBMs) were optimised for conventional, forward-facing, upright occupants. Consequently, there is currently no widely accepted tool designed to evaluate occupant safety in non-traditional seating environments [5,6]. Establishing this capability is critical for assessing countermeasure effectiveness and guiding safety strategies for future ADS vehicle interiors, which require tools that can robustly replicate human-like responses across various seat types, recline angles, and occupant demographics.

To proactively address these gaps, the National Highway Traffic Safety Administration (NHTSA) has undertaken a multi-stage research initiative to evaluate and, if necessary, modify existing biomechanics tools for use in nontraditional seating configurations. The first stage of this initiative has involved establishing biofidelity targets for both male and female PMHS across current or potential ADS seating configurations. The second stage involves evaluating ATD performance against these human targets to identify necessary modifications, ensuring these tools more accurately capture human responses in ADS crash scenarios.

One crash mode of interest involving these unconventional interior designs, particularly in "face-to-face" or carriage style arrangements, is the high-speed rear-facing frontal impact (HSRFFI). Exploratory work investigating this scenario has been ongoing for nearly a decade, beginning with 56 km/h sled tests using midsize male PMHS [7-12]. This crash pulse was selected at the inception of the research series because it comes from the New Car

R. L. Carpenter (e-mail: carpenterr@trcpg.com; tel: 609-864-5767) is a Research Scientist, A. Bendig is a Research Engineer, and A. Hagedorn and V. Pradhan are Research Scientists at the Transportation Research Center, Inc. in East Liberty, Ohio, USA. H. J. Kwon is a General Engineer, J. Stammen is the Division Chief of Crashworthiness, K. Moorhouse is the Division Chief of Applied Biomechanics at NHTSA's Vehicle Research and Test Center in East Liberty, Ohio, USA. Y.-S. Kang is an Associate Professor at the Injury Biomechanics Research Center at the Ohio State University in Columbus, Ohio, USA.

Assessment Program (NCAP) and represents the current standard for modelling high-speed, survivable frontal impact conditions in the absence of an official ADS-specific pulse.

These studies examined occupant responses across two seat angles: 25° (standard, upright) and 45° (reclined), and two original equipment manufacturer (OEM) seat designs representing distinct mechanical boundary conditions: an All-Belts-to-Seat (ABTS) configuration (2018 Honda Odyssey) and a Fixed D-Ring (FDR) configuration (2018 Honda Accord). The ABTS seat featured an integrated belt system and a stiffer, heavier frame that housed a shoulder belt retractor assembly and a rigid transverse crossbar. In contrast, the FDR seat utilised a standard three-point seatbelt with a D-ring fixed to the buck frame which represented the vehicle structure. The FDR seatback frame was simpler, softer, and more symmetric, utilizing thin serpentine springs for suspension rather than a rigid lower crossmember.

Structural differences between the seat designs and the chosen recline angles were found to influence energy management, occupant kinematics, and resulting injury profiles [7,9-12]. The ABTS seat dissipated impact energy more effectively, generally resulting in lower normalized anterior-to-posterior (A-P) chest compressions. In the FDR condition, the seatback allowed the occupant's torso and pelvis to "pocket" deeply into the seatback, leading to higher seatback forces, greater linear x-accelerations at the thoracic spine and pelvis, and larger forward off-axis pelvis rotations. Furthermore, as occupants interacted with the seatback, the shoulder belt in the FDR condition frequently slipped off the shoulder, resulting in larger "ramping" (upward vertical movement along the seatback) compared to the ABTS seat, where the integrated belt more effectively restrained the occupant.

Looking at injuries, nearly all male PMHS sustained rib and pelvic fractures; however, the FDR configuration generally produced a higher total number of rib fractures and more severe pelvic injuries, including pubic rami fractures and sacroiliac (SI) joint damage. In the ABTS seat, the retractor mechanism created a localised "hard spot" on the left side of the frame, causing asymmetric rib fractures and left scapula fractures. For the thorax, the number of rib fractures was higher at 45° despite peak A-P chest compressions that were smaller than those recorded in the upright condition. This identified a complex thoracic injury mechanism involving combined A-P compression and inferior-superior (I-S) deformation caused by occupant "ramping" and the inertial movement of abdominal contents upward into the thoracic cavity. Pelvic injuries were linked to both direct contact with the seatback and inertial loading transmitted from the lower extremities to the acetabulum.

Follow-up HSRFFI evaluations with the 50th percentile male Test device for Human Occupant Restraint (THOR-50M) ATD in ABTS seating at both 25° and 45° recline demonstrated generally good biofidelity for most measurements investigated, but mixed results for head, spine, and pelvis kinematics and for injury prediction capabilities [5]. The authors concluded that the THOR-50M would benefit from targeted revisions, particularly to better reproduce ramping, head/neck-head restraint interaction, and pelvis–seat and seatbelt coupling, to more closely match the PMHS kinematics in HSRFFI. When the autonomous vehicle variant of the THOR 50th percentile male (THOR-AV-50M or THOR-AV) was tested in ABTS HSRFFI conditions, it demonstrated generally good biofidelity, though the authors noted comparable challenges related to the inability to reproduce the ramping behaviour and pelvis-seat and seatbelt interaction observed in the midsize male PMHS tests [6]. Similar efforts are also ongoing to evaluate other midsize male ATDs in these impact conditions.

Critically, relying exclusively on midsize male data has been shown to be insufficient in current vehicle environments, as females have demonstrated higher injury odds and fatality risks under comparable crash conditions and anthropometries [13-15]. In rear-impact research specifically, females have exhibited distinct injury patterns in available field data, such as a disproportionately higher risk of sustaining whiplash injuries compared to males [16-18]. These factors motivated recent research to establish small female PMHS biofidelity corridors for HSRFFIs, while providing a comparison to the midsize male dataset [19]. Across all test conditions, the female PMHS demonstrated consistently lower head restraint, seatback, and lap-belt loads than males. Despite lower inertial loading, females sustained injury patterns distinct from males, including a significantly higher incidence of cervical and thoracic vertebral body fractures (seven out of 12 females compared to only one male) and disc ruptures. Additionally, five females in the FDR conditions and one in the ABTS condition sustained sacral fractures, an injury not observed in any of the male tests. Females also experienced a higher frequency of lower extremity fractures (seven of 12), primarily because their shorter thigh length caused the legs to interact with the front of the seat pan earlier and more forcefully, leading to excessive knee extension. Notably, rib fracture counts were comparable between sexes, which suggested a lower load tolerance for rib fractures in females given their smaller anatomical structures and unique kinematic responses.

Given the variation in impact response and injuries observed across sex in PMHS HSRFFI studies, it is essential that small-female ATDs can capture the sex- and size-specific biomechanical differences. These variations may necessitate targeted modifications to improve ATD biofidelity for HSRFFI scenarios. Similar to the path for midsize male tools, candidate small female ATDs must be evaluated under the same impact conditions and compared to the biofidelity corridors established in matched small female PMHS studies before necessary refinements can be identified [19].

Three primary small female ATDs are currently available for consideration for use in these non-traditional configurations. The Hybrid III 5th percentile female (HIII-5F) is widely utilised in biomechanical testing, though the Hybrid III family possesses hardware limitations, including more rigid spinal construction that has been shown in prior midsize male evaluations to prevent it from achieving the reclined positioning required for HSRFFI testing [5]. The THOR 5th percentile female (THOR-05F) features expanded measurement capabilities and a more flexible spine that allow for adjustable postures representative of a wider range of human seating configurations. As of 2025, NHTSA has released a comprehensive technical package for the THOR-05F, including the drawing package [20], durability report [21], procedures for assembly, disassembly, and inspection (PADI) manual [22], qualification manual [23], and repeatability and reproducibility of qualification testing report [24]. Finally, the THOR-AV-5F is marketed as a modified version of the THOR-05F specifically optimised for ADS-equipped cabins; however, it remains the newest of the three candidates and was not available at the time of testing. The THOR-05F was chosen as the focus for the current study, though future testing will investigate the remaining ATDs to comprehensively assess their capabilities in the HSRFFI condition. Importantly, this selection does not imply that the other ATDs were excluded from consideration within the broader research initiative.

Therefore, the primary objective of this study was to provide an initial evaluation of the THOR-05F responses in 56 km/h HSRFFIs for two seatback recline angles (25° upright and 45° reclined) and two OEM seat types (ABTS and FDR). To accomplish this, (1) test repeatability was first assessed by analysing repeated runs within each seat type and recline angle, wherever possible, (2) THOR-05F biofidelity was quantified using the most recent Biofidelity Ranking System (BRS) [5] against female PMHS corridors collected under comparable conditions [19], and (3) THOR-05F measurement trends across seats and recline angles were compared to physical injuries observed in the female PMHS [19]. Secondary goals included evaluating the sensitivity of THOR-05F measurements to seatback recline and seat type differences and comparing that to the sensitivity observed in the PMHS tests.

II. METHODS

Experimental Testing Overview

A total of 22 HSRFFI sled tests were analysed for this study, conducted at a target velocity of 56 km/h. This dataset comprises 10 new tests performed using the THOR-05F ATD and 12 PMHS tests previously reported by [19]. The PMHS data served as the biofidelity comparison target for the ATD responses. Testing was conducted across two production seat types: a 2018 Honda Odyssey equipped with an ABTS integrated restraint system, and a 2018 Honda Accord equipped with an FDR restraint system. Each seat configuration was evaluated at two seatback recline angles: 25° (standard) and 45° (reclined), resulting in four seating configurations.

Table I summarises the test matrix and the PMHS and THOR-05F subject characteristics. To address anthropometric differences during corridor generation, PMHS responses were previously normalised to a 5th percentile female using the anthropometry values defined in [25]. Detailed information regarding the normalisation procedures and the specific values applied to these subjects can be found in [19].

Experimental Testing Setup and Instrumentation

Methods for setup and instrumentation were adapted from prior studies involving male [7,12] and female PMHS [19], the THOR-50M [5], and THOR-AV [6] under similar seating configurations. At the start of testing, each seat was rigidly mounted to a sled equipped with an instrumented structure to enable detailed analysis of seatback interactions. The head restraint was adjustable in both fore/aft and vertical directions, allowing for more consistent positioning across tests and subjects (Fig. A1, Appendix). A multi-axis load cell (FTSS IF-625 or Humanetics/Denton 1914A, Farmington Hills, MI) mounted behind the head restraint measured forces (Fx, Fy, Fz) and moments (My, Mz) at that location.

TABLE I
TEST MATRIX AND SUBJECT CHARACTERISTICS

Seat/Restraint Type	Seatback Recline (°)	Subject	Age (yrs)	Height (cm)	Weight (kg)	Seated Height (cm)	aBMD L2-L4 (T-Score)	Tests Per Subject	Total per Condition
Accord/FDR	25	PMHS23*	45	162.5	56.0	86.5	1.1	1	5
		PMHS31*	59	159.3	58.5	89.0	-2.2	1	
		PMHS32*	71	158.2	47.2	85.4	-0.9	1	
		THOR-05Fǂ	N/A	151.0	47.3	78.8	N/A	2	
	45	PMHS24*	80	157.5	57.2	79.0	-2.7	1	5
		PMHS28*	73	160.3	57.2	88.7	-1.6	1	
		PMHS30*	36	171.2	53.1	93.8	0.2	1	
		THOR-05Fǂ	N/A	151	47.3	78.8	N/A	2	
Odyssey/ABTS	25	PMHS25*	69	167.2	44.2	89.9	-2.2	1	6
		PMHS34*	69	167.6	52.4	84.1	-1.8	1	
		PMHS35*	68	163.3	51.0	84.8	-1.3	1	
		THOR-05Fǂ	N/A	151	47.3	78.8	N/A	3	
	45	PMHS26*	48	159.5	51.7	89.3	-3.0	1	6
		PMHS36*	75	147.8	43.1	78.3	1.1	1	
		PMHS37*	83	161.5	52.6	88.7	-1.3	1	
		THOR-05Fǂ	N/A	151	47.3	78.8	N/A	3	
Total Number of Tests Used in Analysis									22
Average Female PMHS (SD)*			65 (15)	161.3 (6.0)	52.0 (5.0)	86.5 (4.5)	-1.2 (1.4)	N/A	N/A
5th Percentile Female [25]			N/A	151.3	46.7	81.2	N/A	N/A	N/A

*PMHS tests previously performed and reported in [19]
ǂBased on the 2019 [26] version of the THOR-05F drawing package

The seatback was instrumented with three load cell plates – each containing two multi-axis load cells (FTSS IF-625 or Humanetics/Denton 1914A, Farmington Hills, MI) – positioned at the top, middle, and bottom. Each load cell measured forces (Fx, Fy, Fz) and moments (My, Mz), which were then summed to determine the respective seatback load at each load cell plate location (Fig. A2). Additionally, an accelerometer was mounted on each load cell plate, allowing for inertial compensation of the load cell data during data processing.

Belt routing followed the procedures outlined in [7,12] (Fig. A3, Appendix). The ABTS configuration utilised an integrated three-point belt system with the shoulder belt retractor housed within the top-left side of the seatback frame. The FDR configuration utilised a generic three-point belt attached to a D-ring fixed to the rigidised seatback support frame. Traditional FDR systems utilising static B-pillar anchors cannot maintain proper belt fit in alternative seating configurations and are fundamentally incompatible with these environments without modification. Specifically, in reclined conditions, as the recline angle increases, the shoulder belt would play a diminished role in occupant restraint during a high-speed rear impact due to an increasing gap between the belt and the occupant's torso. This gap would increase the risk of excessive occupant excursion or loss of restraint engagement during ramping. Consequently, for any non-integrated belt system to be viable in future ADS environments that also allow for swivelling or reclining seats, this body of work assumes that the D-ring would feature adaptive capabilities or a mounting point independent of the B-pillar to maintain an anatomical belt fit across a wide range of seating conditions. To model this requirement, the D-ring location for the 45° FDR condition (Fig. A3D, Appendix) was rotated about the seat pivot point to maintain the same relative position to the seatback as in the 25° condition.

The THOR-05F sensors utilised for this analysis are listed in Table AI in the Appendix, alongside corresponding PMHS measurement locations. Instrumentation was configured to record data comparable to the PMHS dataset, as well as instrumentation previously identified to be of interest in HSRFFI conditions but not directly measurable on the PMHS, such as upper neck load cell forces and moments [5,19].

Testing the THOR-05F in a high-speed rear-facing orientation required modifications to the standard instrumentation setup to mitigate damage from posterior impacts. Following protocols established for the THOR-50M [5], instrumentation cable bundles were split and rerouted inside the ribcage, exiting laterally rather than posteriorly, to prevent the cables from being crushed between the ATD and the seatback. Despite these routing countermeasures, minor sensor damage occurred during the FDR tests, ultimately limiting the FDR dataset to two ATD tests per recline angle.

In addition to standard THOR instrumentation, a 40-channel chestband was installed outside the ATD jacket at the mid-sternum level to assess external thoracic deformation during testing. To define the mid-sternum level, the band's bottom edge was aligned with the top of the sternal hole between the ATD breast plates. The chestband was installed with overlap in the front to minimise ribbon cable interaction with the seatback and prevent vertical displacement or damage as the ATD ramped upward. When wrapping the chestband around the THOR-05F chest, a gap was found between the band and the dummy, which could complicate chest deflection measurements. To minimise this gap and prevent vertical displacement, duct tape was used to secure the band tightly to the dummy's contours. A 40-gage band (approximately 1-inch gage spacing) was utilised as prior research suggests this granularity is sufficient to capture focal belt and seatback loading in HSRFFI tests [5].

Positioning

Initial THOR-05F positioning for each seating configuration is shown in Fig. 1, with corresponding measurements in Tables AII–AIII and a reference diagram of the measured angles in Fig. A4. The THOR-05F was positioned in the test seat such that the head, pelvis, thigh, leg, and hip-to-eye angles in the 25° and 45° recline tests were as similar as possible to the predicted 5th percentile female posture in the 23° and 43° seatback conditions, respectively, based on the positioning model reported by the University of Michigan Transportation Research Institute (UMTRI) [27]. The paired female PMHS tests [19] were also positioned according to this procedure. To summarise, using the anthropometry of the THOR-05F reported in Table I (stature, mass, and erect sitting height), specific local 2D coordinates derived from the UMTRI model were targeted to successfully achieve all corresponding postural angles. It is important to note that specific global coordinates were not targeted across seats and recline angles for the first test in each condition, as differences in seat cushioning and design inhibited placement in the same spot across seat types. This approach prioritised matching the angular posture and allowed for natural settling into each respective seat cushion. However, to ensure test-to-test repeatability within the ATD test series, global H-point coordinates were strictly recorded and maintained between runs.

The head restraint was then adjusted to achieve a backset of 80 ± 5 mm for the 25° recline tests and 0 mm (head in contact with the head restraint) for the 45° recline tests. In past HSRFFI studies, a topset of 80 ± 5 mm was targeted [5,19]. Because of the THOR-05F's smaller stature, this target was not achievable, as the headrest could be positioned any lower relative to the seatback; the resulting topset values were larger on average: 108.1 ± 36.3 mm at 25° and 164.1 ± 27.6 mm at 45° recline. Lastly, the THOR-05F lumbar spine pitch angle was positioned to the "erect" setting across both recline angles to allow the ATD to lean further back against the seat.

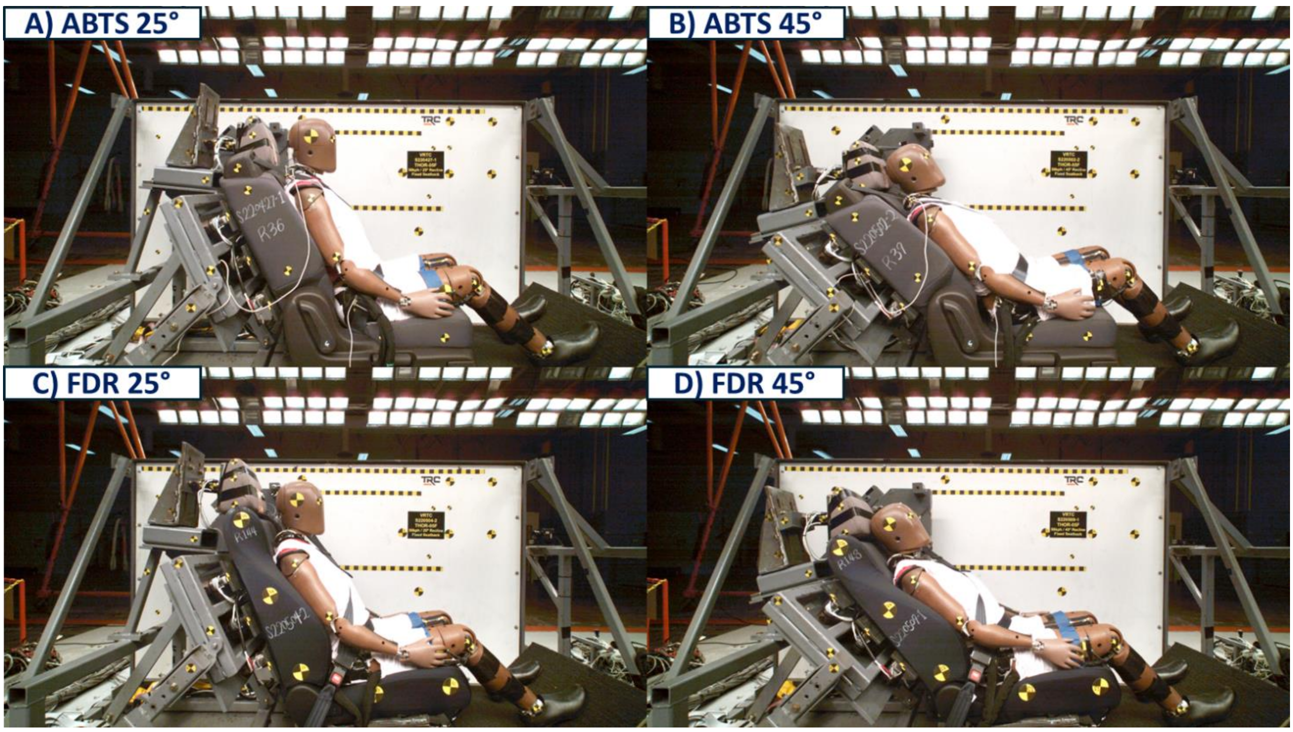

Fig. 1. Examples of the initial positioning of the THOR-05F in: A) ABTS seat at 25°; B) ABTS seat at 45°; C) FDR seat at 25°; and D) FDR seat at 45°. Images are high-speed video stills.

Data Processing

Data were sampled at 20,000 Hz, with coordinate definitions and filter classes per SAE J211 [28], and consistent with previous male and female HSRFFI studies [5,7,12,19]. To isolate the forces experienced by the THOR-05F from the seat, the forces recorded along each of the seat load cells were inertially compensated along the locally mounted x-axis. Following this, the forces and moments recorded in a test where the seat was unoccupied were subtracted from the response using the methods outlined in [5]. Kinematic variables were calculated relative to both the body-local (x, y, z) and global sled (X, Y, Z) coordinate systems. To obtain the global head and pelvis values, accelerometer and ARS measurements were used. Lastly, chestband data were processed with CrashStar v2.8, outputting chestband contours at each time point [5].

Repeatability of the Test Set-up

Repeatability of the 25° and 45° test configurations was assessed for the THOR-05F in the ABTS seat using 43 discrete measurements encompassing seat loads and occupant responses. Repeatability for each measurement was quantified using the mean, standard deviation (SD), and percent coefficient of variation (%CV = (SD / mean) × 100) of the peak values, consistent with prior work in this test condition [5,19]. The final results were then colour-coded based on the three CV thresholds listed in Table BI of the Appendix, which were used to aid in the analysis [5]. Due to complications encountered during the FDR tests specifically regarding sensor damage and seat procurement constraints, only two tests per angle were conducted. Consequently, repeatability calculations could not be performed for the FDR configuration, a limitation addressed further in the Discussion section.

Biofidelity Analysis

Biofidelity was assessed using the BRS published in 2022, consistent with its prior application to the THOR-50M and THOR-AV in the same HSRFFI condition [5,6]. To summarise, the updated scoring system utilises a Shape and Magnitude (SM) score as the BRS score that is reported. The SM score is calculated as the ratio of the Dummy Cumulative Absolute Difference (DCAD) to the Cadaver Cumulative Standard Deviation (CCSD). DCAD is defined as the sum of the absolute differences between the average PMHS response curve and the dummy response curve, while CCSD is the sum of the one standard deviation values from the PMHS mean curve. The method then reports a phase shift known as the Dummy Phase Shift (DPS) as supplemental information. The DPS represents the amount of time shift required to optimally align the phase of the dummy response curve with that of the mean PMHS response curve. The specific equations for these calculations are detailed in the original BRS methodology publication [5].

Prior to calculating the BRS score per the updated methodology, dummy response curves must be shifted in time to best align the dummy response phase to that of the mean PMHS response. The purpose of this optimal phase alignment is to ensure that the SM score reflects the true relative SM difference between the dummy and the cadaver without being artificially inflated by phase differences. Minimizing the DCAD is the primary method used to achieve this alignment. However, because data signals vary widely among subject and test types, a single, stringent mathematical alignment method does not work for all data signals. The updated BRS methodology explicitly allows user flexibility to select the most appropriate curve alignment method for a given dataset to ensure the system works across many types of data. For instance, using the minimum DCAD alignment can sometimes shift the dummy curve to an obviously unreasonable point, such as aligning zero-level post-event data with the primary PMHS event, which fails to compare the common physical parts of the response. Therefore, varying alignment methods are justified to maintain a physically meaningful comparison. When minimum DCAD failed to align common events sensibly, alternative methods were applied, such as aligning the first prominent peaks or leaving the data unshifted.

Measurement data were divided into external seat loading channels (Fig. 2) and internal occupant response channels (Fig. 3). BRS scores for forces and accelerations were then calculated from 0 ms to 100 ms, while belt tensions, angular velocities, moments, rotations, displacements, and chest deflections were calculated from 0 ms to 160 ms, consistent with prior ranges used in this condition [5,6].

For each channel, BRS scores were calculated by averaging results from tests conducted at each recline angle and seat type. This procedure was applied across all channels within each anatomical region; for example, the pelvis region comprised six measures: x-acceleration (Ax), z-acceleration (Az), y-angular rate (ωy), X-displacement (DX), Z-displacement (DZ), and Y-rotation (θY). Channel scores were averaged to produce body region scores (e.g. averaging the six pelvis scores to obtain one pelvis BRS score), and then the four body region scores (head, spine, pelvis, and thorax) were averaged to yield the overall occupant response score. An analogous method was followed to calculate the seat loading score.

Mathematically, a BRS score of 0.0 indicates that the THOR-05F response is identical to the average PMHS response. A score of 1.0 indicates the response is, on average, one standard deviation away from the PMHS response, a score of 2.0 indicates two standard deviations away, and so forth. Therefore, a lower BRS score indicates better biofidelity. Thresholds for interpreting the resulting BRS score are given in Table III and follow a similar classification applied in previous work [6,29]. Specifically, biofidelity was considered “excellent” if the BRS score was less than or equal to 1.0, “good” if greater than 1.0 but less than or equal to 2.0, “marginal” if greater than 2.0 but less than or equal to 3.0, and “poor” if greater than 3.0.

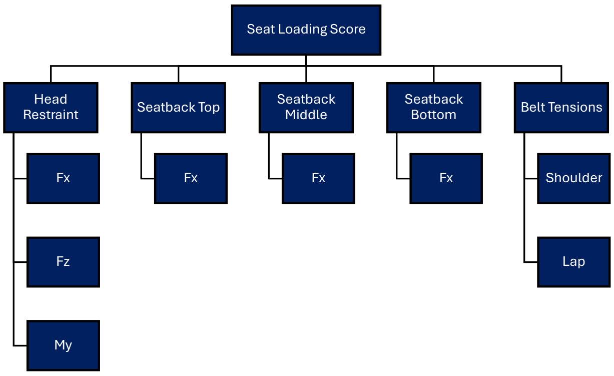

Fig. 2. Components used to compute the seat loading score.

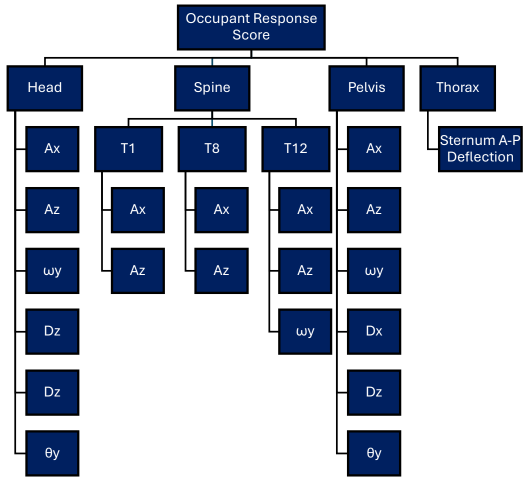

Fig. 3. Components used to compute the occupant response score.

TABLE III
THOR-05F BIOFIDELITY SCALES FOR HSRFFI ANALYSIS

Biofidelity Interpretation	BRS Score [6,29]
Excellent	*BRS score* ≤ 1
Good	1 < *BRS score* ≤ 2
Marginal	2 < *BRS score* ≤ 3
Poor	*BRS score* > 3

Comparison of THOR-05F Measurement Trends to PMHS Injury Locations

Injuries observed in small female PMHS under equivalent test conditions [19] were compared with relevant THOR-05F measures across seat types and recline angles. Evaluated measures include the Head Injury Criterion measured over a maximum 15 ms interval (HIC-15), Brain Injury Criterion (BrIC), upper neck Fx, upper neck Fz, upper neck My, chest resultant deflection (IR-TRACC), acetabulum resultant force, upper tibia compressive Fz, lower tibia Fx and compressive Fz. These measures were selected to most closely align with injury locations observed in the PMHS (e.g., utilizing upper-neck load cell data to assess cervical injuries) and maintain consistency with previous THOR-50M evaluations [5]. When an injury was present, but a corresponding ATD measure was unavailable (e.g. arm, clavicle, or scapula injuries), no investigation could be carried out. It is critical to note that because rear-facing Injury Assessment Reference Values (IARVs) and Injury Risk Functions (IRFs) for the THOR-05F have not yet been established in the HSRFFI condition, these comparisons are intended to identify general biomechanical trends and do not constitute a definitive injury risk evaluation.

III. RESULTS

Repeatability of the Test Set-up

Repeatability results are listed in Table BII in the Appendix. In the ABTS seat at 25° (n=43 measurements), 30 measures (69.77%) had CV < 10%, 11 measures (25.58%) had CV between 10% and 20%, and 2 measures (4.65%) had CV ≥ 20%. In the ABTS seat at 45° (n=43), all CVs were < 20%, with 37 (86.05%) ≤ 10%. Because only two tests were conducted for each FDR seat configuration, a repeatability assessment utilizing CV could not be performed. Instead, the mean measurement values and the absolute differences between the tests for the FDR conditions are documented in Appendix Table BIII.

THOR-05F Biofidelity

Individual BRS scores, DPSs, and methods of dummy curve alignment for the THOR-05F were evaluated across test seat types (FDR and ABTS) and seat recline angles (25° and 45°), as detailed in Tables CI–CVIII in the Appendix, with a summary provided in Table IV, below. Figures C1–C28 overlay each THOR-05F measurement responses with the corresponding PMHS response corridors, where the black curve and grey corridor represent the mean PMHS response and ± 1 SD responses, respectively, the red curve shows the original (unshifted) THOR-05F response, and the blue curve shows the phase-shifted response per the updated BRS methodology. If the THOR-05F response was already aligned with the PMHS mean response, or if no reasonable alignment method existed, the THOR-05F response was left unshifted; in these cases, the DPS was listed as 0 ms. When PMHS data were unavailable, only unshifted (red) curves were shown, and no BRS score was reported. Lastly, the time range for each set of plots represents the time range for the BRS calculation (e.g. the calculations for Fig. C1 were all performed across 100 ms and thus the x-axis for those plots ranges from 0 ms to 100 ms).

TABLE IV
AVERAGE BRS SCORES AND AVERAGE ABSOLUTE DPS FOR 25° AND 45° TESTS

	25°				*45°*			
	ABTS Odyssey		*FDR Accord*		*ABTS Odyssey*		*FDR Accord*	
Location	*BRS Score*	*|DPS| (ms)*	*BRS Score*	*|DPS| (ms)*	*BRS Score*	*|DPS| (ms)*	*BRS Score*	*|DPS| (ms)*
Head Restraint	2.35	1	2.78	2	2.18	3	2.89	4
Seatback Top	2.12	1	2.34	0*	1.62	1	3.35	2
Seatback Middle	0.76	0*	1.61	0	1.40	2	0.86	1
Seatback Bottom	*Not Calculated*		*Not Calculated*		2.39	1	8.18	2
Belt Tensions	2.29	50	2.65	27	1.21	65	1.88	4
Seat Loading	**1.88**	**13**	**2.34**	**7**	**1.76**	**14**	**3.43**	**3**
Head	5.26	1	1.29	1	1.44	2	2.01	2
Spine	1.37	3	1.58	3	1.41	2	1.07	2
Thorax	1.02	1	1.51	1	1.27	0	0.80	0
Pelvis	1.28	0*	1.90	3	1.24	2	1.24	3
Occupant Response	**2.23**	**1**	**1.57**	**2**	**1.34**	**2**	**1.28**	**2**

** Slight Shift (<0.5 ms)*

For the 25° recline tests, ABTS seat loading demonstrated good biofidelity (BRS score = 1.88), while FDR seat loading demonstrated marginal biofidelity (BRS score = 2.34). Across both seats, the head restraint, seatback top, and belt tension regional BRS scores were marginal, with belt tensions exhibiting large phase shifts (50 ms for ABTS and 27 ms for FDR), inflating the average seat-loading DPS values to 13 ms (ABTS) and 7 ms (FDR). THOR-05F occupant response BRS scores showed marginal biofidelity in the ABTS seat (BRS score = 2.23) and good biofidelity in the FDR seat (BRS score = 1.57). For ABTS at 25°, the head region had a worse BRS score than the other regions assessed (BRS score = 5.26). For FDR at 25°, none of the BRS scores for each body region exceeded 2. All average absolute DPS values for the occupant were between 0 ms and 3 ms, with an average occupant response DPS of 1 ms for ABTS and 2 ms for FDR.

For the 45° recline tests, ABTS seat loading demonstrated good biofidelity (BRS score = 1.76), while the FDR seat loading demonstrated poor biofidelity (BRS Score = 3.43). For the FDR seat, the seatback bottom demonstrated a higher BRS score than other regions assessed (BRS score = 8.18). The BRS score for head restraint loads was marginal across both seats. Belt tensions again exhibited the largest phase shifts for ABTS (65 ms), inflating the average seat-loading DPS to 14 ms; FDR seat-loading DPS remained low (3 ms). Occupant response BRS scores indicated good biofidelity in both seats (ABTS BRS score = 1.34; FDR BRS score = 1.28). All ABTS body region BRS scores were between 1 and 2; FDR showed excellent-to-good scores for spine, thorax, and pelvis, while the average head score was near the threshold for good but still marginal (BRS score = 2.01). The average occupant response DPS across both seats was 2 ms.

Additional results supporting the biofidelity analysis – including comparisons of peak seat loads, occupant trajectories, peak occupant kinematics, and a biofidelity analysis where only the unshifted scores were considered – are provided in Appendix D for reference in the Discussion.

Comparison of THOR-05F Measurements to PMHS Injury Locations

The PMHS injuries reported in [19] were compared to corresponding THOR-05F measurements, as summarised in Table V for the ABTS seat, and in Table VI for the FDR seat. In the head and neck region, HIC-15 was elevated across all conditions despite no skull fractures occurring in the PMHS. Upper neck loads (extension moment, shear, and compressive axial loading) were highest in the FDR 45° condition, which aligns with the increased incidence of cervical injuries observed in that specific PMHS test configuration. For the thorax, chest resultant deflections were higher at 25° than at 45° across both seats; however, this trend only correlated with the PMHS rib fracture outcomes in the ABTS seat and was opposite for the FDR seat. Acetabular forces were consistently high across all seats and angles, correlating with the high rate of acetabular and pelvic ring fractures sustained by the female PMHS. Lower extremity responses showed mixed correlation; elevated leg shear forces in the ABTS 45° tests aligned with observed fibula and tibia fractures, but the relatively lower leg loads measured in the FDR conditions did not parallel the multiple lower leg fractures still sustained by the PMHS in that seat. Lastly, comparing THOR-05F measurements to previous THOR-50M baselines under matched ABTS conditions [5] demonstrated that the THOR-05F produced higher values exclusively in the head, neck, and lower leg regions.

TABLE V
COMPARISON OF THOR-05F MEASUREMENTS TO PMHS INJURIES IN ABTS CONDITIONS

Measurement	THOR-05F 25° (n=3)	Female PMHS Injuries 25°	THOR-05F 45° (n=3)	Female PMHS Injuries 45°
HIC-15	**5061**	No skull fractures; brain injury not assessed; thoracic vertebral body fractures (n=3); thoracic disc herniation (n=1)	**2241**	No skull fractures; brain injury not assessed; cervical spinous process fracture (n=1); cervical disc rupture (n=1)
BrIC	0.404		0.305	
Upper Neck Fx (N)	-459		**-1103**	
Upper Neck Fz (N)	1528		**-2519**	
Upper Neck My (Nm)	23.2		**-43.6**	
Chest Resultant Deflection (IR-TRACC) (mm)	41.2	Avg. 15 rib fractures per PMHS	30.5	Avg. 10 rib fractures per PMHS
Acetabulum FR (N)	4690	Pelvic ring fractures (n=2); acetabular fractures (n=1)	6005	Pelvic ring fractures (n=2)
Lower Tibia Fx (N)	**-2320**	No injuries reported	**-3174**	Fibula fractures (n=3); tibia fractures (n=1)
Upper Tibia Compressive Fz (N)	**1300**		**1469**	
Lower Tibia Compressive Fz (N)	1524		1247	

Note: Bolded values reflect measures that were higher in the THOR-05F when compared to THOR-50M measurements from [5].

TABLE VI
COMPARISON OF THOR-05F MEASUREMENTS TO PMHS INJURIES IN FDR CONDITIONS

Measurement	THOR-05F 25° (n=2)	Female PMHS Injuries 25°	THOR-05F 45° (n=2)	Female PMHS Injuries 45°
HIC-15	4595	No skull fractures; brain injury not assessed; cervical vertebral body fracture (n=1)	1939	No skull fractures; brain injury not assessed; multiple cervical/thoracic vertebral body fractures (n=3); cervical disc rupture (n=1)
BrIC	0.431		0.674	
Upper Neck Fx (N)	-538		-1793	
Upper Neck Fz (N)	-3137		-3236	
Upper Neck My (Nm)	42.3		-79.7	
Chest Resultant Deflection (IR-TRACC) (mm)	48.9	Avg. 11 rib fractures per PMHS	32	Avg. 20 rib fractures per PMHS
Acetabulum FR (N)	5504	Pelvic ring fracture (n=2)	5737	Multiple pelvic ring fractures (n=3)
Lower Tibia Fx (N)	216	Fibula fracture (n=2); Tibia fracture (n=1)	-1171	Fibula fracture (n=2); Tibia fracture (n=1)
Upper Tibia Compressive Fz (N)	534		862	
Lower Tibia Compressive Fz (N)	434		856	

IV. DISCUSSION

The goal of this study was to provide a preliminary evaluation of the performance of the THOR-05F in a HSRFFI across two seatback recline angles and two seat configurations, with the intent of determining the modifications required for future HSRFFI evaluations. To accomplish this, the analysis focused on: (1) assessing test repeatability through repeated runs within each seat type and recline angle, when possible; (2) quantifying THOR-05F biofidelity using the most recent BRS [5]; and (3) comparing THOR-05F measurement trends to physical injuries observed in the female PMHS [19]. Secondary goals included evaluating the sensitivity of THOR-05F measurements to seatback recline and seat type differences and comparing that to the sensitivity observed in the PMHS tests. A discussion on the findings is presented below and is organised according to the study's research objectives.

Repeatability of the Test Set-up

Repeatability was assessed using %CV, in accordance with [5]. Overall, repeatability of the test set-up and THOR-05F measurements in the ABTS seat was high at both recline angles. The 45° tests demonstrated marginally better repeatability than the 25° tests for this seat, with all measurement CVs ≤ 20% at 45°, compared to 95.4% of measurement CVs ≤ 20%.

For the FDR configuration, repeatability could not be formally assessed due to both logistical and physical constraints that prevented the completion of a third repeat run. The primary constraint was the availability of the specific OEM seats, which are no longer in production. An exhaustive search for additional units to this point has yielded only secondary-market seats that were either structurally inconsistent or showed signs of prior fatigue, making them unsuitable for high-severity sled testing.

Furthermore, physical damage to the ATD was observed during the FDR tests that was not present throughout the ABTS tests. While damage to ATDs under HSRFFI conditions has been documented previously in THOR-50M testing [5], a root-cause analysis was conducted to investigate the specific failure mode for the small female platform. The analysis revealed that, consistent with midsize male testing, damage resulted from external cabling pinching between the ATD and the seatback load cell plates during deep seatback compression. Although the cable-routing scheme recommended in previous HSRFFI studies was implemented, it proved sufficient only for the stiffer ABTS seat. The failure to prevent damage in the FDR seat is attributed to its more compliant frame, which allowed for deeper occupant "pocketing" and generated consistently higher peak seatback forces (Tables DI and DII) [7].

Caution is advised when interpreting the FDR seat results due to the absence of a formal repeatability assessment. Consequently, these conditions cannot be assigned the same statistical weight as the ABTS conditions, for which repeatability has been established. Despite these limitations, all available tests were retained to satisfy the study's objective of providing a preliminary evaluation of the THOR-05F in the HSRFFI condition and identifying potential hardware modifications. Notably, concerns regarding the tool's durability appear specific to the unique interactions of this test mode, and not the THOR-05F design specifically, as the THOR-05F has previously demonstrated acceptable durability under high-energy qualification test conditions [21]. Further, this behaviour has been observed previously with other ATDs in this test mode, and it is anticipated that similar challenges will persist with other small female ATDs if they utilise external cabling. Therefore, while further routing modifications are still under investigation, the most robust recommendation for future HSRFFI research is the transition to the In-Dummy Data Acquisition System variant of the THOR-05F, which does not utilise external cabling.

THOR-05F Biofidelity at 25° Recline

Seat Loading

Overall trends regarding head restraint and seatback loading were noted for the THOR-05F across both seats, with the THOR-05F generally producing higher peak loads relative to the PMHS (Table DI). Differences in seat loading behaviour across subjects likely reflect the effective-mass and stiffness differences between the ATD and PMHS: for impacts with similar mass, a stiffer body produces larger deformation of the seatback and thus higher forces.

At 25° recline in the ABTS seat, the overall seat-loading BRS score indicated good biofidelity (BRS score = 1.88; |DPS| = 13 ms); however, regional scores for the head restraint (BRS score = 2.35; |DPS| = 1 ms), seatback top (BRS score = 2.12; |DPS| = 1 ms), and belt loads (BRS Score = 2.29; |DPS| = 50 ms) were marginal, and the belt loads exhibited high average DPS values. The head-restraint results appear driven by differences in head-to-head-restraint interaction: PMHS heads tended to wrap around the restraint during contact, whereas the THOR-05F head compressed into it, producing combined neck flexion and axial compression. Consistent with this, head-restraint compression magnitudes were, on average, 2.04 kN larger in the THOR-05F tests. Although average seatback peak timing was similar between THOR-05F (41.7 ± 1.4 ms) and PMHS (42.1 ± 0.9 ms), the spatial load distribution differed: THOR-05F loads were concentrated toward the seatback bottom, while PMHS loads concentrated at the seatback top (Table DI).

The belt tension regional score in the ABTS seat was largely a product of differing lap-belt loading (BRS score = 3.76), as the THOR-05F lap-belt loads were lower in magnitude compared to the PMHS. More notably, average DPS values were 57 ms for the lap belt and 43 ms for the shoulder belt, indicating substantially delayed belt engagement relative to the PMHS; by contrast, PMHS average and maximum phase shifts for these measures were within 5 ms. These findings are consistent with prior THOR-50M and THOR-AV evaluations in the ABTS seat at this recline angle [5,6], suggesting that (1) modifications are needed to improve THOR-05F belt-interaction biofidelity for this condition, and (2) similar updates may be applicable across THOR ATDs. One reason for this behaviour stems from differences in occupant kinematics, with belt loading serving to restrain the PMHS during ramping, while the THOR-05F tended to "spring forward" off the seat with minimal vertical displacement (Fig. D5A and Fig. D6A, Appendix), and the belt loading served primarily to restrain forward movement (Fig. D3). This mechanism is examined further in a later section.

The FDR seat at 25° recline yielded an overall seat-loading BRS score that indicated marginal biofidelity (BRS score = 2.34; |DPS| = 7 ms). Regional scores for the head restraint (BRS score = 2.78; |DPS| = 2 ms), seatback top (BRS score = 2.34; |DPS| < 0.5 ms), and belt-loads (BRS score = 2.65; |DPS| = 27 ms) were marginal. Belt loads again showed elevated DPS values (though lower than in the ABTS seat). Head restraint contact differed between the dummy and PMHS; the THOR-05F contacted harder and lower on the restraint, resulting in a higher X force (Fig. C21C) and a large negative spike in Y-moment during initial head contact that was not observed in the PMHS (Fig. C23C).

This altered head restraint interaction is likely a function of different initial head vertical positioning, as the THOR head was positioned lower on average in the seat relative to the PMHS (topset 147.6 mm vs 111.9 mm; Table AIII). Topset variation could not be controlled for the THOR-05F in the same way as previous midsize male ATD HSRFFI research (i.e., the headrest could not be positioned any lower to account for slight differences in seated height relative to the PMHS) [6,19]. It is possible that the poorer seat loading scores in the FDR condition are a product of these differences, as they could alter initial head restraint engagement and subsequent load distribution, though the full downstream effects are unknown. This represents a limitation in the present work, though an important consideration for future testing. It is important to note, however, that topset differences are not the sole explanation; topsets were more closely aligned in the ABTS condition, yet differences in head restraint interaction persisted.

Regarding seatback interaction, the THOR-05F did not exhibit the "spring-forward" behaviour in the FDR seat and more closely reproduced PMHS pelvis Z-displacements. However, for a given Z-displacement, pelvis X-displacements were consistently larger, with the dummy remaining more pressed into the seat as it moved upward (Fig. D5B). This greater engagement helps explain the increase in seatback force relative to the PMHS data, and relative to the THOR-05F in the ABTS seat (Table DI) and would contribute to the marginal seatback loading scores. It also accounts for the marginal belt-load scores and elevated DPS: because the dummy loaded the seatback more heavily during ramping, its rebound phase lagged the PMHS, resulting in delayed belt engagement.

Occupant Response

At 25° recline in the ABTS seat, the overall occupant response BRS score demonstrated marginal biofidelity (BRS score = 2.23; |DPS| = 1 ms), despite good regional scores for the spine (BRS score = 1.37; |DPS| = 3 ms), thorax (BRS score = 1.02; |DPS| = 1 ms), and pelvis (BRS score = 1.28; |DPS| < 0.5 ms). The primary contributor to this was the elevated head BRS score (BRS score = 5.26), which was driven mainly by a poor head Z-displacement outlier score (BRS score = 22.82).

Inspection of this measurement trace (Fig. C5A) revealed that the high score resulted from the relatively narrow PMHS corridors in this condition (far narrower than the other head Z-displacement traces in Fig. C5B-C5D), and from substantial differences in movement directionality across subjects. Notably, the THOR-05F head failed to replicate the PMHS vertical kinematics and instead exhibited the distinctive "spring forward" behaviour characterised by the minimal upward displacement discussed above. This discrepancy may also be related to the differences in the head-to-head restraint interaction also discussed above, a notion further supported by marginal head angular kinematic BRS scores (ω_y: 2.04; θ_y: 2.44). When this outlier was excluded, the ABTS head BRS score improved to 1.74, and the overall occupant response score improved to 1.35, indicating good biofidelity in the remaining response measures.

In the FDR seat, the overall occupant response BRS score showed good biofidelity, with good body region scores. In the FDR seat, the head Z-displacement score was elevated compared to other measures (BRS score = 2.38), but not nearly as high as the ABTS condition. This is largely because, despite the initial differences in head restraint contact discussed above, the THOR-05F was largely able to reproduce the PMHS vertical ramping behaviour in this seat as the event progressed, and thus the score was lower. Instead, the largest occupant scores were in the pelvis region, with higher pelvis X-displacements into the seatback (BRS score = 3.16), and higher angular kinematic scores (ωy: 2.16; θy: 3.66). Therefore, despite similarities in the vertical ramping behaviour relative to the PMHS, the THOR-05F pelvis translated further into the seatback (Fig. D6B) and displayed more anterior rotation during initial contact with the seatback (Fig. C9 and Fig. C12).

Differences in pelvis rotation likely also contributed to the marginal belt loading score and lower magnitudes of lap-belt loading in the THOR-05F discussed above: PMHS exhibited an early rearward rotation (Fig. C9 and Fig. C12) that was absent in the THOR-05F, and which appears to reduce subsequent forward rotation from upper-body inertia and seatback contact, and which might also help to explain the more pronounced submarining behaviour observed during rebound in the THOR-05F tests, which was present across both seats and can be observed in the belt loading stills in Fig. D3 and D4 in the Appendix.

THOR-05F Biofidelity 45°

Seat Loading

At 45° recline in the ABTS seat, the overall seat-loading BRS score indicated good biofidelity (BRS score = 1.76; |DPS| = 14 ms); however, regional scores for the head restraint (BRS score = 2.18; |DPS| = 3 ms) and seatback bottom loads (BRS score = 2.39; |DPS| = 1 ms) were marginal, and the belt loads (BRS score = 1.21) again exhibited high DPS values (|DPS| = 65 ms). While there was a gap between the head and the head restraint targeted in the 25° tests, there was no gap targeted in the 45° tests. This lowered the amount of compression loading from THOR-05F into the head restraint relative to the 25° condition (-1.65 kN relative to ABTS 25°; Table DII), and changed the timing of seat loading (head restraint peaking before seatback loads), though the ATD still exhibited higher head X-displacement into the head restraint relative to the PMHS at 45° (Fig. C9A), and consequently saw higher head restraint X-forces (+3.32 kN relative to PMHS ABTS 45°).

Differences in the seatback bottom response appear linked to a positive X-force spike that occurs near the end of seatback unloading, as the initial compression magnitudes were similar across subjects (0.11 kN difference). Upon inspection of the high-speed video, the “spring-forward” behaviour observed at 25° was also present at 45°; the rebound timing coincides with this positive spike, suggesting an interaction where some part of the ATD or seatback structure is “pulling” on the bottom load cell plate. This point is examined further in a dedicated section below. Finally, because the rebound behaviour persisted at 45°, a similar explanation applies to the large DPS values: THOR-05F belt loading primarily acts as a horizontal restraint of the ATD during rebound, whereas in the PMHS, the belts contribute much earlier to restrain the body during vertical ramping.

In the FDR seat, overall seat-loading indicated poor biofidelity (BRS score = 3.43; |DPS| = 3 ms), driven primarily by poor scores at the seatback top (BRS score = 3.35; |DPS| = 2 ms) and bottom (BRS score = 8.18; |DPS| = 2 ms). The bottom plate score was exceptionally high relative to other calculated channels. largely due to differences in peak compression magnitude (+8.39 kN higher for THOR-05F) and load duration across subjects (Table CII). While overall THOR-05F pelvis X and Z displacements were similar to the PMHS, the dummy displaced further in the X direction for a given Z excursion, driving deeper into the seat as it ramped (Fig. C10B). The comparatively lower loading at the seatback top in the THOR-05F is likely a result of the I-S thoracic motion observed in the PMHS tests caused by inertial shifting of soft tissue and internal organs during ramping [19]. This movement may have shifted load toward the seatback top and reduced seatback bottom forces for the PMHS. The THOR-05F did not reproduce this inertial effect, which may explain why the measured load distribution remained concentrated toward the seatback-bottom.

Occupant Response

At 45° recline in the ABTS seat, both the overall occupant response BRS score (BRS score = 1.34; |DPS| = 2 ms), and all body region scores – including the head (BRS score = 1.44; |DPS| = 2 ms), spine (BRS score = 1.41; |DPS| = 2 ms), thorax (BRS score = 1.27; |DPS| = 0 ms), and pelvis (BRS score = 1.24; |DPS| = 2 ms) – indicated good biofidelity. This is largely attributed to the larger vertical head Z displacements in the 45° condition when compared to 25°. While the head Z-displacement BRS score improved to marginal (BRS score = 2.99), it remained elevated relative to other measures – a discrepancy still seemingly tied to the "spring forward" behaviour that was also observed during the 25° tests. Again, this rebound was not driven by early belt loading, as belt engagement occurred much later than the peak seatback loads in THOR-05F relative to PMHS (|DPS| = 65 ms).

The FDR seat also showed good biofidelity for the overall occupant response score at this angle (BRS score = 1.28; |DPS| = 2 ms), supported by good-to-excellent scores at the spine (BRS score = 1.07; |DPS| = 2 ms), thorax (BRS score = 0.80; |DPS| = 0 ms), and pelvis (BRS score = 1.24; |DPS| = 3 ms). The lone exception was the head region (BRS score = 2.01; |DPS| = 2 ms), which was marginal but close to the threshold for good biofidelity. This was due to the THOR-05F head displacing further in the -X direction (into the seatback) during the test combined with the narrower PMHS corridor observed for this condition (BRS Score = 3.88; Fig. C4D). This, along with the marginal head restraint BRS score for the same tests, also indicates different head-to-head restraint interaction. This appears to be related to topset differences across subjects, which were largest in the FDR 45° tests for the THOR-05F.

Additional Comments on the THOR-05F Biofidelity Evaluation

The updated BRS methodology explicitly isolates the SM score from the phase response so that timing differences do not obscure the evaluation of a curve's morphology [5]. The primary goal of shifting the dummy data is to align common events in time, ensuring that shape and magnitude can be fairly compared against the PMHS mean. Although the phase shift is no longer part of the SM calculation, it remains a critical consideration in the overall analysis; phase mismatches alone can indicate non-biofidelic behaviour despite a good SM score.

Recognising that the ability to manually align common events may be met with scepticism, the biofidelity analysis was repeated without any phase shifts (detailed in Appendix C and Table DIII). It is important to note that while phase shifting generally improved the BRS scores, there were multiple instances where aligning common events worsened the score, preventing the ATD from artificially benefiting from non-biofidelic alignment. These generally occurred for the head and pelvis kinematics which were discussed previously.

Seat loading scores generally benefited the most from phase alignment. However, these improvements were contextualised in the preceding sections, which appropriately penalised the ATD for requiring massive phase alignments or for still producing marginal-to-poor scores even after shifting. Occupant response scores, by contrast, were largely unaffected and remained within the same thresholds. Thus, while the unshifted values are provided for full transparency, the act of phase shifting did not alter the overall conclusions, as both the BRS scores and the DPS values were evaluated holistically in the present analysis.

Comparison of THOR-05F Measures to PMHS Injuries

To examine the sensitivity of THOR-05F to changing recline angles and seating configurations at capturing the injury trends observed during PMHS testing, measurements previously evaluated for the THOR-50M [5] were also evaluated for the THOR-05F. At the time of publication, injury risk assessment metrics for the THOR-05F have not been developed for rear-facing impact conditions. Consequently, general trends relative to prior THOR-50M values were also considered to aid in contextualising the results, with the expectation that the analysis can be revisited if specific criteria become available.

When THOR-05F measures in the ABTS seat were compared with previous ABTS tests conducted using the THOR-50M (Table V), two primary regions were found to exhibit generally elevated values for the THOR-05F: the head/neck region and the lower leg (tibia/fibula) region. These findings align with the PMHS data, which indicated a greater incidence of injuries in female PMHS tests compared to male tests for these same regions [19], suggesting the elevated measures may be attributable to size or sex differences across subjects that is being captured across ATDs. Specifically, seven out of the 12 female PMHS tested sustained vertebral body fractures at either the cervical or thoracic levels [19], whereas only one male PMHS sustained a vertebral body fracture, which was attributed to a pre-existing osteophyte bridging T11-T12 [12]. Further, seven out of the 12 female PMHS tested sustained fractures to the tibia or fibula, while only two males sustained any type of lower leg injury.

Regarding the head measures, the increased HIC-15 values are attributed to head contact with the rigidised but padded head restraint. Further investigation demonstrated that the results correlated well to the HIC-15 values recorded in the female PMHS tests [19], though the THOR-05F consistently recorded higher magnitudes on average. Specifically, in the ABTS seat, the THOR-05F recorded HIC-15 values of 5061 at 25° and 2241 at 45°, compared to the PMHS means of 3629.7 (±973.7) and 1224.7 (±203.6), respectively. Similarly, in the FDR seat, the THOR-05F measured 4595 at 25° and 1939 at 45°, exceeding the corresponding PMHS means of 4033.0 (±393.1) and 1273.0 (±216.5). Lastly, the absence of skull fractures in the PMHS tests despite the elevated HIC-15 values is not unreasonable given that HIC-15 was not developed for rear impacts.

The observed differences in upper neck loading and the THOR-05F's ability to correlate with injury patterns across seating configurations are attributed to variations in head restraint interaction. In the FDR seat at 45°, the THOR-05F was positioned lower, resulting in a larger average topset distance (50.1 mm larger compared to THOR-05F ABTS at 45°). As the ATD moved upward within the FDR seat, contact occurred with the lower portion of the headrest, generating increased compressive forces and subsequent neck extension as the head was driven upward and inward. This was accompanied by noticeably greater compression of the headrest cushioning (Fig. D8). This observation supports the injury mechanism described in prior literature [19], which emphasises a large vertical shear force potentially combined with neck extension components from head restraint interaction. The THOR-05F test data suggest that upper neck compression may also play a critical role, as all test cases with cervical injury in the female PMHS corresponded to high compressive Fz values recorded in the THOR-05F (specifically ABTS at 45° and FDR at both 25° and 45°). Conversely, in the ABTS 25° test condition, where no cervical injury was noted in the PMHS, the dominant loading mode was tension, and the magnitude was much lower (1,528 N) than the other conditions. It is possible that these results may be specific to the fixed head restraint and seatback configurations used in this test series. However, the findings suggest the need for further investigation into head restraint interactions and upper neck loading in future rear-impact research involving small-statured subjects.

Higher THOR-05F chest IR-TRACC deflections were observed in 25° conditions compared to 45° and are attributed to the more upright seat during testing, which, relative to the sled motion, permits more chest compression during seatback loading. A similar trend was observed in the chestband data (Fig. C20, Appendix). The female PMHS sustained numerous rib fractures, though there were contrasting trends relative to the THOR-05F patterns. In the ABTS seat, the PMHS injury patterns followed a similar trend as the THOR-05F IR-TRACC measurements, with more rib fractures sustained at 25°; in the FDR seat, however, there were not only more rib fractures at 45°, but this condition also had the highest number of fractures out of any female test.

This disconnect may be related to prior reports that anterior-posterior chest deflection underpredicts rib fracture risk in reclined rear-facing impacts, where I-S deformation from ramping and abdominal inertia meaningfully contributes to injury [5,19]. Investigations into the individual X and Z component measurements of the THOR-05F IR-TRACC data demonstrated that while Z-deflections were comparable in magnitude to X-deflections, there were no clear trends in the Z data to explicitly support the I-S injury mechanisms discussed for the PMHS. Ultimately, more investigation is needed to evaluate the ability of the THOR-05F in identifying thoracic injuries in rear-facing seats, paralleling the findings from the THOR-50M investigation [5]. There may be utility in considering multi-axis thoracic injury metrics for future HSRFFI testing, though again this was not discernible from the IR-TRACC or chestband data alone.

At present, there are no established THOR-05F pelvis IRFs specific to rear-facing impacts. To provide contextualisation, the acetabular loads – a common metric for pelvic injury in other crash modes – were evaluated. Across all test conditions, the recorded loads exceeded the 50% risk threshold developed by [30] for frontal impacts. While this is not a statement of injury risk given the different boundary conditions, it highlights that the ATD was subjected to severe pelvic loading relative to existing benchmarks.

In the context of HSRFFI testing, peak acetabular force alone may be insufficient to explain the sex-specific outcomes: five of six female PMHS sustained sacral fractures (five in FDR, one in ABTS), while none of the male PMHS did. The original study attributed this to seat geometry and PMHS posture. Other studies investigating the mass coupling behaviour in the KTH complex have hypothesised that mobility (laxity) differences across sex within the pelvis-sacrum-lumbar spine articulating joints (hip, sacroiliac, sacrococcygeal) could affect how forces are modulated at the hip from impact loading [31]. Imaging and posture studies show females have larger sacral-slope and pelvic-tilt changes and reduced L4-S lordosis when sitting [32], and sex * chair effects (especially with a backrest) shift centre of mass/pressure between sexes [33]. For application in HSRFFIs, these shifts could place the sacrum in orientations that amplify sacral stress for a given seatback load.

The scope of modifications required to capture these PMHS sacral injury mechanisms in an ATD is not yet known, but one potential target is the lumbar spine. Prior work has inferred that the THOR-05F lumbar is stiffer than human tissue [34]. Further, while there have been different spinal postures noted in humans with different seated or standing postures [32,33], the THOR lumbar spine pitch adjustment is less robust, especially in the current study where it was fixed in an "erect" posture across both seating positions. This could help explain why the ATD was unable to capture the dynamic pelvic rotations observed in the PMHS (if there were differences in spinal curvature in females when sitting [32]), and may explain the lower seatback-bottom Fx in FDR tests despite more pelvis injuries, suggesting mechanisms beyond simple horizontal pelvis translation and axial compression. The THOR-05F also currently lacks the ability to measure sacral-specific load transmission and stresses, as well as the off axis pelvis rotation behaviour reported in prior HSRFFI PMHS tests [10] (since there is only one Pelvis ARS block in the THOR-05F compared to two used in the PMHS study), which may also contribute. Ultimately, future rear-impact research should continue investigating this mechanism, as it might necessitate additional ATD pelvis instrumentation, or updated IRFs for future application with HSRFFI.

Increased lower-leg measures for the THOR-05F when compared to the THOR-50M are consistent with the PMHS explanation from [19], that shorter thigh length and reduced posterior leg-to-seat pan gap in smaller females produce earlier and larger tibia loading. This severity increases at 45° recline due to larger pelvis X-excursions, with THOR-05F tibia shear forces increasing by 854 N in the ABTS seat and 955 N in the FDR seat between angles. A difference was noted in that PMHS testing produced more tibia and fibula fractures in FDR than in ABTS, while THOR-05F loads were larger in ABTS. For this, two explanations are plausible. First, PMHS lower-leg injuries were concentrated in the smaller subjects and the ABTS 25° PMHS group was relatively tall (163.3-167.6 cm versus 151.3 cm for a typical small female). Second, seat-dependent pelvis kinematics differed for THOR-05F: greater vertical pelvis displacement in FDR led to tibia unloading at peak pelvis XZ excursion in FDR while tibia contact was retained in ABTS; PMHS leg behaviour was observed to more closely match the ABTS contact pattern, remaining largely in seat-pan contact through peak pelvis excursion (Fig. D1 & D7). Similar behaviour was also observed in the THOR-50M ABTS tests, which was described as the inertia of the upper body and pelvis “pulling” the lower legs upward and into the front of the seat pan, elevating the Fz vector [5].

Potential Contributors to the “Spring Forward” Mechanism Observed

Given that (1) the THOR-05F exhibited a “spring forward” behaviour in the ABTS seat across both recline angles, (2) this behaviour was not present in the FDR condition, where the ATD exhibited comparable levels of ramping to the PMHS, and (3) similar behaviour has been reported in prior THOR-50M and THOR-AV evaluations in the ABTS seat [5,6], it is possible that the behaviour stems from a combination of ATD design limitations and specific seat architecture differences. Prior ABTS HSRFFI research has suggested that the PMHS upper body mass (which shifts due to soft tissue inertia) and the increased flexibility in the spine allow the subjects to conform to the seatback geometry more closely, which then pulls the pelvis up off the seat pan and up the seatback. The THOR-50M spine by comparison could not replicate this behaviour, contributing to its “spring forward” rebound behaviour [5]. This appears to be a plausible explanation for the THOR-05F in this testing, supported by the differences in peak T12 (Fig. C19, Appendix), and pelvis (Fig. C9 & C12, Appendix) angular kinematics during initial seat contact, which were more pronounced at 25°. This suggests that targeted revisions are needed for the THOR-05F spine to improve its ability to conform to the seatback. Increasing spinal flexibility could achieve this, as noted in the previous section, though it risks introducing durability concerns under high-severity impact conditions.

The observation that the THOR-05F was better able to produce the vertical ramping behaviour in the FDR seat, which was not part of the prior THOR-50M evaluation, suggests that seat specific architecture may have

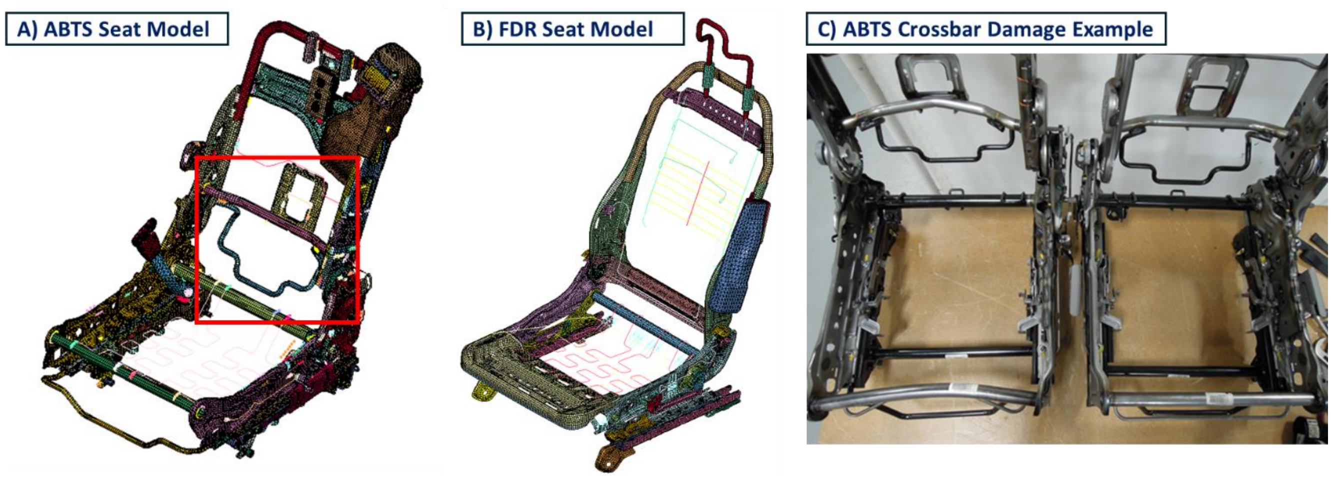

Fig. 4. Potential seatback cross-member interaction contributing to the “spring forward” rebound in ABTS tests: A) ABTS seatback frame (cover removed) showing the transverse cross-member and rectangular plate; B) FDR frame (cover removed) lacking that cross-member; C) ABTS plate deformation after testing (*left*) versus a new frame (*right*).

exacerbated any underlying subject-seat coupling differences. Unlike the FDR seat (Fig. 4B), the ABTS seatback features a lower horizontal cross-member (Fig. 4A). Post-test inspections of the ABTS frame revealed substantial deformation of this cross-member and the rectangular plate above it (Fig. 4C). This deformation likely acted as a vertical restraint, snagging the ATD and facilitating the "spring forward" mechanism. This aligns with findings in [35], where seated height and pelvis position differences caused the GHBMC model to interact with metal seatback components in ways the PMHS did not. This would also explain why the 45° tests (where the ATD sits lower with a larger topset) allowed more vertical travel before engaging the cross-member relative to the 25° tests, and why tensile loads were recorded on the seatback plate during unloading (the bent plate may have caught the load-cell plate and "pulled" on it as the dummy translated forward). Beyond seat specific differences, it is also important to note that the rigidised seatback and seatback plates may have further contributed to the "spring forward" behaviour; future work should investigate the occurrence of this mechanism in an ABTS seat without a rigidised seatback.

Representativeness of the Crash Pulse

This body of work focuses on the HSRFFI, formulated as one possible crash scenario that could emerge in future ADS vehicles. In the absence of a specific ADS pulse, this work operates under the premise that occupants will continue to receive equivalent baseline protections afforded in current frontal crash tests. Therefore, to simulate a HSRFFI, vehicle crash accelerations, velocities, and durations were compiled from USNCAP testing [12]. As collision mitigation technologies continue to advance, real-world crash pulses are anticipated to become increasingly modulated in magnitude, duration, and overall shape. Because of this, this pulse will ideally represent more of a worst-case scenario in future collisions. However, until further research justifies altering current regulatory standards for novel seating arrangements, and until there is empirical evidence and industry consensus defining an ADS-specific frontal pulse, abandoning the established high-speed NCAP severity appears premature and is currently unjustified. Ultimately, this study provides a critical biomechanical baseline for evaluating safety tool performance under known high-speed, survivable frontal impact conditions, which can be iteratively refined as more characteristic ADS crash data becomes available.

Representativeness of the Seat Types

The current test series utilises both ABTS and FDR seat types for the investigation. In highly automated vehicles, ABTS designs are anticipated to be the primary restraint solution. This is driven by two critical factors: (1) ABTS systems reduce the risk of excessive occupant excursions during high-speed rear impacts, particularly in reclined postures, and (2) future ADS seating is expected to require consistent restraint performance across a broad range of recline angles enabled by flexible interior layouts [12]. For the FDR condition, this body of work assumes that the D-ring would feature adaptive capabilities or a mounting point independent of the B-pillar to be compatible across a wide range of seating conditions. To model this, the D-ring location for the 45° FDR condition was rotated about the seat pivot to maintain a consistent belt position relative to the seatback across recline angles. This is still ultimately an assumption, and future work should continue to evaluate the applicability of this assumption and adjust boundary conditions as more production ADS seating geometries are introduced.

Additional Limitations

Beyond the limitations discussed above, there are additional limitations in this work. First, the female PMHS corridors used for biofidelity comparisons were based on three tests per configuration. When sensor issues occurred in one or more tests for a given measurement region, corridors could not be established and corresponding BRS scores could not be computed. Second, the evaluation relies on anthropometric normalization, which is an imperfect tool that may have inadvertently impacted the biofidelity evaluation in ways unknown at the present time. While a representative subject pool large enough to eliminate the need for normalization is the ideal solution, this is rarely feasible, especially for small female subjects. Next, in this study the most updated BRS method was used to quantify differences in time-history responses between the THOR-05F and female PMHS. However, alternative comparison approaches (e.g. CORA, ISO/TS 18571, SPM) and other BRS variants exist. Those methods can yield different scores and interpretations, and future work should apply and compare multiple time-history methods to assess the robustness of the findings. Finally, because the THOR-05F was designed for frontal impacts, some biofidelity differences may stem from adapting the ATD to HSRFFI scenarios, implying that (1) if modifications are desired, they may need to be HSRFFI-specific, and (2) if future biofidelity improvements are implemented for the THOR-05F for use in frontal crash investigations, it could inadvertently alter the current findings.

V. CONCLUSION

This study provided a preliminary evaluation of the THOR-05F ATD in a HSRFFI scenario across two seatback recline angles and two seat configurations, using matched female PMHS test data as reference. The objective was to assess the extent to which the ATD reproduced the sex- and size-specific biomechanical trends previously identified in PMHS testing and to identify areas for refinement in future ADS-relevant occupant protection evaluations. The biofidelity comparison showed that the THOR-05F generally performed better at 45° recline than at 25°, with improved occupant response scores across both seat types and better seat loading scores for the ABTS configuration. The THOR-05F was also generally more repeatable at 45° recline than at 25° for the ABTS condition. However, several areas were identified where the THOR-05F could be improved, specifically regarding seatback loading, belt loading, pelvic angular kinematics, and head restraint interaction. Furthermore, the ATD experienced sensor damage during FDR testing and currently lacks the measurement capabilities and validated injury criteria necessary to fully capture the complex female PMHS injury mechanisms observed during testing. Together, these results indicate that targeted hardware modifications and further investigation into HSRFFI-specific injury criteria are needed before the THOR-05F is suitable for use in future HSRFFI testing.

VI. ACKNOWLEDGEMENTS

The following research was funded by the National Highway Traffic Safety Administration (NHTSA) under contract number 693JJ918D000019. The authors would also like to acknowledge the numerous contributions from the test support personnel at the Transportation Research Center (TRC) in East Liberty, Ohio. The authors would like to thank the Dummy Lab for THOR-05F preparations, Colton Thomas and Brian Suntay for chestband installation and data-processing, and Mike Van Voorhis for TEMA analysis. Further, this report is published in the interest of advancing motor vehicle safety research. While the report may provide results from research or tests using specifically identified manufacturers' names, it is not intended to make conclusions about the safety performance or safety compliance of those products or manufacturers, and no such conclusions should be drawn.

VII. REFERENCES

[1] Östling, M. and Larsson, A. Occupant activities and sitting positions in automated vehicles in China and Sweden, in *Proceedings of the 26th International Technical Conference on the Enhanced Safety of Vehicles (ESV)*. 2019: Eindhoven, Netherlands. p. 10-13.

[2] Koppel, S., Jimenez Octavio, J., et al. Seating configuration and position preferences in fully automated vehicles. *Traffic Inj Prev*, 2019. 20(sup2): p. S103-S109

[3] Jorlöv, S., Bohman, K., and Larsson, A. Seating positions and activities in highly automated cars - a qualitative study of future automated driving scenarios, in *Proceedings of the International Conference on the Biomechanics of Impact (IRCOBI)*. 2017: Antwerp, Belgium.

[4] McMurry, T.L., Poplin, G.S., Shaw, G., and Panzer, M.B. Crash safety concerns for out-of-position occupant postures: A look toward safety in highly automated vehicles. *Traffic Inj Prev*, 2018. 19(6): p. 582-587

[5] Hagedorn, A., Stammen, J., et al. Biofidelity Evaluation of THOR-50M in Rear-Facing Seating Configurations Using an Updated Biofidelity Ranking System. *SAE International Journal of Transportation Safety*, 2022. 10(2): p. 291-375

[6] Wang, Z.J. Biomechanical Responses of the THOR-AV ATD in Rear Facing Test Conditions. *SAE International Journal of Advances and Current Practices in Mobility*, 2022. 04(6): p. 2089-2105

[7] Kang, Y.-S., Stammen, J., et al. Effects of Seatback Recline and Belt Restraint Type on PMHS Responses and Injuries in Rear-Facing Frontal Impacts. *SAE International Journal of Transportation Safety*, 2022. 10(2): p. 235-289

[8] Kang, Y.S., Baker, G.H., et al. Thoracic Responses and Injuries of Male Post-Mortem Human Subjects in a Homogeneous Rear-Facing Seat During High-Speed Frontal Impact. *Ann Biomed Eng*, 2025. 53(2): p. 520-535

[9] Kang, Y.S., DeWitt, T., et al. Responses and Injuries of Male Post-Mortem Human Subjects (PMHS) Seated in an Unreinforced Production Seat in Rear-facing Frontal Impacts, in *Proceedings of the International Research Council on the Biomechanics of Impact (IRCOBI)*. 2024: Stockholm, Sweden.

[10] Kang, Y.S., Pradhan, V., et al. Pelvic Responses and Injuries to Male Post-Mortem Human Subjects (PMHS) in Rear-Facing Seat Configurations in High-Speed Frontal Impacts, in *Proceedings of the International Research Council on the Biomechanics of Impact (IRCOBI)*. 2024: Stockholm, Sweden.

[11] Kang, Y.S., Stammen, J., et al. Thoracic responses and injuries to male postmortem human subjects (PMHS) in rear-facing seat configurations in high-speed frontal impacts. *Traffic Inj Prev*, 2023. 24(sup1): p. S47-S54

[12] Kang, Y.S., Stammen, J., et al. Biomechanical Responses and Injury Assessment of Post Mortem Human Subjects in Various Rear-facing Seating Configurations. *Stapp Car Crash J*, 2020. 64: p. 155-212

[13] Parenteau, C.S., Zuby, D., Brolin, K.B., Svensson, M.Y., Palmertz, C., and Wang, S.C. Restrained Male and Female Occupants in Frontal Crashes: Are We Different?, in *Proceedings of the International Research Council on the Biomechanics of Impact (IRCOBI)*. 2013: Gothenburg, Sweden. p. 803-817.
[14] Bose, D., Segui-Gomez, M., and Crandall, J.R. Vulnerability of female drivers involved in motor vehicle crashes: an analysis of US population at risk. *Am J Public Health*, 2011. 101(12): p. 2368-73
[15] Forman, J., Poplin, G.S., et al. Automobile injury trends in the contemporary fleet: Belted occupants in frontal collisions. *Traffic Inj Prev*, 2019. 20(6): p. 607-612
[16] Jakobsson, L. and Norin, H. AIS1 Neck Injury Reducing Effect of WHIPS (Whiplash Protection System). *Proceedings of Proceedings of the International Research Council on the Biomechanics of Impact (IRCOBI)*, 2004. Graz, Austria
[17] Storvik, S.G., Stemper Bd Fau - Yoganandan, N., Yoganandan N Fau - Pintar, F.A., and Pintar, F.A. Population-based estimates of whiplash injury using nass cds data - biomed 2009. (0067-8856 (Print))
[18] Carlsson, A., Linder, A., Davidsson, J., Hell, W., Schick, S., and Svensson, M. Dynamic kinematic responses of female volunteers in rear impacts and comparison to previous male volunteer tests. *Traffic Inj Prev*, 2011. 12(4): p. 347-57
[19] Kang, Y.-S., Baker, G.H., et al. Comparison of Female and Male Post Mortem Human Subject Kinematic Responses and Injuries in Rear-Facing Seat Configurations in High-Speed Frontal Impacts. *Stapp Car Crash Journal*, 2026
[20] Administration, N.H.T.S. Drawings and Specifications for THOR-05F Advanced Female Frontal Crash Test Dummy. 2025, National Highway Traffic Safety Administration, Vehicle Research and Test Center: East Liberty, Ohio.
[21] Administration, N.H.T.S. THOR-05F Durability Report. 2025, National Highway Traffic Safety Administration, Vehicle Research and Test Center: East Liberty, Ohio.
[22] Administration, N.H.T.S. THOR 5th Percentile Female (THOR-05F) Procedures for Assembly, Disassembly, and Inspection (PADI). 2025, National Highway Traffic Safety Administration, Vehicle Research and Test Center: East Liberty, Ohio.
[23] Administration, N.H.T.S. THOR 5th Percentile Female (THOR-05F) Qualification Procedures and Requirements. 2025, National Highway Traffic Safety Administration, Vehicle Research and Test Center: East Liberty, Ohio.
[24] Administration, N.H.T.S. THOR-05F Repeatability and Reproducibility of Qualification Tests. 2025, National Highway Traffic Safety Administration, Vehicle Research and Test Center: East Liberty, Ohio.
[25] Mertz, H.J., Jarrett, K., Moss, S., Salloum, M., and Zhao, Y. The Hybrid III 10-Year-Old Dummy. *Stapp Car Crash J*, 2001. 45: p. 319-28
[26] Administration, N.H.T.S. Drawings and Specifications for THOR-05F Advanced Female Frontal Crash Test Dummy. 2019, National Highway Traffic Safety Administration, Vehicle Research and Test Center: East Liberty, Ohio.
[27] Reed, M.P., Ebert, S.M., and Jones, M.L.H. Posture and belt fit in reclined passenger seats. *Traffic Inj Prev*, 2019. 20(sup1): p. S38-S42
[28] International, S. Instrumentation for Impact Test Part 1 - Electronic Instrumentation, in *Surface Vehicle Recommended Practice*. Rev. Aug. 2022.
[29] Wang, Z.J., Ramachandra, R., Bolte IV, J.H., and Lee, E. THOR 5th Female Biofidelity Evaluation in Gold Standard Sled Test Condition, in *Proceedings of the International Research Council on the Biomechanics of Impact (IRCOBI)*. 2021: Held Online.
[30] Carpenter, R.L., Donlon, J.P., and Forman, J.L. Development and Evaluation of Methodology for Assessing Female Knee-Thigh-Hip Injury Risk in Frontal Impacts Using Female ATD Load Cell Measurements, in *Proceedings of the International Research Council on the Biomechanics of Impact (IRCOBI)*. 2025: Vilnius, Lithuania.
[31] Carpenter, R.L., Berthelson, P.R., Donlon, J.P., and Forman, J.L. Comparison of the Knee-Thigh-Hip Response in Small Female ATDs with Female PMHS. *Proceedings of Proceedings of the International Research Council on the Biomechanics of Impact (IRCOBI)*, 2024. Stockholm, Sweden
[32] Mizukoshi, R., Yagi, M., et al. Gender differences in spinal mobility during postural changes: a detailed analysis using upright CT. *Sci Rep*, 2024. 14(1): p. 9154
[33] Dunk, N.M. and Callaghan, J.P. Gender-based differences in postural responses to seated exposures. *Clin Biomech (Bristol)*, 2005. 20(10): p. 1101-10
[34] Wang, Z.J., Below, J., Loeber, B., and Greenlees, B. Biofidelity Report of the THOR 5th Percentile Anthropomorphic Test Device, U.S.D.o. Transportation, Editor. 2020, National Highway Traffic Safety Administration.
[35] Pradhan, V.V., Ramachandra, R., et al. Biofidelity assessment of the GHBMC M50-O in a rear-facing seat configuration during high-speed frontal impact. *Comput Methods Biomech Biomed Engin*, 2024. 27(10): p. 1287-1302

VIII. APPENDIX

Appendix A: Test Information and Diagrams

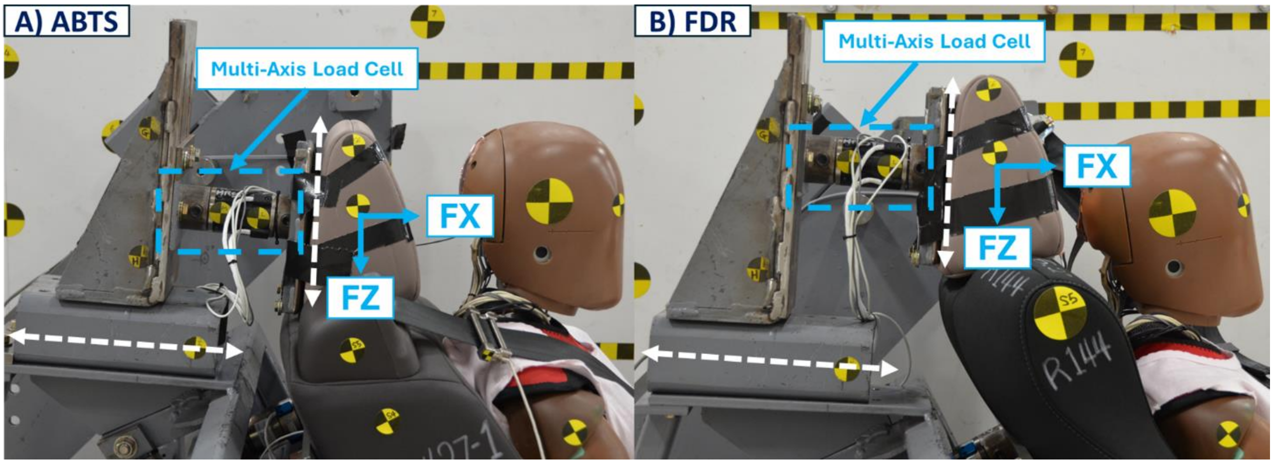

Fig. A1. Fixed, adjustable head restraint assembly for A) the ABTS seat and B) the FDR seat. Load cell location and coordinate axes are shown in blue; directions of adjustability are indicated by white arrows.

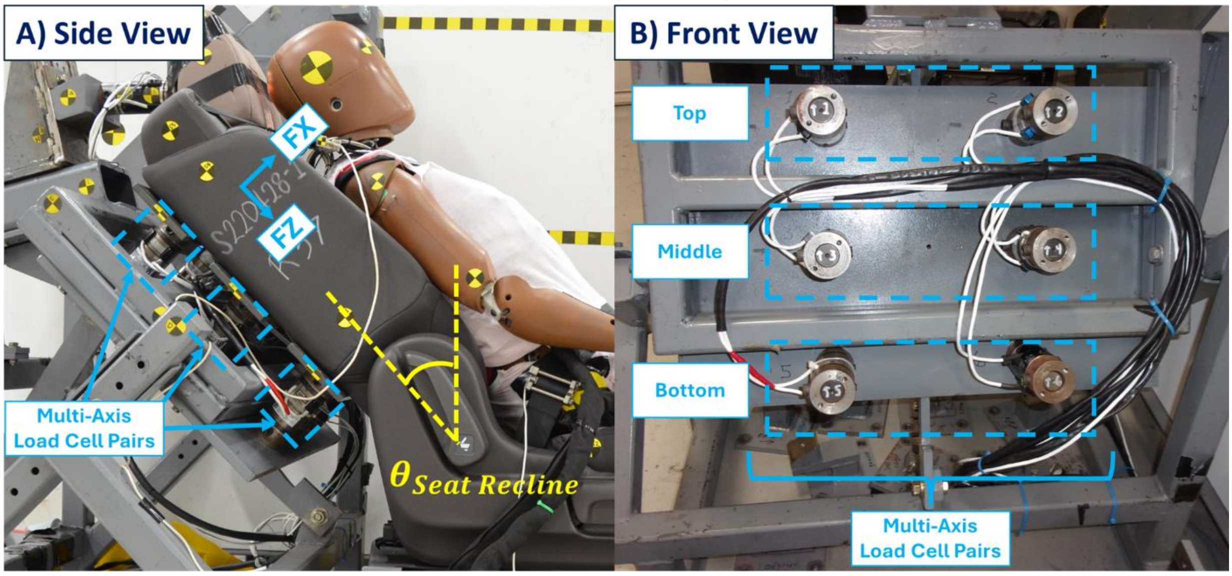

Fig. A2. Fixed, adjustable seatback assembly used in testing from the A) side view (fully assembled, ABTS seat example) and B) front view (during assembly). Locations of load-cell pairs (each containing two multi-axis load cells) and coordinate axes are shown in blue; seatback adjustability is indicated by yellow lines.

TABLE AI
THOR-05F AND PMHS SENSORS USED DURING TESTING

Sensor	THOR-05F	Small Female PMHS [19]
Head Accelerometers and Angular Rate Sensors (ARS)	X	X
Upper and Lower Neck Forces and Moments	X	
Upper and Lower Thorax IR-TRACCs	X	
Chestband (External)	X	X
T1 Accelerometers and ARS	X	X
T8 Accelerometers and ARS	X	X
T12 Accelerometers and ARS	X	X
Acetabulum Forces	X	
Pelvis Accelerometers and ARS	X	X
Femur Force and Moments	X	
Femur Accelerometers, ARS, Strain Gages		X
Tibia Force and Moments	X	
Tibia Accelerometers, ARS, Strain Gages		X

Fig. A3. Fixed recline seatback, fixed head restraint sled test configuration (front view) showing the THOR-05F belt routing in: A) ABTS seat at 25° recline; B) ABTS seat at 45° recline; C) FDR seat at 25° recline; and D) FDR seat at 45° recline. Images are high-speed video stills.

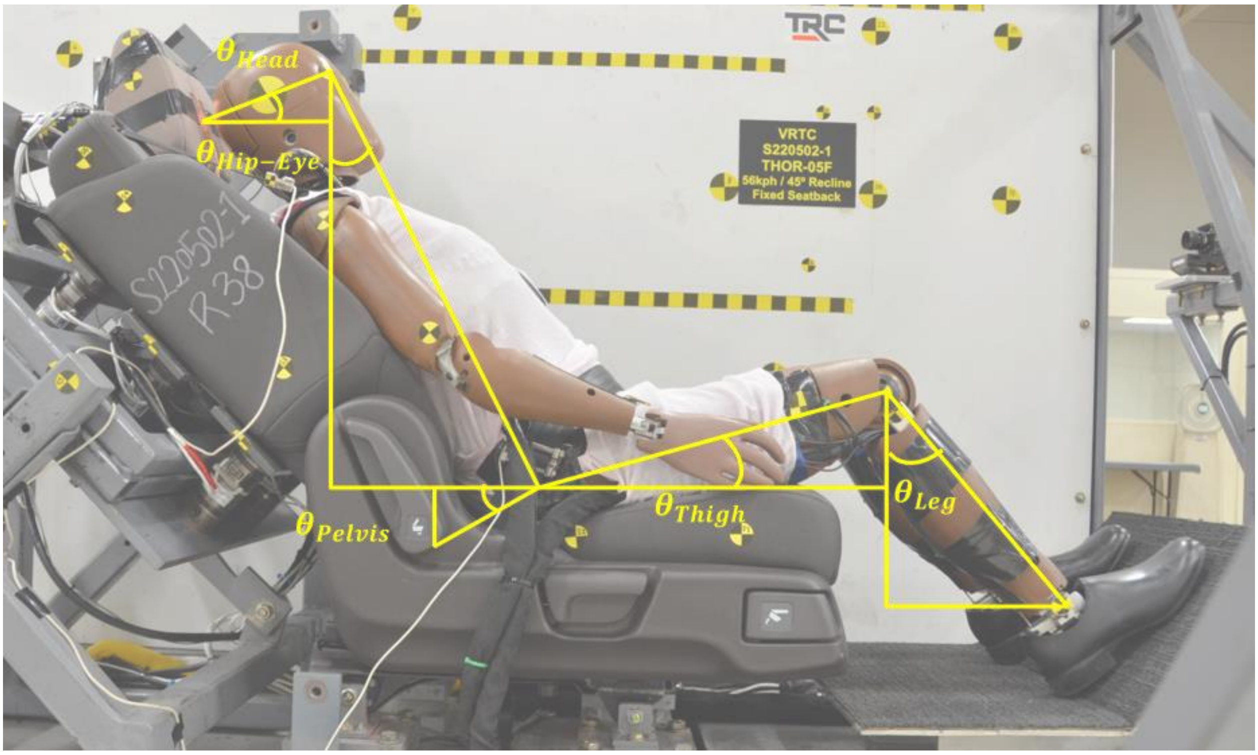

Fig. A4. UMTRI angle definitions [27], consistent with previous ADS studies [5,19].

TABLE AII

THOR-05F 25° SEAT RECLINE POSITIONING MEASUREMENTS

Seat	Test	Head Angle (deg.)	Pelvis Tilt Sensor (deg.)	Thigh Angle (deg.)	Leg Angle (deg.)	Hip-to-Eye Angle (deg.)	Backset (mm)	Topset (mm)
Accord	*S211209-1*	-0.3	22.3	12.1	46.2	13.1	81.0	145.0
	S220504-2	1.4	22.3	11.7	46.9	11.3	79.0	150.3
Odyssey	*S220425-1*	0.8	20.6	13.0	48.0	9.7	75.0	86.6
	S220426-1	0.8	20.2	12.2	45.1	10.9	75.1	81.3
	S220427-1	0.6	20.1	11.7	47.4	10.5	76.0	77.3
THOR-05F Mean (SD)		**0.7 (0.6)**	**21.1 (1.1)**	**12.1 (0.5)**	**46.7 (1.1)**	**11.1 (1.3)**	**77.2 (2.7)**	**108.1 (36.3)**
PMHS Mean (SD) [19]		**0.6 (0.3)**	**42.4 (7.4)** ±	**11.0 (0.6)**	**46.0 (1.9)**	**--**	**81.0 (3.1)**	**95.3 (16.6)**

±UMTRI Pelvis Angle; offset from THOR-05F pelvis tilt sensor reading by ~25.2° (estimated from [26] drawing package).

TABLE AIII

THOR-05F 45° SEAT RECLINE POSITIONING MEASUREMENTS

Seat	Test	Head Angle (deg.)	Pelvis Tilt Sensor (deg.)	Thigh Angle (deg.)	Leg Angle (deg.)	Hip-to-Eye Angle (deg.)	Backset (mm)	Topset (mm)
Accord	*S220104-1*	31.1	36.6	11.5	47.0	34.6	0*	198.7
	S220509-1	31.3	35.8	11.3	46.2	31.2	0	189.7
Odyssey	*S220428-1*	33.0	35.2	12.2	40.9	33.1	0*	143.5
	S220502-1	32.9	34.6	12.6	41.9	32.9	0*	143.8
	S220502-2	32.1	34.2	12.3	40.7	30.3	0*	145.0
THOR-05F Mean (SD)		**32.1 (0.9)**	**35.3 (1.0)**	**12.0 (0.6)**	**43.3 (3.0)**	**32.4 (1.7)**	**0 (0)***	**164.1 (27.6)**
PMHS Mean (SD) [19]		**26.3 (2.2)**	**36.3 (8.1)±**	**10.7 (1.0)**	**47.1 (3.1)**	**--**	**0.0 (0.0)**	**85.7 (29.8)**

**Head not touching head restraint; gap too small to measure.*

±UMTRI Pelvis Angle; offset from THOR-05F pelvis tilt sensor reading by ~25.2° (estimated from [26] drawing package).

Appendix B: Repeatability Results

TABLE BI
THOR-05F REPEATABILITY SCALES FOR HSRFFI ANALYSIS

CV (%) [5]
0 ≤ CV ≤ 10
10 < CV ≤ 20
CV > 20

TABLE BII
THOR-05F REPEATABILITY RESULTS ABTS HONDA ODYSSEY SEAT (N=3 TESTS PER ANGLE, 43 MEASUREMENTS PER TEST)

		25°			45°	
Measurement	Mean	SD	CV (%)	Mean	SD	CV (%)
HIC-15	5060.76	568.28	11.23	2241.08	115.05	5.13
Head Ax (g)	364.98	30.08	8.24	237.03	9.13	3.85
Head Az (g)	47.25	4.03	8.53	89.43	5.94	6.64
Head Ry (deg/s)	-716.35	71.71	10.01	-454.44	33.08	7.28
*Head RotY (deg)**	-29.94	6.05	20.21	-13.36	2.52	18.85
*Head DX (mm)**	-198.59	2.21	1.11	-150.08	1.86	1.24
*Head DZ (mm)**	-10.71	0.68	6.34	-46.48	3.87	8.32
BrIC	0.40	0.07	16.89	0.30	0.02	8.04
Upper Neck Fx (N)	-458.77	71.43	15.57	-1102.59	44.89	4.07
Upper Neck Fz (N)	1528.28	66.57	4.36	-2518.80	214.26	8.51
Upper Neck My (Nm)	23.17	0.36	1.57	-43.63	5.33	12.21
T1 Ax (g)	140.20	0.85	0.61	107.56	4.75	4.42
T1 Az (g)	38.67	2.55	6.60	58.81	4.29	7.30
T8 Ax (g)	110.56	1.96	1.78	75.27	1.32	1.76
T8 Az (g)	97.22	5.19	5.34	110.38	2.88	2.61
T12 Ax (g)	121.80	3.63	2.98	74.75	5.46	7.30
T12 Az (g)	81.70	5.06	6.19	104.93	3.67	3.50
T12 Ry (deg/s)	293.39	37.48	12.78	-341.59	19.74	5.78
Chest Resultant Deflection (Internal IR-TRACC) (mm)	41.20	0.63	1.52	30.50	1.18	3.88
Pelvis Ax (g)	125.15	6.13	4.90	108.28	4.33	4.00
Pelvis Az (g)	41.49	2.73	6.57	-107.35	4.17	3.89
Pelvis Ry (deg/s)	-2504.78	54.37	2.17	-2142.86	47.33	2.21
*Pelvis RotY (deg)**	-22.43	1.03	4.58	-20.90	0.16	0.78
*Pelvis DX (mm)**	-137.00	1.86	1.36	-189.00	3.36	1.78
*Pelvis DZ (mm)**	-14.66	2.23	15.18	-61.89	10.80	17.46
Left Acetabulum FR (N)	4229.90	113.08	2.67	5272.25	71.29	1.35
Right Acetabulum FR (N)	4690.12	135.58	2.89	6004.85	243.45	4.05
Left Femur Compressive Fz (N)	1163.12	25.59	2.20	1793.98	91.66	5.11
Right Femur Compressive Fz (N)	1255.06	90.35	7.20	1674.80	41.73	2.49
LL Tibia Fx (N)	-2123.11	207.78	9.79	-2858.18	287.64	10.06
RL Tibia Fx (N)	-2218.19	236.46	10.66	-3120.33	399.08	12.79
LU Tibia Compressive Fz (N)	1300.09	138.63	10.66	1468.87	196.40	13.37
RU Tibia Compressive Fz (N)	903.12	45.25	5.01	1256.40	73.21	5.83
LL Tibia Compressive Fz (N)	1441.72	236.56	16.41	1204.75	61.10	5.07
RL Tibia Compressive Fz (N)	1323.72	95.37	7.20	1214.14	92.18	7.59
Head Restraint Fx (N)	-10721.54	434.25	4.05	-8977.64	205.53	2.29
Head Restraint Fz (N)	1708.25	241.85	14.16	-2648.25	69.15	2.61
Head Restraint My (Nm)	128.46	19.35	15.06	238.47	5.76	2.41
Seatback Top Fx	-8912.80	458.50	5.14	-5473.53	92.78	1.70
Seatback Middle Fx	-3845.50	226.35	5.89	-4303.76	145.98	3.39
Seatback Bottom Fx	-10712.93	278.27	2.60	-8437.99	199.57	2.37
Lap Belt (N)	542.58	178.89	32.97	1126.71	29.27	2.60
Shoulder Belt (N)	777.52	58.67	7.55	775.85	69.94	9.01

**Denotes Global Measurement.*

TABLE BIII

THOR-05F RESULTS FDR HONDA ACCORD SEAT (N=2 TESTS PER ANGLE, 43 MEASUREMENTS PER TEST)

	25°		45°	
Measurement	Mean	Difference	Mean	Difference
HIC-15	4595.28	354.38	1939.41	805.04
Head Ax (g)	326.61	43.09	193.85	45.31
Head Az (g)	42.38	10.17	79.48	23.44
Head Ry (deg/s)	-1354.14	6.42	-1146.64	1.28
*Head RotY (deg)**	-40.57	7.65	-24.66	6.01
*Head DX (mm)**	-224.3	3.25	-151.98	8.93
*Head DZ (mm)**	-48.33	28.72	-168.58	26.65
BrIC	0.43	0.01	0.67	0.53
Upper Neck Fx (N)	-538.08	147.26	-1792.7	147.77
Upper Neck Fz (N)	-3137.23	670.4	-3235.79	1168
Upper Neck My (Nm)	42.29	7.98	-79.69	28.93
T1 Ax (g)	326.61	43.09	126.75	15.81
T1 Az (g)	*Sensor Failed in First Test*		29.63	17.68
T8 Ax (g)	149.39	6.72	70.94	6.56
T8 Az (g)	66.94	27.34	55.38	8.74
T12 Ax (g)	126.44	2.97	75.88	2.54
T12 Az (g)	62.06	30.67	45.52	2.95
T12 Ry (deg/s)	-485.19	15.3	-497.93	91.76
Chest Resultant Deflection (Internal IR-TRACC) (mm)	48.88	0.01	29.38	2.34
Pelvis Ax (g)	130.1	0.87	90.88	2.55
Pelvis Az (g)	37.59	6.65	48.91	6.77
Pelvis Ry (deg/s)	-1824.49	220.06	-1403.54	41.5
*Pelvis RotY (deg)**	-20.23	3.73	-14.65	1.64
*Pelvis DX (mm)**	-144.28	18.23	-212.3	28.17
*Pelvis DZ (mm)**	-89.8	5.72	-151.3	0.46
Left Acetabulum FR (N)	5690.51	478.96	5737.11	458.81
Right Acetabulum FR (N)	5503.6	98.48	5667.44	348.1
Left Femur Compressive Fz (N)	1435.06	90.45	1767	436.55
Right Femur Compressive Fz (N)	1442.94	124.84	1694.94	67.69
LL Tibia Fx (N)	*Data Only Available for Second Test*		-865.72	21.1
RL Tibia Fx (N)			-1170.52	319.23
LU Tibia Compressive Fz (N)			784.75	301.7
RU Tibia Compressive Fz (N)			834.72	91.03
LL Tibia Compressive Fz (N)			807.59	61.34
RL Tibia Compressive Fz (N)			850.3	169.6
Head Restraint Fx (N)	-11570.63	11.31	-9371	2171.05
Head Restraint Fz (N)	-2942.88	104.67	-2581.95	11.13
Head Restraint My (Nm)	-357.36	146.1	-255.85	149.02
Seatback Top Fx	-14999.43	53.45	*Sensor Failed in First Test*	
Seatback Middle Fx	-6976.81	69.73	-5376.33	564.45
Seatback Bottom Fx	-16526.98	1169.69	*Sensor Failed in Second Test*	
Lap Belt (N)	867.65	201.13	1293.3	170.59
Shoulder Belt (N)	2196.56	498.51	*Sensor Failed in Second Test*	

**Denotes Global Measurement.*

Appendix C: BioRank Data

TABLE CI

SEAT LOADING BRS SCORES AND DPS FOR 25° ABTS TESTS

Location	*Measure*	*Test ID*	*BRS Score (Unshifted)*	*BRS Score*	*DPS (ms)*	*Alignment Method*	*Mean BRS Score (Unshifted)*	*Mean BRS Score*	*Mean |DPS| (ms)*
Head Restraint	*Fx*	*S220425-1*	5.28	2.41	2.2	MinDCAD	6.12	2.64	3
		S220426-1	6.37	2.50	2.9	MinDCAD			
		S220427-1	6.71	3.01	2.8	MinDCAD			
	Fz	*S220425-1*	*PMHS Corridor Data Not Available*						
		S220426-1							
		S220427-1							
	My	*S220425-1*	2.55	2.07	3.0	MinDCAD	2.68	2.07	3
		S220426-1	2.71	2.05	3.8	MinDCAD			
		S220427-1	2.77	2.09	3.6	MinDCAD			
Head Restraint Region Averages							**4.40**	**2.35**	**3**
Seatback Top	*Fx*	*S220425-1*	2.49	2.41	1.1	MinDCAD	2.27	2.12	1
		S220426-1	2.18	1.98	1.5	MinDCAD			
		S220427-1	2.13	1.96	1.6	MinDCAD			
Seatback Top Region Averages							**2.27**	**2.12**	1
Seatback Middle	*Fx*	*S220425-1*	0.69	0.67	0.2	MinDCAD	0.78	0.76	0*
		S220426-1	0.91	0.88	0.5	MinDCAD			
		S220427-1	0.75	0.73	0.4	MinDCAD			
Seatback Middle Region Averages							**0.78**	**0.76**	**0***
Seatback Bottom	*Fx*	*S220425-1*	*PMHS Corridor Data Not Available*						
		S220426-1							
		S220427-1							
Seatback Bottom Region Averages (Not Available)									
Belt Tensions	*Lap*	*S220425-1*	6.82	4.69	-59.2	MinDCAD	7.09	3.76	57
		S220426-1	6.87	3.86	-56.4	MinDCAD			
		S220427-1	7.58	2.72	-56.6	MinDCAD			
	Shoulder	*S220425-1*	2.10	0.97	-43.7	MinDCAD	2.11	0.82	43
		S220426-1	2.10	0.56	-43.0	MinDCAD			
		S220427-1	2.12	0.94	-41.8	MinDCAD			
Seatbelt Region Averages							**4.60**	**2.29**	**50**
Overall Seat Loading Averages							**3.01**	**1.88**	**13**

** Slight Shift (<0.5 ms)*

TABLE CII

SEAT LOADING BRS SCORES AND DPS FOR 25° FDR TESTS

Location	*Measure*	*Test ID*	*BRS Score (Unshifted)*	*BRS Score*	*DPS (ms)*	*Alignment Method*	*Mean BRS Score (Unshifted)*	*Mean BRS Score*	*Mean |DPS| (ms)*
Head Restraint	*Fx*	*S211209-1*	2.56	2.23	-0.8	MinDCAD	2.30	2.11	1
		S220504-2	2.05	1.99	0.3	MinDCAD			
	Fz	*S211209-1*	4.61	4.23	3.1	Negative Peaks	4.67	4.29	3
		S220504-2	4.73	4.35	3.0	Negative Peaks			
	My	*S211209-1*	2.10	1.86	-2.0	MinDCAD	2.10	1.93	2
		S220504-2	2.11	2.01	-1.1	MinDCAD			
Head Restraint Region Averages							**3.02**	**2.78**	**2**
Seatback Top	*Fx*	*S211209-1*	2.59	2.58	0.2	MinDCAD	2.41	2.34	0*
		S220504-2	2.23	2.10	0.5	MinDCAD			
Seatback Top Region Averages							**2.41**	**2.34**	**0***
Seatback Middle	*Fx*	*S211209-1*	1.83	1.83	0.0	Unshifted	1.61	1.61	0
		S220504-2	1.40	1.40	0.0	Unshifted			
Seatback Middle Region Averages							**1.61**	**1.61**	**0**
Seatback Bottom	*Fx*	*S211209-1*	*PMHS Corridor Data Not Available*						
		S220504-2							
Seatback Bottom Region Averages (Not Available)									
Belt Tensions	*Lap*	*S211209-1*	4.06	2.49	-21.7	MinDCAD	4.38	2.65	27
		S220504-2	4.70	2.81	-33.2	MinDCAD			
	Shoulder	*S211209-1*	*PMHS Corridor Data Not Available*						
		S220504-2							
Seatbelt Region Averages							**4.38**	**2.65**	**27**
Overall Seat Loading Averages							**2.80**	**2.27**	**8**

** Slight Shift (<0.5 ms)*

TABLE CIII

OCCUPANT RESPONSE BRS SCORES AND DPS FOR 25° ABTS TESTS

Location	*Measure*	*Test ID*	*BRS Score (Unshifted)*	*BRS Score*	*DPS (ms)*	*Alignment Method*	*Mean BRS Score (Unshifted)*	*Mean BRS Score*	*Mean |DPS| (ms)*
Head	*Ax*	*S220425-1*	2.68	1.15	1.4	MinDCAD	3.66	1.42	2
		S220426-1	4.03	1.42	2.1	MinDCAD			
		S220427-1	4.26	1.70	2.0	MinDCAD			
	Az	*S220425-1*	2.13	1.78	3.4	MinDCAD 0-45 ms	2.16	1.80	4
		S220426-1	2.16	1.77	3.6	MinDCAD 0-45 ms			
		S220427-1	2.19	1.85	3.7	MinDCAD 0-45 ms			
	Wy	*S220425-1*	2.29	2.29	0.0	Unshifted	2.04	2.04	0
		S220426-1	1.82	1.82	0.0	Unshifted			
		S220427-1	2.01	2.01	0.0	Unshifted			
	DX	*S220425-1*	2.25	2.25	0.0	Unshifted	1.11	1.11	0
		S220426-1	0.44	0.44	0.0	Unshifted			
		S220427-1	0.64	0.64	0.0	Unshifted			
	DZ	*S220425-1*	23.38	23.38	0.0	Unshifted	22.82	22.82	0
		S220426-1	21.82	21.82	0.0	Unshifted			
		S220427-1	23.28	23.28	0.0	Unshifted			
	RotY	*S220425-1*	3.38	3.20	3.5	Positive Peaks	2.44	2.34	2
		S220426-1	2.04	1.98	1.7	Positive Peaks			
		S220427-1	1.90	1.84	1.9	Positive Peaks			
		Head Region Averages					**5.71**	**5.26**	**1**
T1	*Ax*	*S220425-1*	2.47	1.68	5.0	MinDCAD	2.56	1.68	5
		S220426-1	2.62	1.73	5.4	MinDCAD			
		S220427-1	2.60	1.64	5.6	MinDCAD			
	Az	*S220425-1*	1.74	**1.73**	**1.6**	Positive Peaks	1.74	1.73	2
		S220426-1	1.75	**1.73**	**2.6**	Positive Peaks			
		S220427-1	1.73	**1.73**	**2.0**	Positive Peaks			
T8	*Ax*	*S220425-1*	1.06	**1.05**	**-0.7**	MinDCAD	1.03	1.01	1
		S220426-1	0.96	**0.95**	**-0.4**	MinDCAD			
		S220427-1	1.06	**1.03**	**-0.8**	MinDCAD			
	Az	*S220425-1*	1.30	1.24	-1.7	MinDCAD	1.26	1.23	2
		S220426-1	1.26	1.24	-1.5	MinDCAD			
		S220427-1	1.21	1.20	-1.6	MinDCAD			
T12	*Ax*	*S220425-1*	1.38	1.17	1.7	MinDCAD	1.49	1.23	2
		S220426-1	1.55	1.24	2.2	MinDCAD			
		S220427-1	1.53	1.27	1.9	MinDCAD			
	Az	*S220425-1*	1.86	**1.65**	**-2.9**	MinDCAD	1.85	1.71	2
		S220426-1	1.85	**1.74**	**-2.4**	MinDCAD			
		S220427-1	1.83	**1.74**	**-1.9**	MinDCAD			
	Wy	*S220425-1*	1.14	1.06	4.4	MinDCAD	1.11	0.98	4
		S220426-1	1.05	0.90	3.6	MinDCAD			
		S220427-1	1.14	0.97	4.2	MinDCAD			
		Spine Region Averages					**1.58**	**1.37**	**3**
Thorax	*Sternum Half Deflection*	*S220425-1*	0.94	0.91	1.9	MinDCAD	1.04	1.02	1
		S220426-1	1.06	1.06	-0.3	MinDCAD			
		S220427-1	1.11	1.10	0.8	MinDCAD			
		Thorax Region Averages					**1.04**	**1.02**	**1**
Pelvis	*Ax*	*S220425-1*	1.19	1.16	-0.4	MinDCAD	1.16	1.14	0
		S220426-1	1.15	1.15	-0.1	MinDCAD			
		S220427-1	1.13	1.12	-0.3	MinDCAD			
	Az	*S220425-1*	0.96	0.96	0.0	Unshifted	0.95	0.95	0
		S220426-1	0.98	0.98	0.0	Unshifted			
		S220427-1	0.91	0.91	0.0	Unshifted			
	Wy	*S220425-1*	2.43	2.35	1.1	Negative Peaks	2.47	2.37	1
		S220426-1	2.40	2.28	1.6	Negative Peaks			
		S220427-1	2.59	2.46	1.4	Negative Peaks			
	DX	*S220425-1*	0.33	0.33	0.3	MinDCAD	0.54	0.53	0
		S220426-1	0.89	0.89	0.4	MinDCAD			
		S220427-1	0.38	0.37	0.4	MinDCAD			
	DZ	*S220425-1*	0.94	0.94	0.0	Unshifted	0.96	0.96	0
		S220426-1	0.81	0.81	0.0	Unshifted			
		S220427-1	1.12	1.12	0.0	Unshifted			
	RotY	*S220425-1*	1.72	1.72	0.0	Unshifted	1.71	1.71	0
		S220426-1	1.67	1.67	0.0	Unshifted			

Location	Measure	Test ID	BRS Score (Unshifted)	BRS Score	DPS (ms)	Alignment Method	Mean BRS Score (Unshifted)	Mean BRS Score	Mean |DPS| (ms)
		S220427-1	1.73	1.73	0.0	Unshifted			
		Pelvis Region Averages					**1.30**	**1.28**	**0**
		Overall Occupant Response Averages					**2.40**	**2.23**	**1**

TABLE CIV

OCCUPANT RESPONSE BRS SCORES AND DPS FOR 25° FDR TESTS

Location	*Measure*	*Test ID*	*BRS Score (Unshifted)*	*BRS Score*	*DPS (ms)*	*Alignment Method*	*Mean BRS Score (Unshifted)*	*Mean BRS Score*	*Mean |DPS| (ms)*
Head	*Ax*	*S211209-1*	1.62	0.93	-1.3	MinDCAD	1.30	0.96	1
		S220504-2	0.98	0.98	0.0	MinDCAD			
	Az	*S211209-1*	1.53	1.53	-0.3	MinDCAD	1.53	1.52	1
		S220504-2	1.53	1.51	0.9	MinDCAD			
	Wy	*S211209-1*	1.75	1.55	-2.5	Positive Peaks	1.83	1.65	2
		S220504-2	1.91	1.76	-2.1	Positive Peaks			
	DX	*S211209-1*	0.51	0.51	0.0	Unshifted	0.52	0.52	0
		S220504-2	0.54	0.54	0.0	Unshifted			
	DZ	*S211209-1*	1.57	1.57	0.0	Unshifted	2.38	2.38	0
		S220504-2	3.18	3.18	0.0	Unshifted			
	RotY	*S211209-1*	0.66	0.65	-0.9	MinDCAD 0-50 ms	0.72	0.71	1
		S220504-2	0.77	0.76	-1.6	MinDCAD 0-50 ms			
		Head Region Averages					**1.38**	**1.29**	**1**
T1	*Ax*	*S211209-1*	2.14	1.38	2.7	MinDCAD	2.23	1.39	3
		S220504-2	2.33	1.41	3.2	MinDCAD			
	Az	*S211209-1*	*Sensor Issue During Test*				1.03	0.95	2
		S220504-2	1.03	0.95	-1.9	MinDCAD			
T8	*Ax*	*S211209-1*	2.29	1.77	-1.9	MinDCAD	2.19	1.63	2
		S220504-2	2.10	1.50	-1.9	MinDCAD			
	Az	*S211209-1*	2.00	1.77	-2.8	MinDCAD	2.10	1.91	2
		S220504-2	2.19	2.05	-2.1	MinDCAD			
T12	*Ax*	*S211209-1*	3.20	2.30	-2.3	MinDCAD	3.23	2.25	3
		S220504-2	3.26	2.20	-2.8	MinDCAD			
	Az	*S211209-1*	2.64	1.73	-8.9	MinDCAD	2.65	1.80	9
		S220504-2	2.66	1.87	-8.3	MinDCAD			
	Wy	*S211209-1*	1.12	1.06	-1.4	Positive Peaks	1.17	1.14	1
		S220504-2	1.23	1.21	-0.3	Positive Peaks			
		Spine Region Averages					**2.09**	**1.58**	**3**
Thorax	*Sternum Half Deflection*	*S211209-1*	1.43	1.41	-0.6	MinDCAD	1.53	1.51	1
		S220504-2	1.63	1.61	1.9	MinDCAD			
		Thorax Region Averages					**1.53**	**1.51**	**1**
Pelvis	*Ax*	*S211209-1*	0.87	0.87	0.0	MinDCAD	0.99	0.87	1
		S220504-2	1.10	0.86	-1.9	MinDCAD			
	Az	*S211209-1*	0.96	0.73	-3.8	MinDCAD	0.93	0.75	5
		S220504-2	0.89	0.77	-6.1	MinDCAD			
	Wy	*S211209-1*	2.06	1.84	-2.7	MinDCAD	2.48	2.16	4
		S220504-2	2.91	2.49	-5.0	MinDCAD			
	DX	*S211209-1*	2.10	2.09	0.2	MinDCAD	3.20	3.16	1
		S220504-2	4.31	4.24	1.1	MinDCAD			
	DZ	*S211209-1*	0.94	0.86	3.4	MinDCAD	0.86	0.81	2
		S220504-2	0.78	0.76	-0.9	MinDCAD			
	RotY	*S211209-1*	3.07	2.98	-2.3	Negative Peaks	3.73	3.66	4
		S220504-2	4.39	4.33	-5.0	Negative Peaks			
		Pelvis Region Averages					**2.03**	**1.90**	**3**
		Overall Occupant Response Averages					**1.76**	**1.57**	**2**

TABLE CV

SEAT LOADING BRS SCORES AND DPS FOR 45° ABTS TESTS

Location	*Measure*	*Test ID*	*BRS Score (Unshifted)*	*BRS Score*	*DPS (ms)*	*Alignment Method*	*Mean BRS Score (Unshifted)*	*Mean BRS Score*	*Mean |DPS| (ms)*
Head Restraint	Fx	S220428-1	2.53	2.01	-2.5	MinDCAD	2.51	2.03	2
		S220502-1	2.45	1.95	-2.6	MinDCAD			
		S220502-2	2.56	2.13	-2.4	MinDCAD			
	Fz	S220428-1	3.41	2.73	7.1	Negative Peaks	3.53	2.86	7
		S220502-1	3.53	2.87	6.9	Negative Peaks			
		S220502-2	3.63	2.97	7.0	Negative Peaks			
	My	S220428-1	1.61	1.61	0.0	Unshifted	1.64	1.64	0
		S220502-1	1.65	1.65	0.0	Unshifted			
		S220502-2	1.65	1.65	0.0	Unshifted			
Head Restraint Region Averages							**2.56**	**2.18**	**3**
Seatback Top	Fx	S220428-1	1.85	1.74	-1.3	MinDCAD	1.73	1.62	1
		S220502-1	1.74	1.52	-1.7	MinDCAD			
		S220502-2	1.61	1.61	0.1	MinDCAD			
Seatback Top Region Averages							**1.73**	**1.62**	**1**
Seatback Middle	Fx	S220428-1	2.35	1.58	-2.4	MinDCAD	2.10	1.40	2
		S220502-1	2.19	1.50	-2.4	MinDCAD			
		S220502-2	1.77	1.12	-1.6	MinDCAD			
Seatback Middle Region Averages							**2.10**	**1.40**	**2**
Seatback Bottom	Fx	S220428-1	3.46	3.09	-1.3	MinDCAD	2.63	2.39	1
		S220502-1	2.38	2.10	-0.9	MinDCAD			
		S220502-2	2.06	1.98	-0.4	MinDCAD			
Seatback Bottom Region Averages (Not Available)							**2.63**	**2.39**	**1**
Belt Tensions	Lap	S220428-1	4.88	0.83	-74.6	MinDCAD	4.78	0.83	72
		S220502-1	4.87	0.83	-71.4	MinDCAD			
		S220502-2	4.59	0.83	-68.8	MinDCAD			
	Shoulder	S220428-1	1.53	1.48	-56.0	MinDCAD 0-70 ms	1.57	1.58	58
		S220502-1	1.58	1.78	-54.4	MinDCAD 0-70 ms			
		S220502-2	1.59	1.50	-62.7	MinDCAD 0-70 ms			
Seatbelt Region Averages							**3.17**	**1.21**	**65**
Overall Seat Loading Averages							**2.44**	**1.76**	**14**

TABLE CVI

SEAT LOADING BRS SCORES AND DPS FOR 45° FDR TESTS

Location	*Measure*	*Test ID*	*BRS Score (Unshifted)*	*BRS Score*	*DPS (ms)*	*Alignment Method*	*Mean BRS Score (Unshifted)*	*Mean BRS Score*	*Mean |DPS| (ms)*
Head Restraint	Fx	S220104-1	4.37	3.81	-3.0	MinDCAD	4.12	3.73	2
		S220104-2	3.86	3.64	-1.6	MinDCAD			
	Fz	S220104-3	2.99	2.23	7.7	MinDCAD	3.32	2.55	8
		S220104-4	3.65	2.87	9.1	MinDCAD			
	My	S220104-5	2.46	2.46	0.0	Unshifted	2.39	2.40	0
		S220104-6	2.33	2.33	0.0	Unshifted			
Head Restraint Region Averages							**3.28**	**2.89**	**4**
Seatback Top	Fx	S220104-1	*Sensor Issue During Test*				3.38	3.35	2
		S220509-1	3.38	3.35	-2.4	MinDCAD			
Seatback Top Region Averages							**3.38**	**3.35**	**1**
Seatback Middle	Fx	S220104-1	1.00	0.63	-1.4	Negative Peaks	1.12	0.86	1
		S220509-1	1.24	1.08	-0.8	Negative Peaks			
Seatback Middle Region Averages							**1.12**	**0.86**	**1**
Seatback Bottom	Fx	S220104-1	8.23	8.18	1.9	MinDCAD	8.23	8.18	2
		S220509-1	*Sensor Issue During Test*						
Seatback Bottom Region Averages							**8.23**	**8.18**	**2**
Belt Tensions	Lap	S220104-1	2.52	2.49	-1.9	MinDCAD	2.58	2.31	4
		S220509-1	2.64	2.13	-6.3	MinDCAD			
	Shoulder	S220104-1	0.77	0.77	0.0	Unshifted	0.77	0.77	0
		S220509-1	*Sensor Issue During Test*						
Seatbelt Region Averages							**2.14**	**1.88**	**2**
Overall Seat Loading Averages							**3.58**	**3.43**	**3**

TABLE CVII

OCCUPANT RESPONSE BRS SCORES AND DPS FOR 45° ABTS TESTS

Location	*Measure*	*Test ID*	*BRS Score (Unshifted)*	*BRS Score*	*DPS (ms)*	*Alignment Method*	*Mean BRS Score (Unshifted)*	*Mean BRS Score*	*Mean |DPS| (ms)*
		S220428-1	3.06	1.18	-4.2	MinDCAD			
	Ax	*S220502-1*	3.11	1.23	-4.1	MinDCAD	3.06	1.23	4
		S220502-2	3.01	1.28	-3.9	MinDCAD			
		S220428-1	1.71	1.59	-1.6	MinDCAD			
	Az	*S220502-1*	1.90	1.76	-1.7	MinDCAD	1.80	1.68	2
		S220502-2	1.78	1.68	-1.5	MinDCAD			
		S220428-1	1.39	1.41	2.7	Positive Peaks			
	Wy	*S220502-1*	1.42	1.41	3.2	Positive Peaks	1.45	1.44	3
		S220502-2	1.53	1.51	2.9	Positive Peaks			
Head		*S220428-1*	0.41	0.41	0.0	Unshifted			
	DX	*S220502-1*	0.49	0.49	0.0	Unshifted	0.55	0.55	0
		S220502-2	0.75	0.75	0.0	Unshifted			
		S220428-1	2.65	2.80	-5.1	MinDCAD 0-50 ms			
	DZ	*S220502-1*	3.35	3.57	-5.8	MinDCAD 0-50 ms	2.83	2.99	5
		S220502-2	2.51	2.61	-4.4	MinDCAD 0-50 ms			
		S220428-1	0.73	0.73	0.0	Unshifted			
	RotY	*S220502-1*	0.79	0.79	0.0	Unshifted	0.75	0.75	0
		S220502-2	0.73	0.73	0.0	Unshifted			
		Head Region Averages					**1.74**	**1.44**	**2**
		S220428-1	1.37	1.33	-0.7	MinDCAD			
	Ax	*S220502-1*	1.33	1.32	-0.3	MinDCAD	1.35	1.34	0*
		S220502-2	1.35	1.35	-0.3	MinDCAD			
T1		*S220428-1*	1.60	1.60	0.0	Unshifted			
	Az	*S220502-1*	1.72	1.72	0.0	Unshifted	1.65	1.65	0
		S220502-2	1.64	1.64	0.0	Unshifted			
		S220428-1	1.48	1.04	-2.5	MinDCAD			
	Ax	*S220502-1*	1.53	1.11	-2.5	MinDCAD	1.41	1.04	2
		S220502-2	1.21	0.98	-1.9	MinDCAD			
T8		*S220428-1*	1.71	1.46	-3.7	MinDCAD			
	Az	*S220502-1*	1.89	1.60	-3.5	MinDCAD	1.77	1.52	3
		S220502-2	1.71	1.51	-2.8	MinDCAD			
		S220428-1	2.46	1.92	-3.4	MinDCAD			
	Ax	*S220502-1*	2.46	1.94	-2.8	MinDCAD	2.36	1.94	3
		S220502-2	2.16	1.96	-1.7	MinDCAD			
		S220428-1	1.72	1.34	-6.8	MinDCAD			
T12	*Az*	*S220502-1*	1.89	1.42	-6.7	MinDCAD	1.77	1.35	6
		S220502-2	1.69	1.29	-5.9	MinDCAD			
		S220428-1	1.03	0.99	2.1	Positive Peaks			
	Wy	*S220502-1*	1.04	1.01	1.2	Positive Peaks	1.05	1.01	2
		S220502-2	1.09	1.03	1.8	Positive Peaks			
		Spine Region Averages					**1.62**	**1.41**	**2**
	Sternum	*S220428-1*	1.31	1.31	0.0	Unshifted			
Thorax	*Half*	*S220502-1*	1.50	1.50	0.0	Unshifted	1.27	1.27	0
	Deflection	*S220502-2*	0.98	0.98	0.0	Unshifted			
		Thorax Region Averages					**1.27**	**1.27**	**0**
		S220428-1	1.91	0.87	-5.8	MinDCAD			
	Ax	*S220502-1*	1.98	0.91	-5.9	MinDCAD	1.88	0.89	6
		S220502-2	1.75	0.88	-5.2	MinDCAD			
		S220428-1	1.16	1.16	0.0	Unshifted			
	Az	*S220502-1*	1.18	1.18	0.0	Unshifted	1.18	1.18	0
		S220502-2	1.20	1.20	0.0	Unshifted			
		S220428-1	1.63	1.26	-3.6	MinDCAD			
Pelvis	*Wy*	*S220502-1*	1.81	1.37	-4.1	MinDCAD	1.72	1.34	4
		S220502-2	1.72	1.39	-3.3	MinDCAD			
		S220428-1	0.81	0.81	0.0	Unshifted			
	DX	*S220502-1*	1.01	0.99	1.3	MinDCAD	0.94	0.92	1
		S220502-2	1.00	0.97	1.9	MinDCAD			
		S220428-1	1.56	1.56	0.0	Unshifted			
	DZ	*S220502-1*	1.63	1.63	0.0	Unshifted	1.62	1.62	0
		S220502-2	1.67	1.67	0.0	Unshifted			
	RotY	*S220428-1*	1.26	1.23	-1.8	MinDCAD	1.49	1.47	1

		S220502-1	1.55	1.53	-1.8	MinDCAD			
		S220502-2	1.66	1.66	-0.8	MinDCAD			
Pelvis Region Averages							**1.47**	**1.24**	**2**
Overall Occupant Response Averages							**1.53**	**1.34**	**2**

** Slight Shift (<0.5 ms)*

TABLE CVIII

OCCUPANT RESPONSE BRS SCORES AND DPS FOR 45° FDR TESTS

Location	*Measure*	*Test ID*	*BRS Score (Unshifted)*	*BRS Score*	*DPS (ms)*	*Alignment Method*	*Mean BRS Score (Unshifted)*	*Mean BRS Score*	*Mean |DPS| (ms)*
Head	Ax	S211209-1	4.02	1.72	-4.6	MinDCAD	3.47	1.44	4
		S220504-2	2.91	1.16	-3.1	MinDCAD			
	Az	S211209-1	2.08	1.91	-4.2	Positive Peaks	1.81	1.69	4
		S220504-2	1.55	1.47	-3.1	Positive Peaks			
	Wy	S211209-1	2.42	2.42	0.0	Unshifted	2.23	2.23	0
		S220504-2	2.05	2.05	0.0	Unshifted			
	DX	S211209-1	3.85	3.83	1.0	MinDCAD 0-40 ms	3.91	3.87	1
		S220504-2	3.97	3.90	1.4	MinDCAD 0-40 ms			
	DZ	S211209-1	1.53	1.39	-4.8	MinDCAD 0-40 ms	1.12	0.98	4
		S220504-2	0.71	0.56	-3.4	MinDCAD 0-40 ms			
	RotY	S211209-1	2.01	2.01	0.0	Unshifted	1.84	1.84	0
		S220504-2	1.67	1.67	0.0	Unshifted			
Head Region Averages							**2.40**	**2.01**	**2**
T1	Ax	S211209-1	1.03	0.85	-1.9	MinDCAD	1.04	0.92	2
		S220504-2	1.06	1.00	-1.2	MinDCAD			
	Az	S211209-1	0.87	0.87	0.0	Unshifted	0.83	0.83	0
		S220504-2	0.78	0.78	0.0	Unshifted			
T8	Ax	S211209-1	1.31	1.20	-2.1	MinDCAD	1.24	1.17	2
		S220504-2	1.18	1.14	-1.0	MinDCAD			
	Az	S211209-1	1.00	0.93	-3.9	MinDCAD	1.01	0.95	3
		S220504-2	1.03	0.97	-2.8	MinDCAD			
T12	Ax	S211209-1	2.01	1.43	-2.4	Positive Peaks	1.78	1.31	2
		S220504-2	1.54	1.19	-1.5	Positive Peaks			
	Az	S211209-1	1.22	0.80	-6.1	MinDCAD	1.18	0.85	5
		S220504-2	1.15	0.89	-4.9	MinDCAD			
	Wy	S211209-1	1.51	1.43	-1.7	MinDCAD 0-25 ms	1.54	1.43	3
		S220504-2	1.58	1.44	-4.1	MinDCAD 0-25 ms			
Spine Region Averages							**1.23**	**1.07**	**2**
Thorax	Sternum Half Deflection	S211209-1	*Sensor Issue During Test*				0.80	0.80	0
		S220504-2	0.80	0.80	0.0	Unshifted			
Thorax Region Averages							**0.80**	**0.80**	**0**
Pelvis	Ax	S211209-1	1.30	1.13	-3.7	MinDCAD	1.33	1.12	3
		S220504-2	1.35	1.11	-2.1	MinDCAD			
	Az	S211209-1	0.82	0.64	-4.7	MinDCAD	0.82	0.68	6
		S220504-2	0.82	0.72	-6.5	MinDCAD			
	Wy	S211209-1	2.14	1.93	-3.4	Negative Peaks	1.98	1.77	3
		S220504-2	1.82	1.6	-3.4	Negative Peaks			
	DX	S211209-1	2.33	2.31	1.0	MinDCAD	1.73	1.72	1
		S220504-2	1.14	1.12	0.8	MinDCAD			
	DZ	S211209-1	1.25	1.03	-3.9	MinDCAD	1.18	0.97	4
		S220504-2	1.10	0.91	-3.2	MinDCAD			
	RotY	S211209-1	1.29	1.28	-0.7	MinDCAD 0-40 ms	1.19	1.18	1
		S220504-2	1.10	1.09	-0.5	MinDCAD 0-40 ms			
Pelvis Region Averages							**1.37**	**1.24**	**3**
Overall Occupant Response Averages							**1.45**	**1.28**	**2**

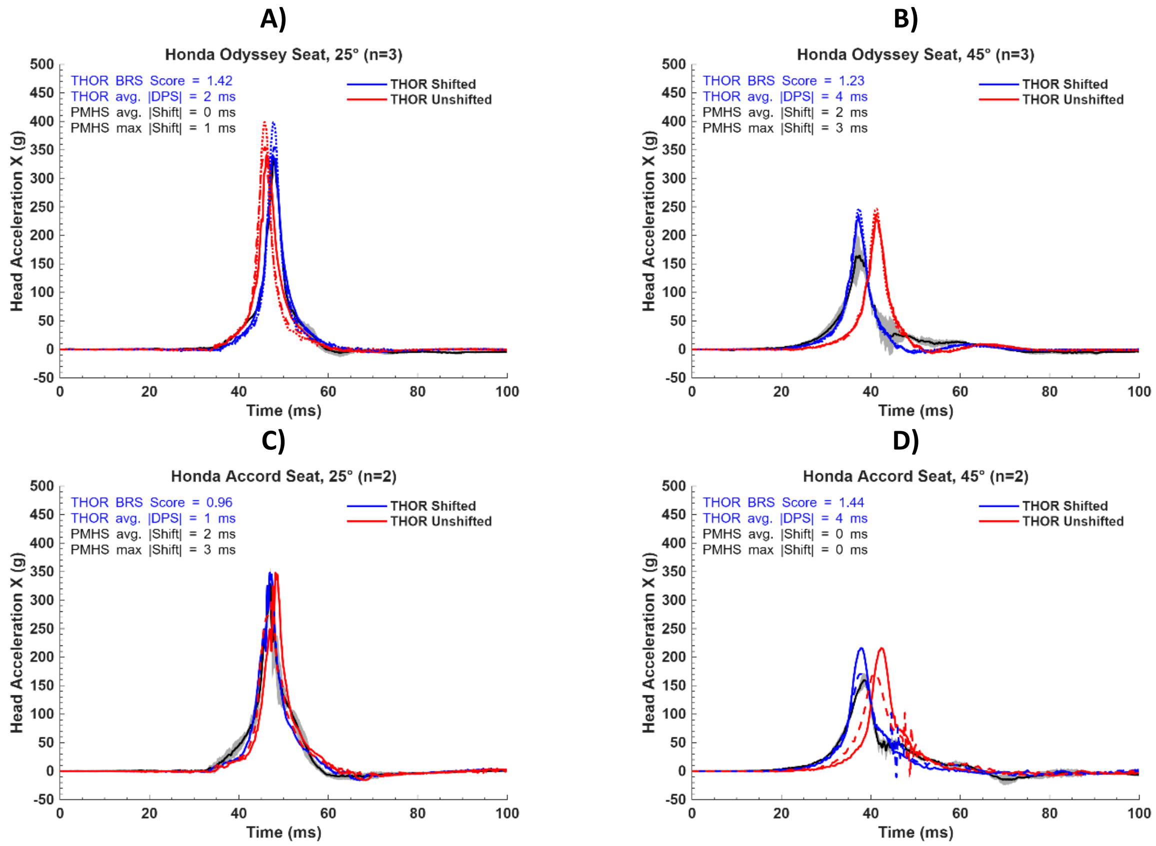

Fig. C1. Comparison of local head X-acceleration between the THOR-05F and female PMHS in four conditions: A) ABTS seat at 25° recline; B) ABTS seat at 45° recline; C) FDR seat at 25° recline; and D) FDR seat at 45° recline.

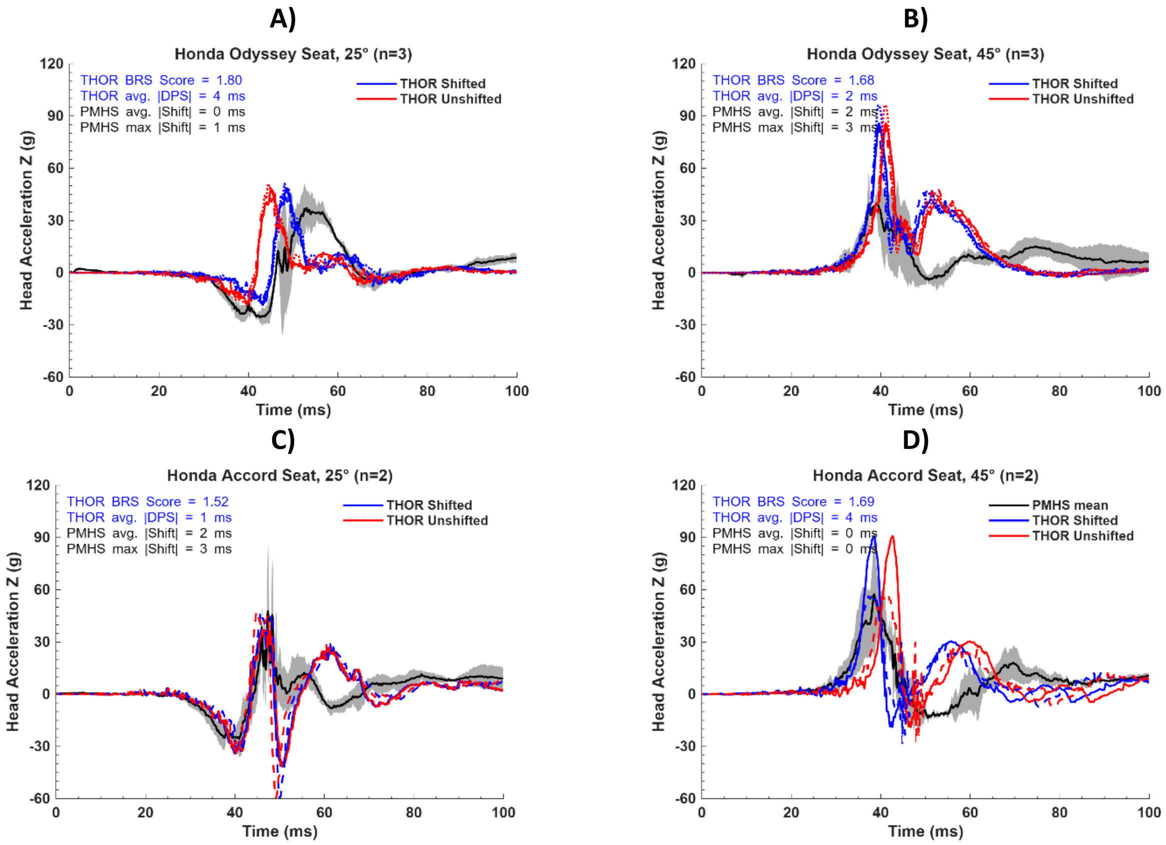

Fig. C2. Comparison of local head z-acceleration between the THOR-05F and female PMHS in four conditions: A) ABTS seat at 25° recline; B) ABTS seat at 45° recline; C) FDR seat at 25° recline; and D) FDR seat at 45° recline.

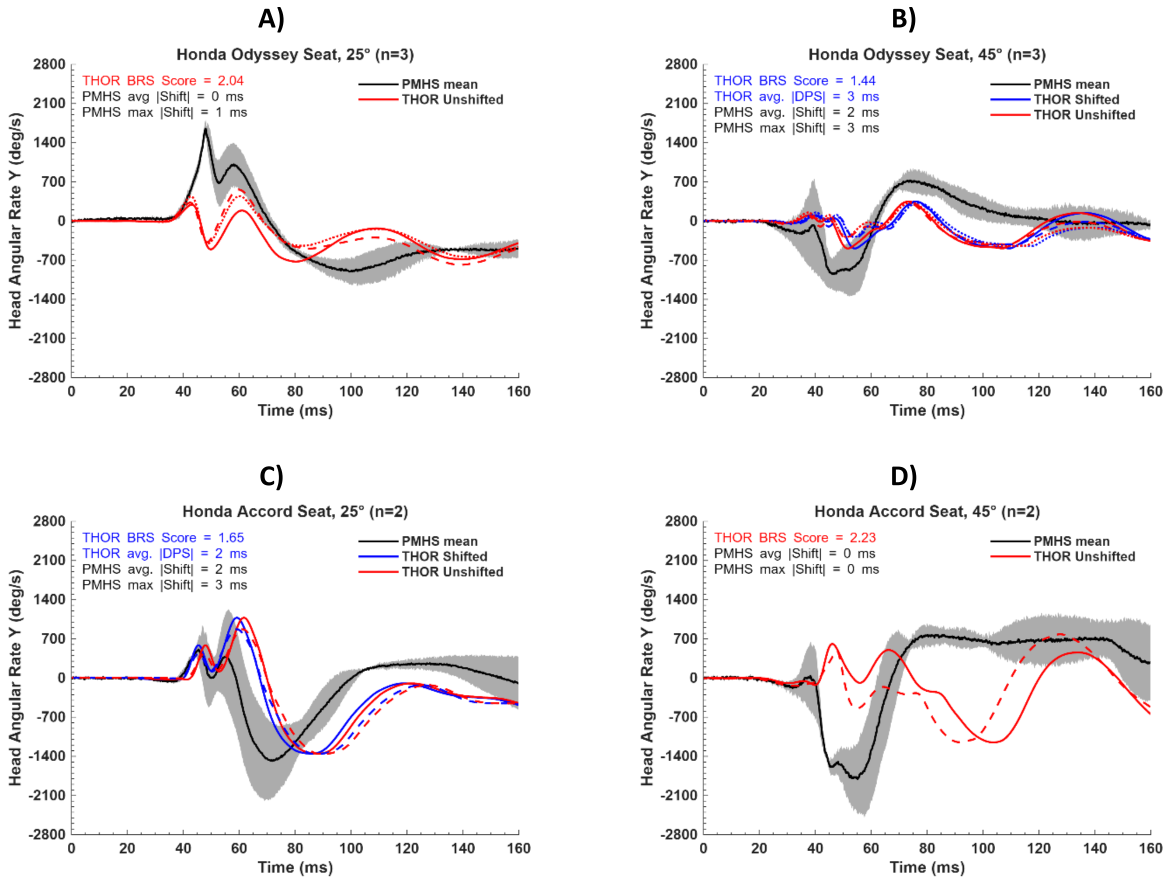

Fig. C3. Comparison of local head y-angular rate between the THOR-05F and female PMHS in four conditions: A) ABTS seat at 25° recline; B) ABTS seat at 45° recline; C) FDR seat at 25° recline; and D) FDR seat at 45° recline.

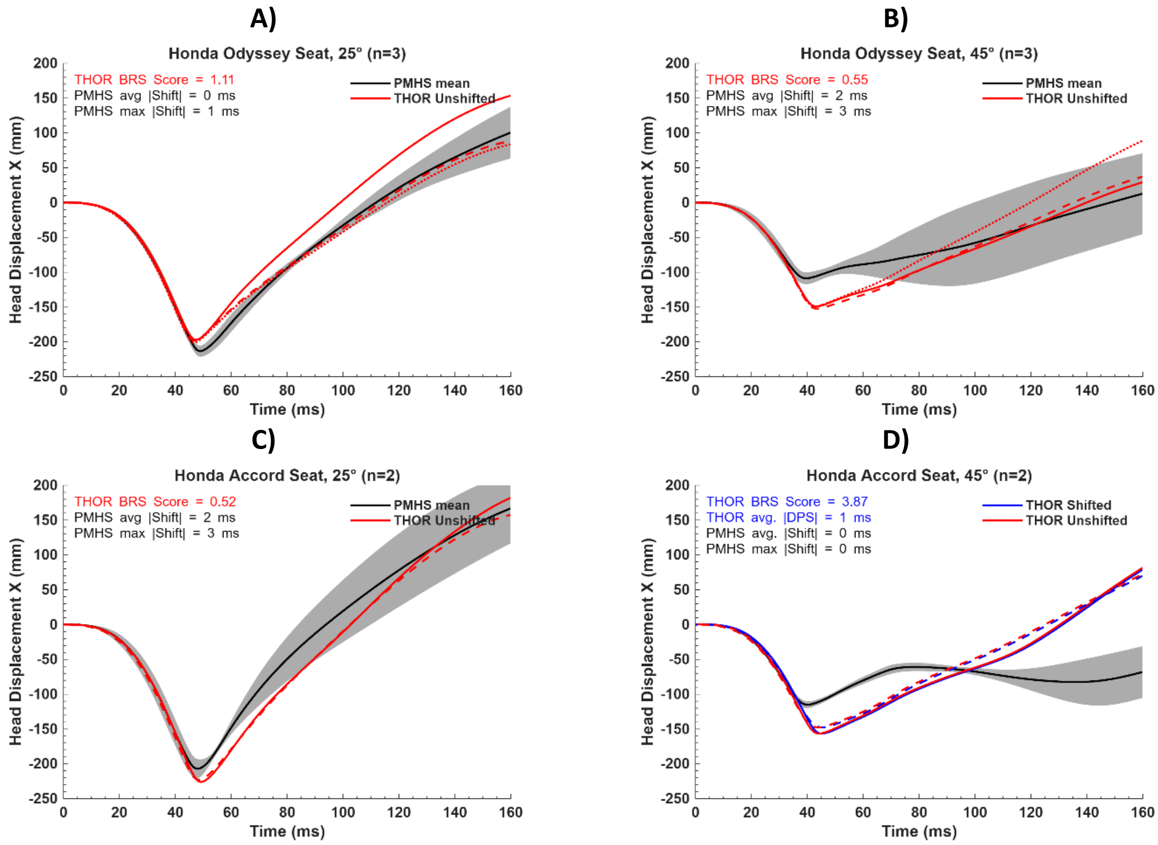

Fig. C4. Comparison of global head X-displacement between the THOR-05F and female PMHS in four conditions: A) ABTS seat at 25° recline; B) ABTS seat at 45° recline; C) FDR seat at 25° recline; and D) FDR seat at 45° recline.

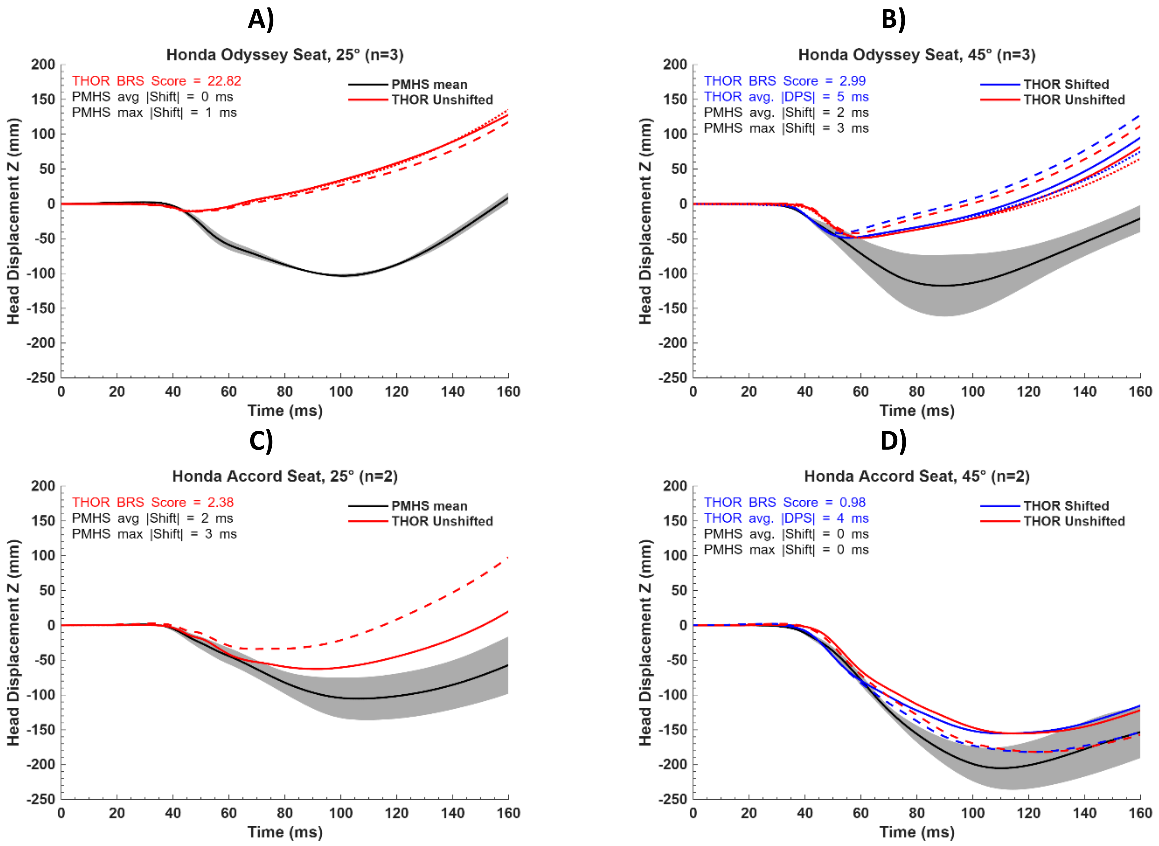

Fig. C5. Comparison of global head Z-displacement between the THOR-05F and female PMHS in four conditions: A) ABTS seat at 25° recline; B) ABTS seat at 45° recline; C) FDR seat at 25° recline; and D) FDR seat at 45° recline.

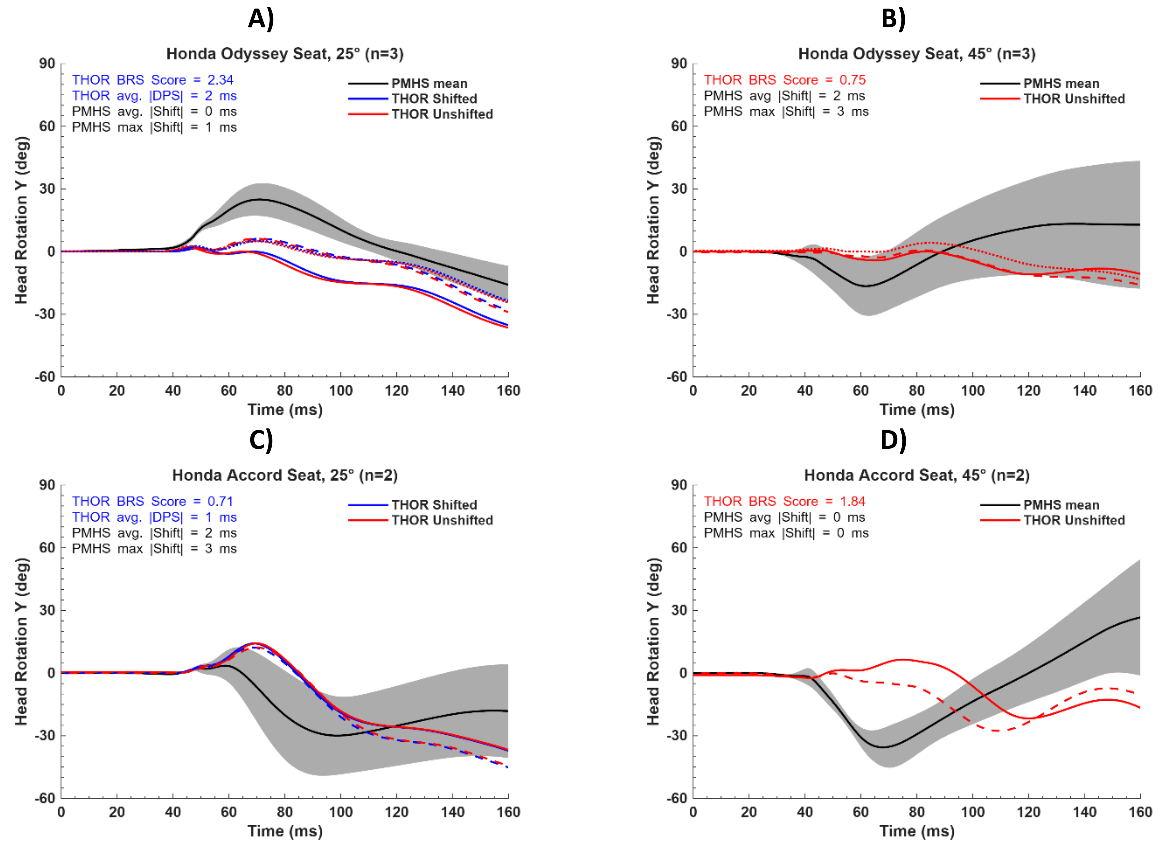

Fig. C6. Comparison of global head Y-rotation between the THOR-05F and female PMHS in four conditions: A) ABTS seat at 25° recline; B) ABTS seat at 45° recline; C) FDR seat at 25° recline; and D) FDR seat at 45° recline.

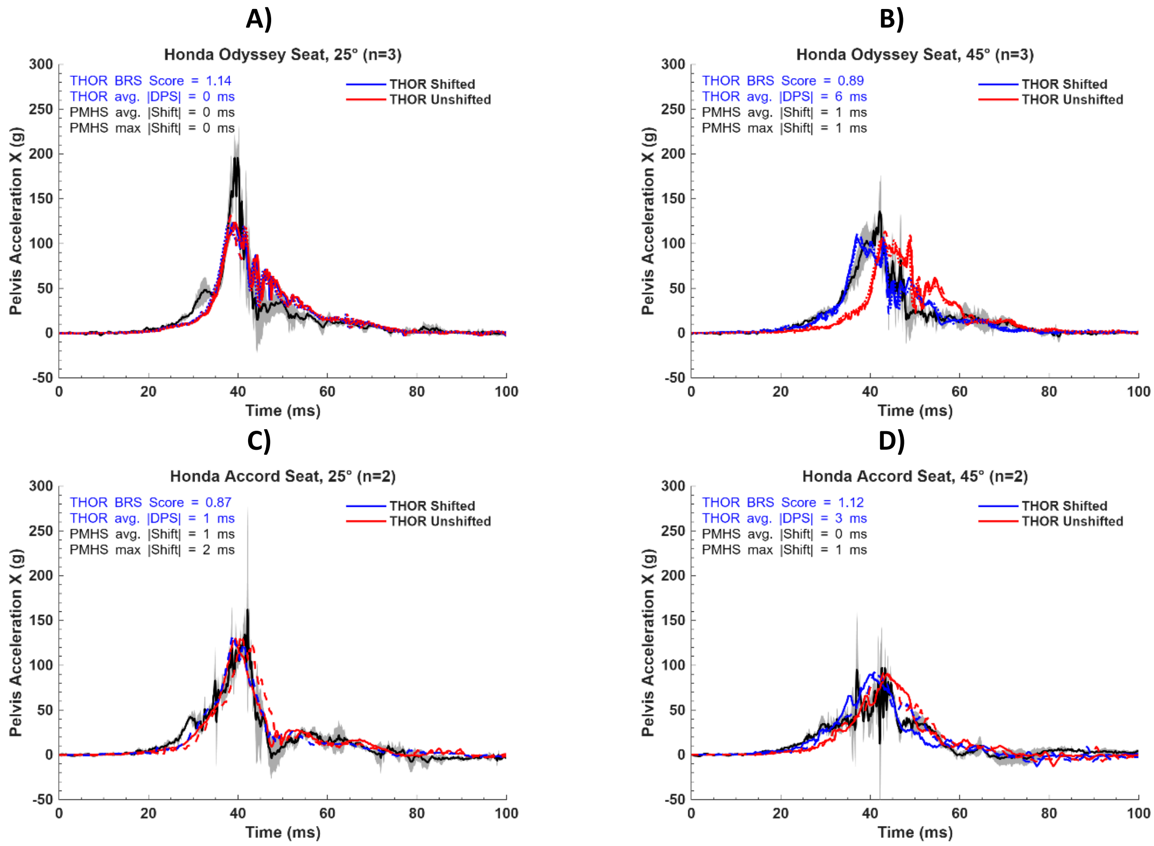

Fig. C7. Comparison of local pelvis x-acceleration between the THOR-05F and female PMHS in four conditions: A) ABTS seat at 25° recline; B) ABTS seat at 45° recline; C) FDR seat at 25° recline; and D) FDR seat at 45° recline.

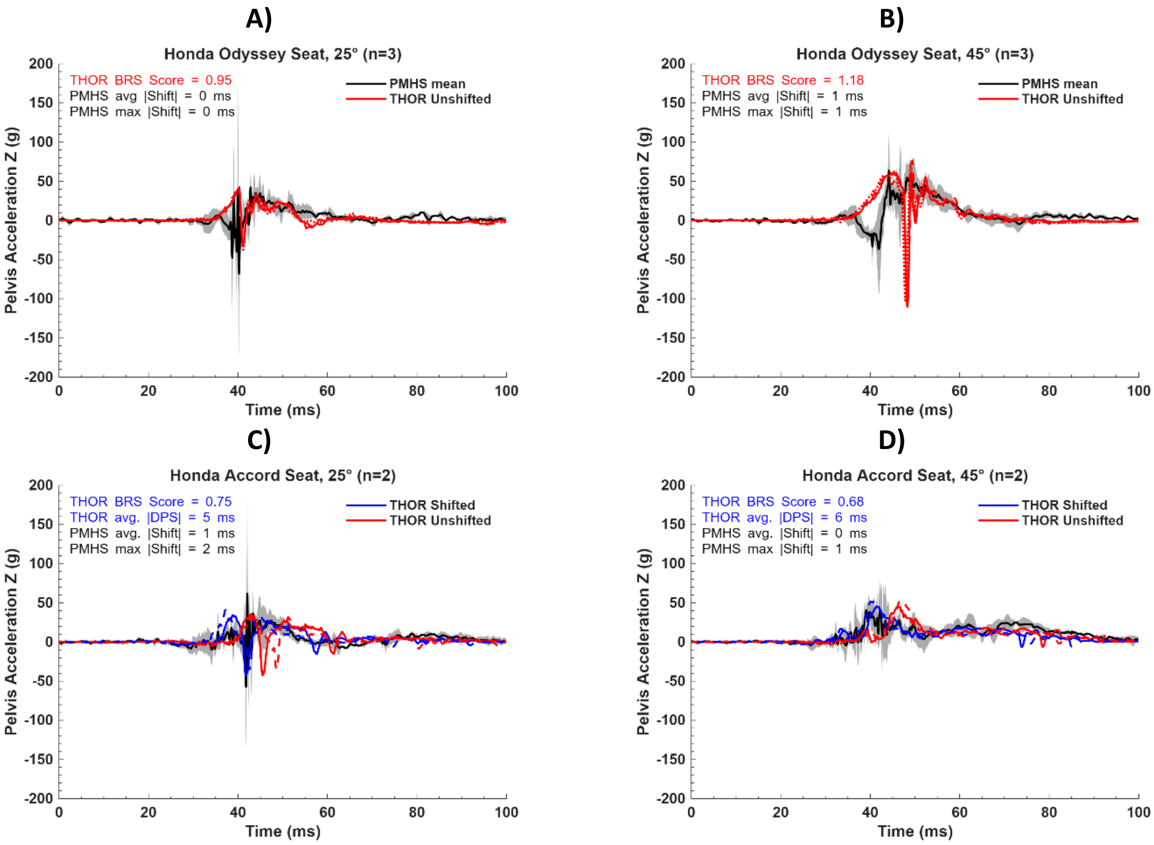

Fig. C8. Comparison of local pelvis z-acceleration between the THOR-05F and female PMHS in four conditions: A) ABTS seat at 25° recline; B) ABTS seat at 45° recline; C) FDR seat at 25° recline; and D) FDR seat at 45° recline.

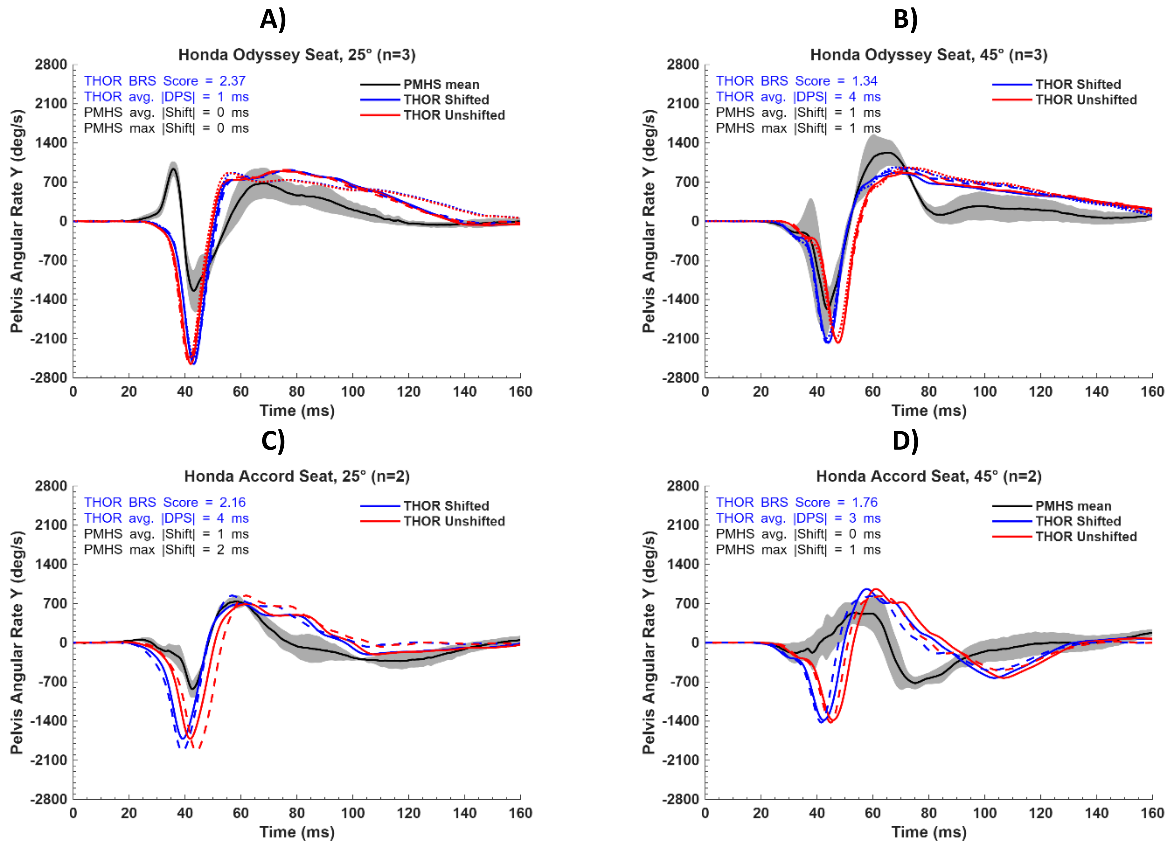

Fig. C9. Comparison of local pelvis y-angular rate between the THOR-05F and female PMHS in four conditions: A) ABTS seat at 25° recline; B) ABTS seat at 45° recline; C) FDR seat at 25° recline; and D) FDR seat at 45° recline.

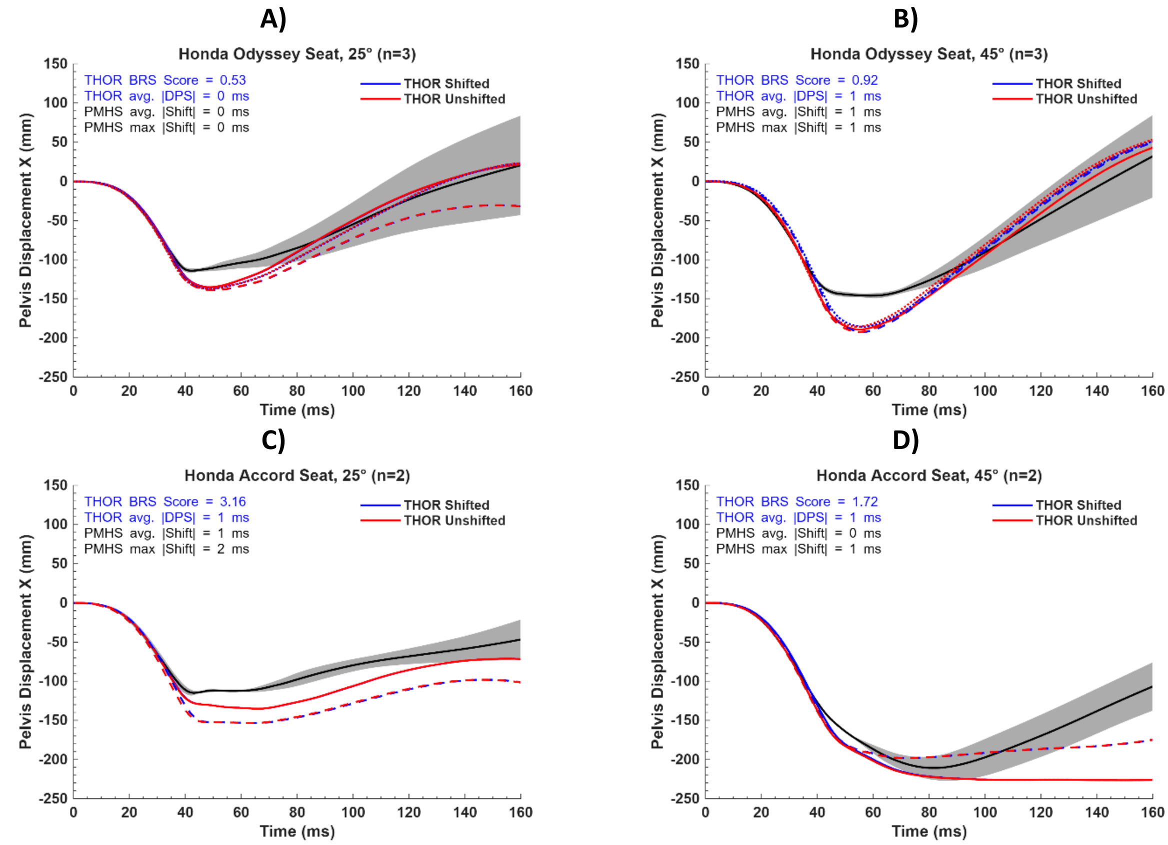

Fig. C10. Comparison of global pelvis X-displacement between the THOR-05F and female PMHS in four conditions: A) ABTS seat at 25° recline; B) ABTS seat at 45° recline; C) FDR seat at 25° recline; and D) FDR seat at 45° recline.

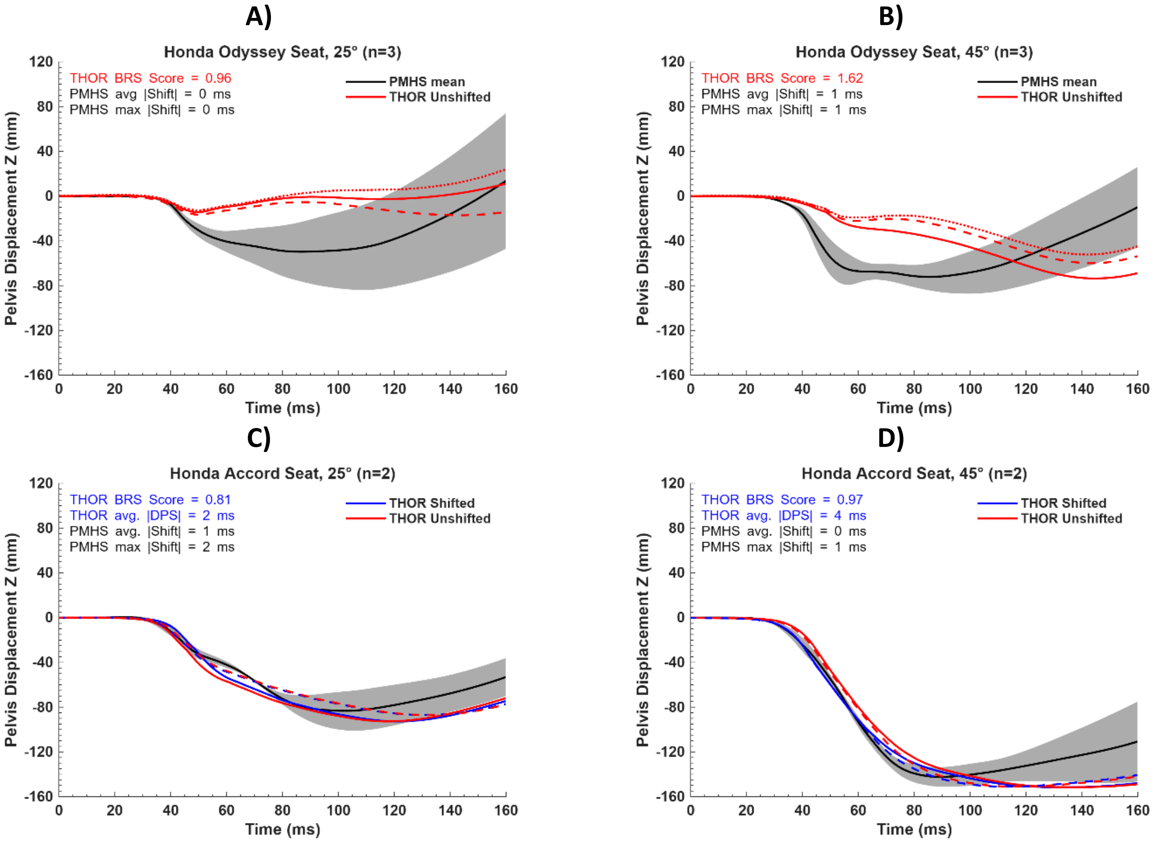

Fig. C11. Comparison of global pelvis Z-displacement between the THOR-05F and female PMHS in four conditions: A) ABTS seat at 25° recline; B) ABTS seat at 45° recline; C) FDR seat at 25° recline; and D) FDR seat at 45° recline.

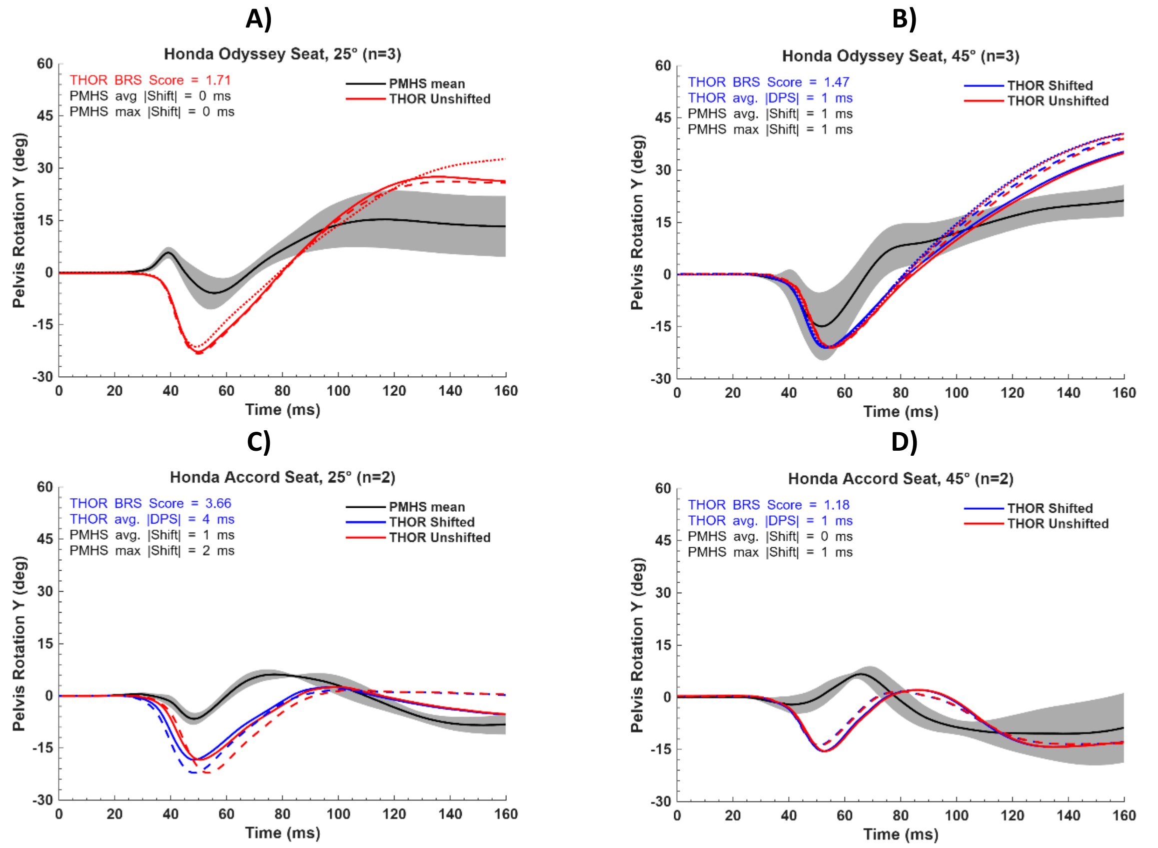

Fig. C12. Comparison of global pelvis Y-rotation between the THOR-05F and female PMHS in four conditions: A) ABTS seat at 25° recline; B) ABTS seat at 45° recline; C) FDR seat at 25° recline; and D) FDR seat at 45° recline.

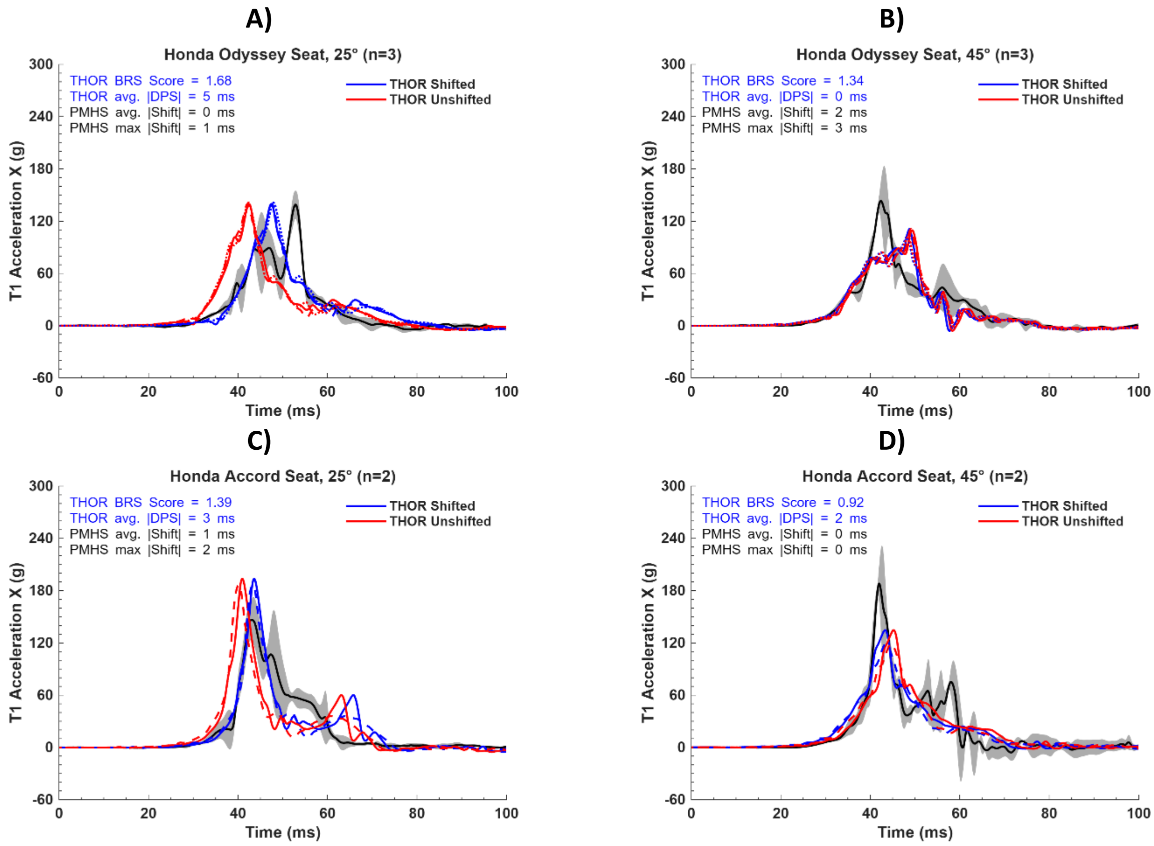

Fig. C13. Comparison of local T1 x-acceleration between the THOR-05F and female PMHS in four conditions: A) ABTS seat at 25° recline; B) ABTS seat at 45° recline; C) FDR seat at 25° recline; and D) FDR seat at 45° recline.

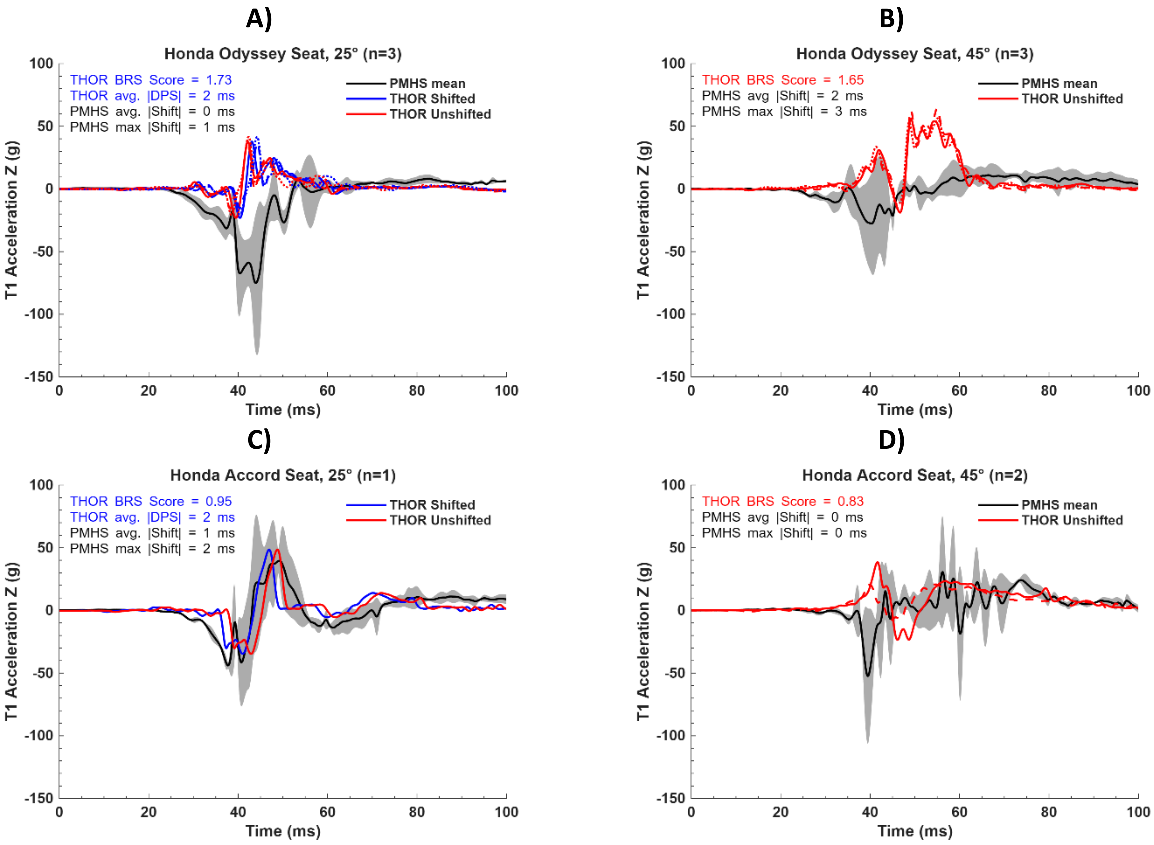

Fig. C14. Comparison of local T1 z-acceleration between the THOR-05F and female PMHS in four conditions: A) ABTS seat at 25° recline; B) ABTS seat at 45° recline; C) FDR seat at 25° recline; and D) FDR seat at 45° recline.

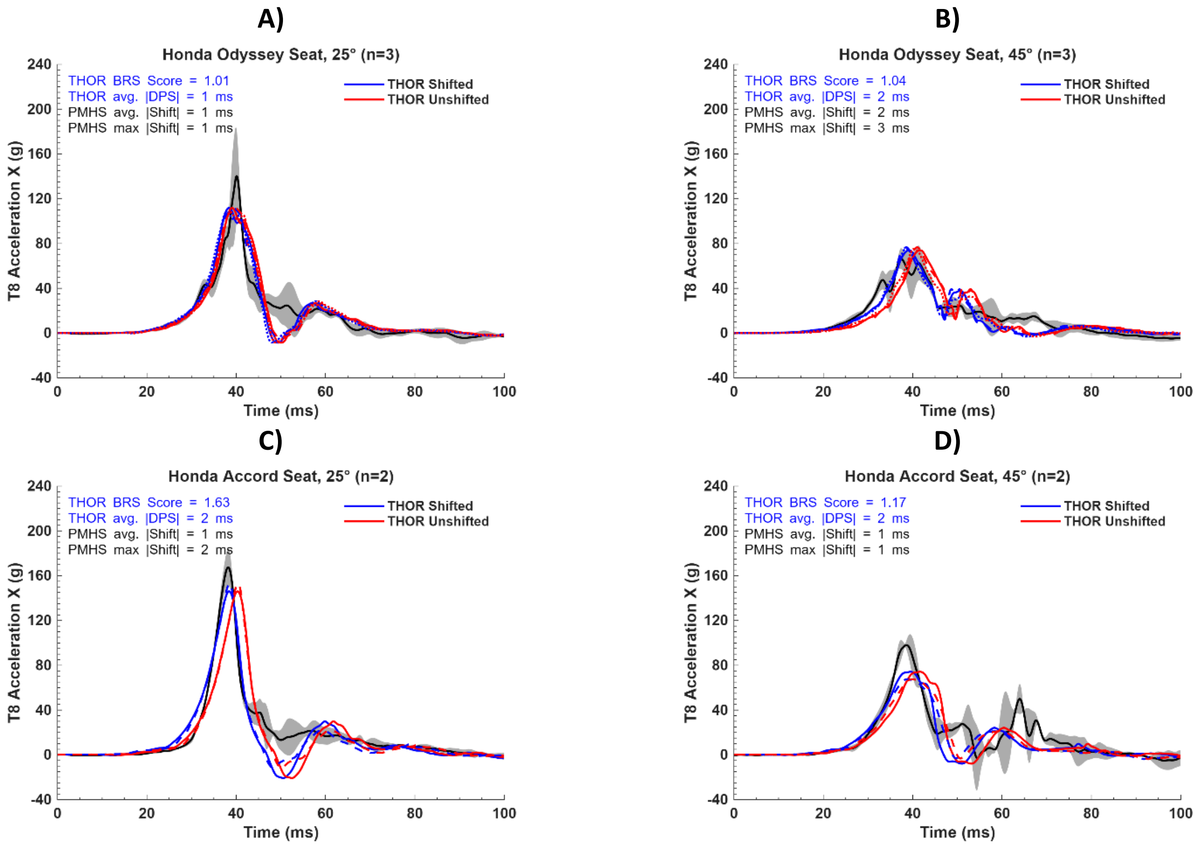

Fig. C15. Comparison of local T8 x-acceleration between the THOR-05F and female PMHS in four conditions: A) ABTS seat at 25° recline; B) ABTS seat at 45° recline; C) FDR seat at 25° recline; and D) FDR seat at 45° recline.

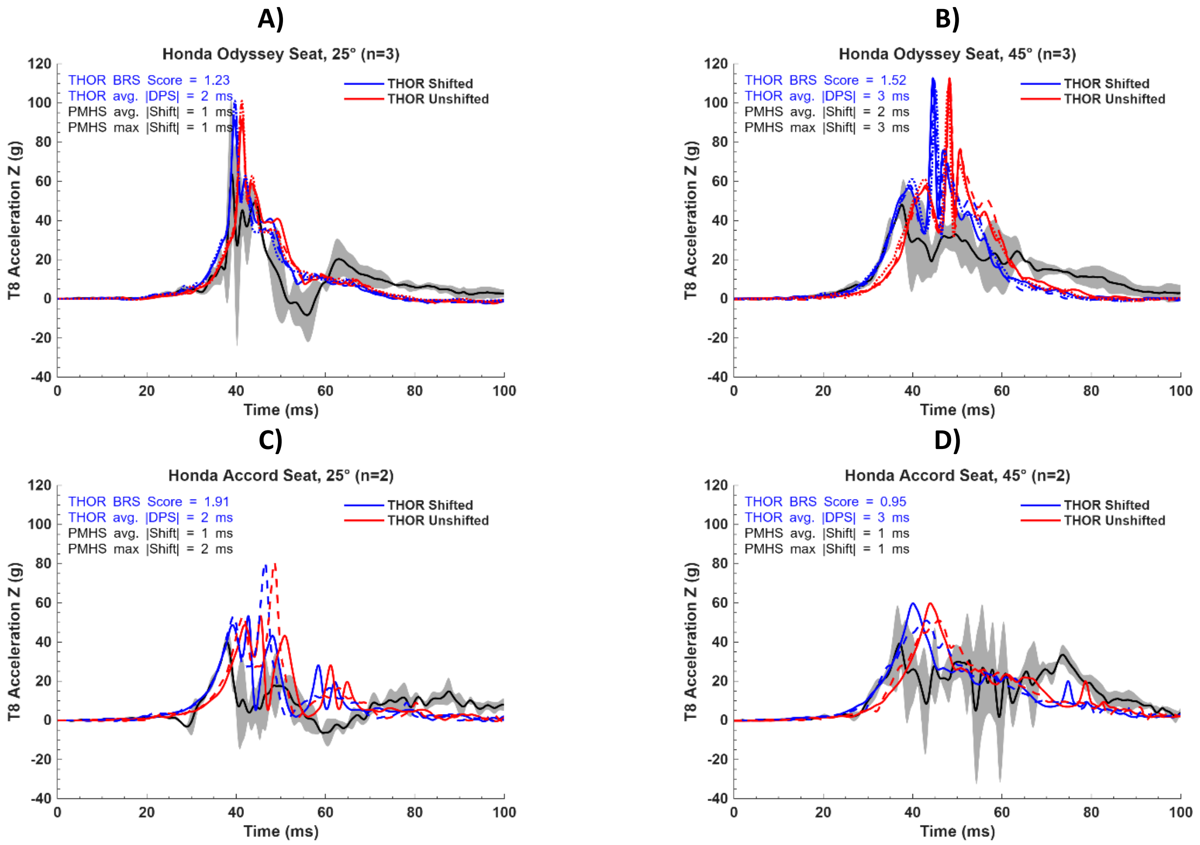

Fig. C16. Comparison of local T8 z-acceleration between the THOR-05F and female PMHS in four conditions: A) ABTS seat at 25° recline; B) ABTS seat at 45° recline; C) FDR seat at 25° recline; and D) FDR seat at 45° recline.

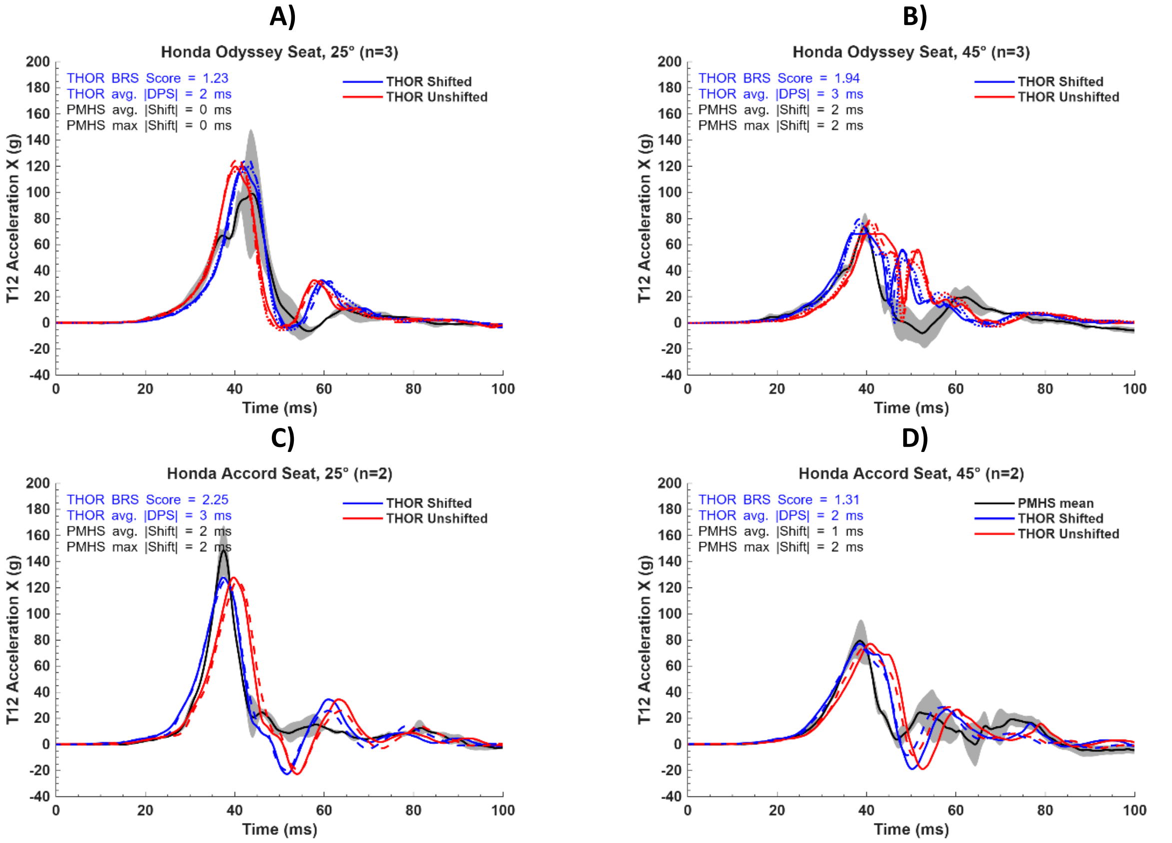

Fig. C17. Comparison of local T12 x-acceleration between the THOR-05F and female PMHS in four conditions: A) ABTS seat at 25° recline; B) ABTS seat at 45° recline; C) FDR seat at 25° recline; and D) FDR seat at 45° recline.

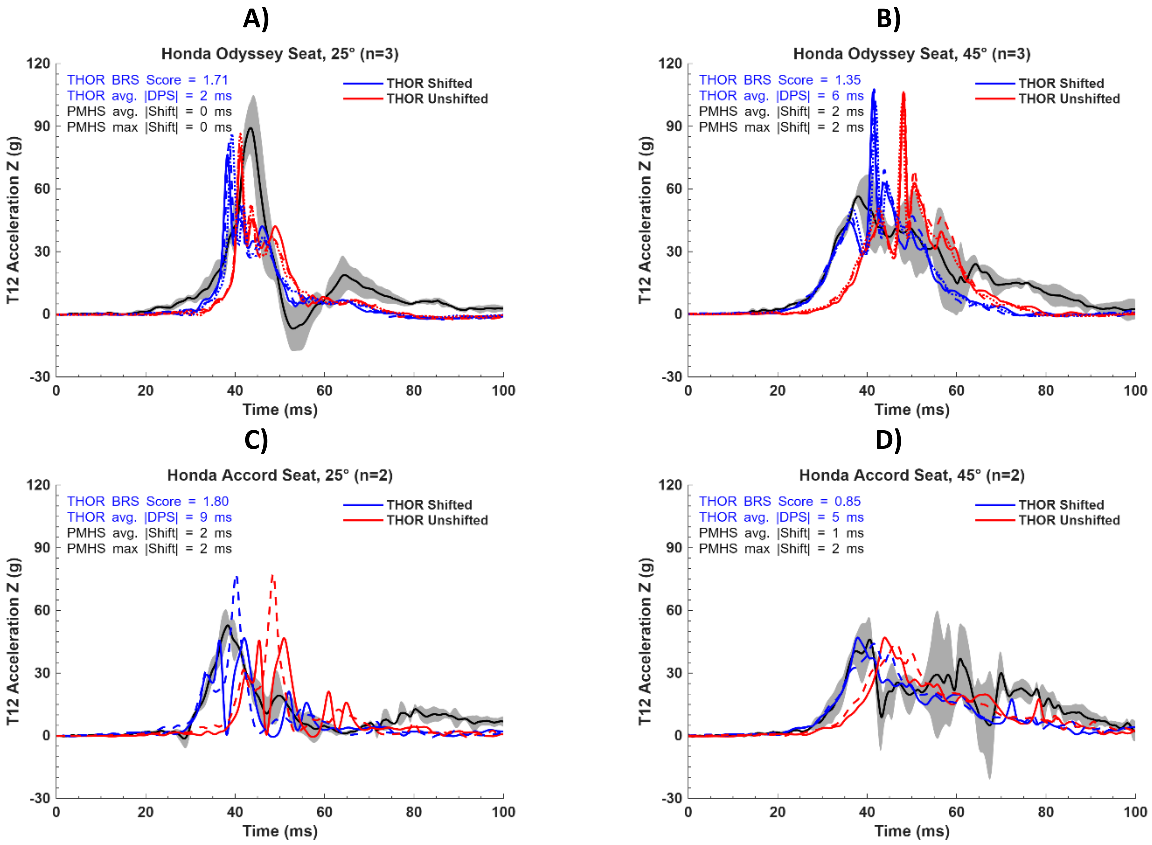

Fig. C18. Comparison of local T12 z-acceleration between the THOR-05F and female PMHS in four conditions: A) ABTS seat at 25° recline; B) ABTS seat at 45° recline; C) FDR seat at 25° recline; and D) FDR seat at 45° recline.

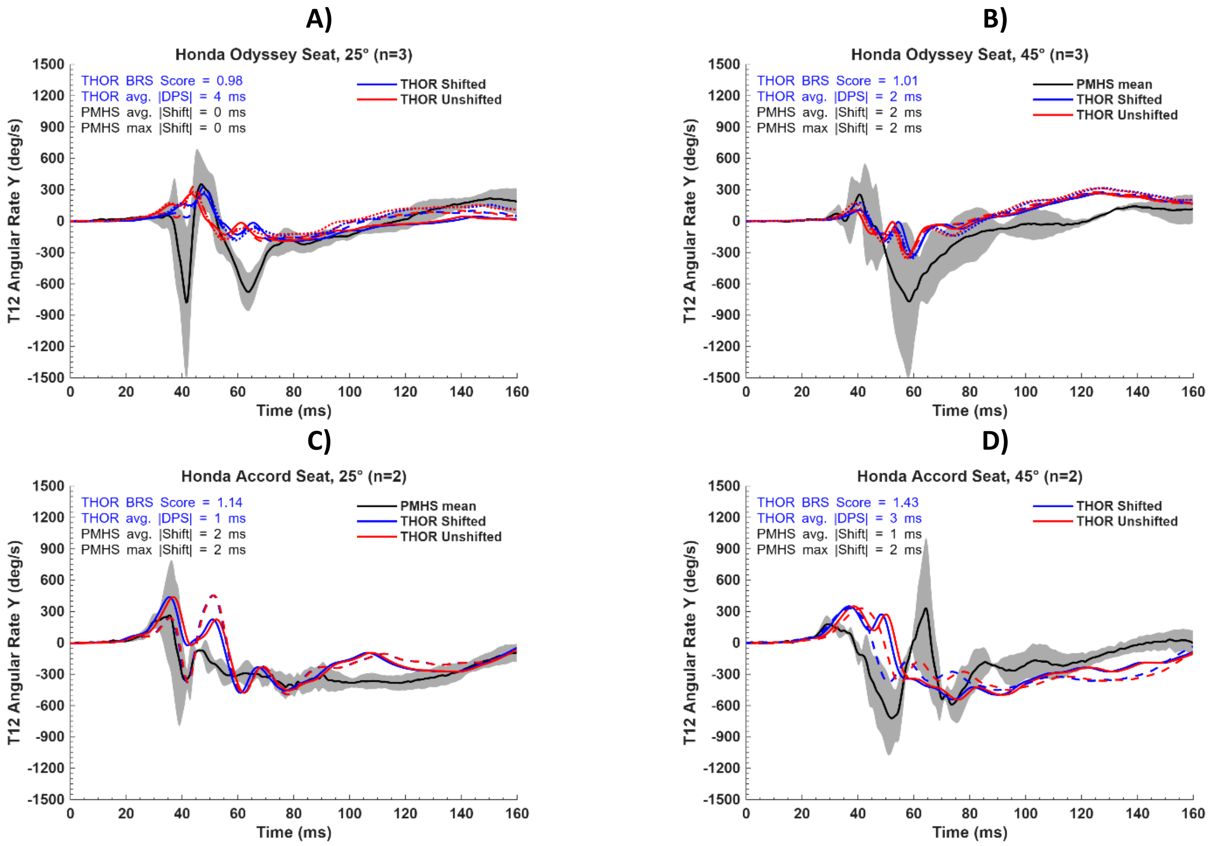

Fig. C19. Comparison of local T12 y-angular rate between the THOR-05F and female PMHS in four conditions: A) ABTS seat at 25° recline; B) ABTS seat at 45° recline; C) FDR seat at 25° recline; and D) FDR seat at 45° recline.

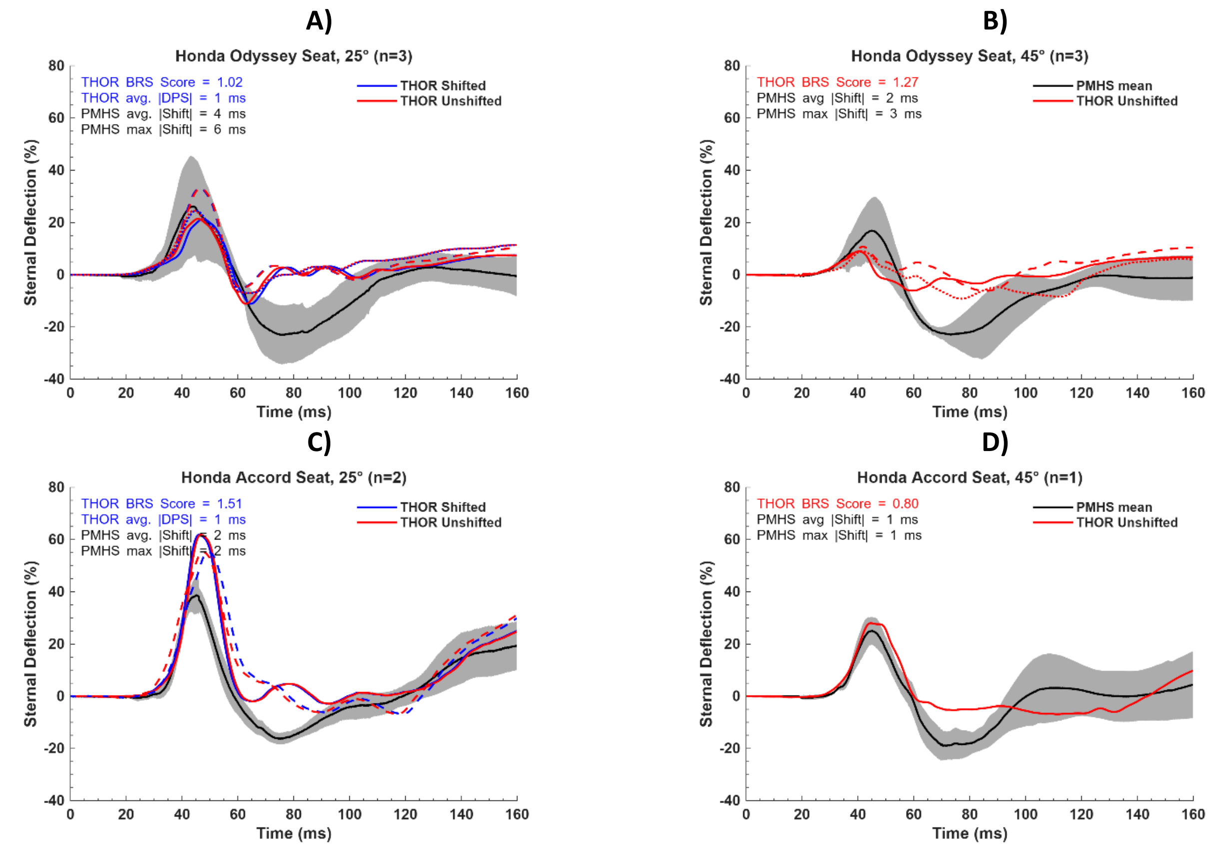

Fig. C20. Comparison of sternal deflection percentage between the THOR-05F and female PMHS in four conditions: A) ABTS seat at 25° recline; B) ABTS seat at 45° recline; C) FDR seat at 25° recline; and D) FDR seat at 45° recline.

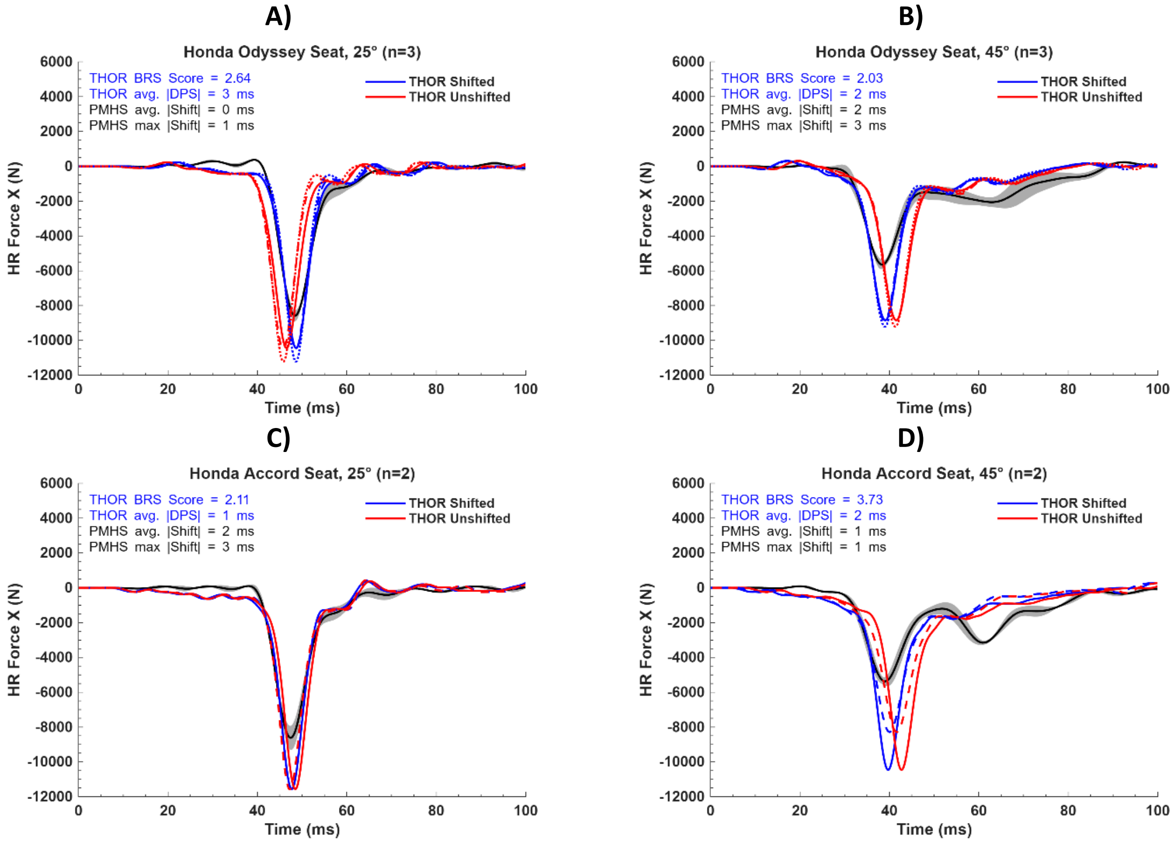

Fig. C21. Comparison of head restraint x-force between the THOR-05F and female PMHS in four conditions: A) ABTS seat at 25° recline; B) ABTS seat at 45° recline; C) FDR seat at 25° recline; and D) FDR seat at 45° recline.

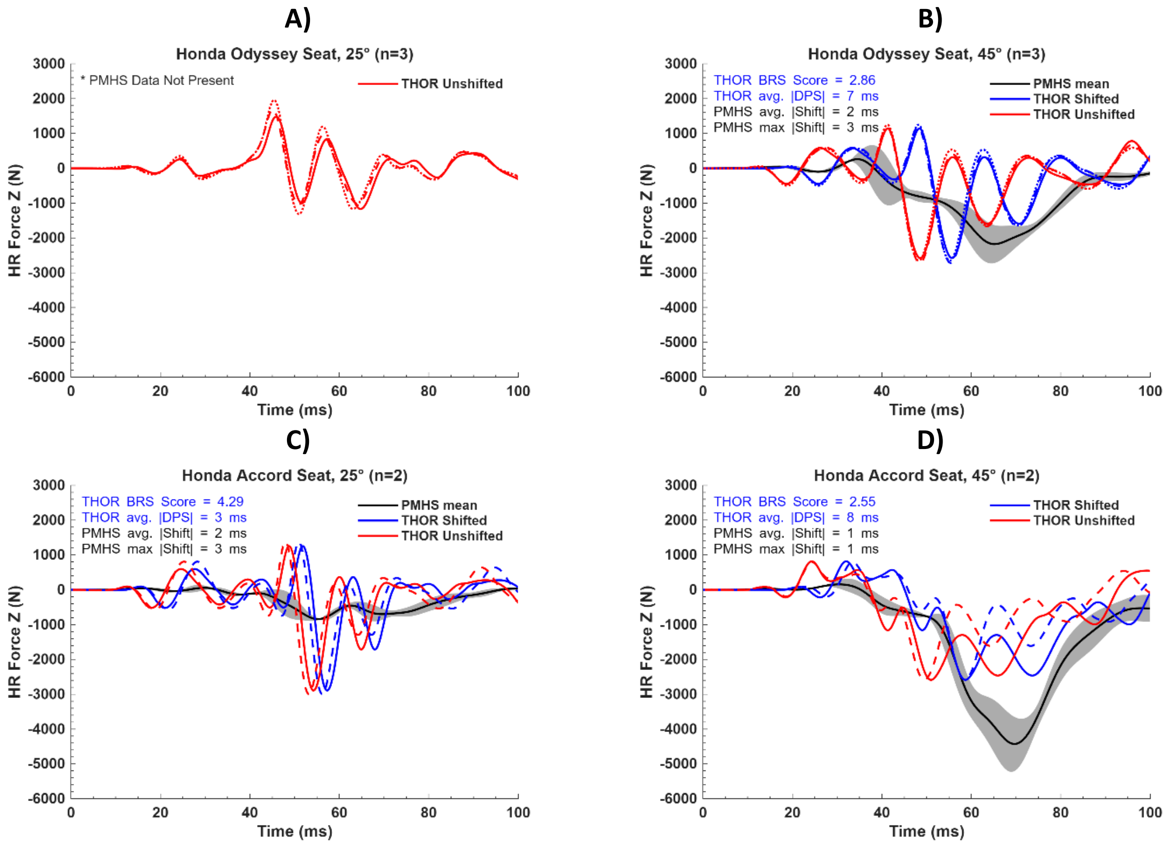

Fig. C22. Comparison of head restraint z-force between the THOR-05F and female PMHS in four conditions: A) ABTS seat at 25° recline; B) ABTS seat at 45° recline; C) FDR seat at 25° recline; and D) FDR seat at 45° recline. Note that, for the ABTS 25° recline condition, PMHS corridors were not present.

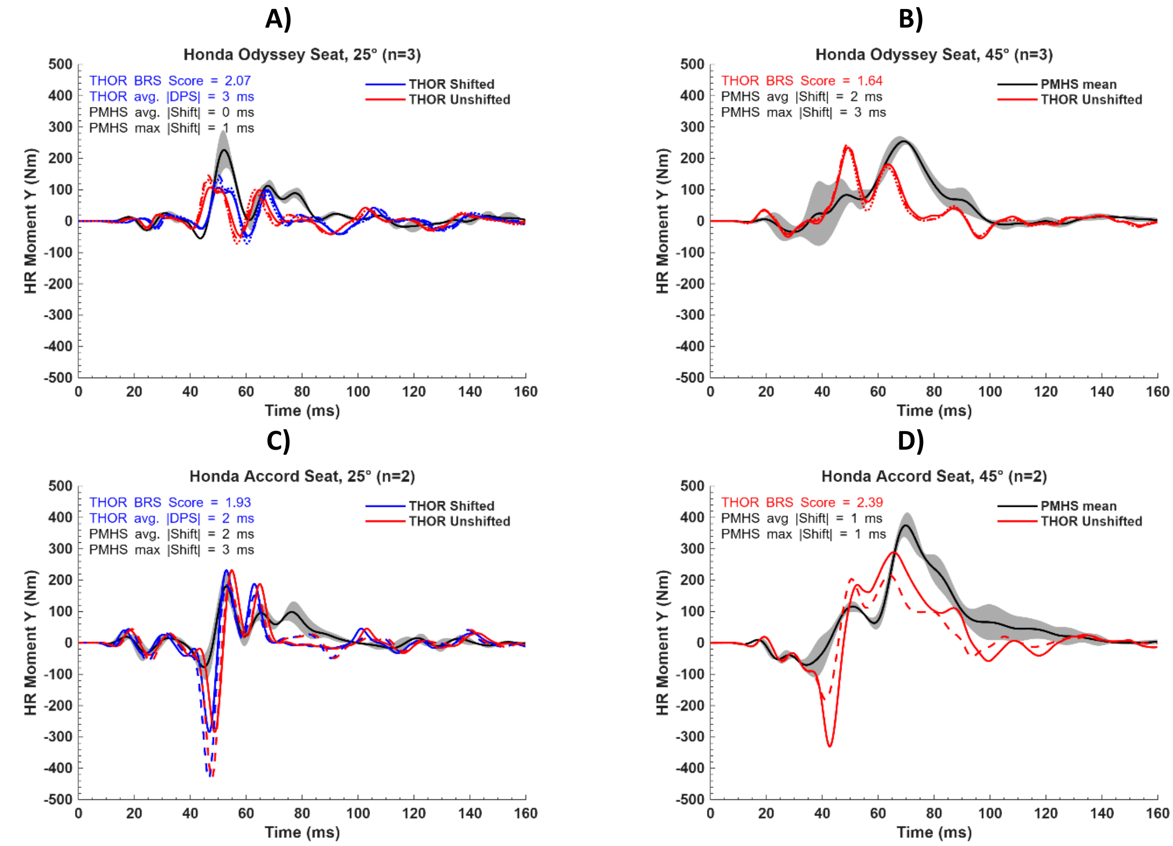

Fig. C23. Comparison of head restraint y-moment between the THOR-05F and female PMHS in four conditions: A) ABTS seat at 25° recline; B) ABTS seat at 45° recline; C) FDR seat at 25° recline; and D) FDR seat at 45° recline.

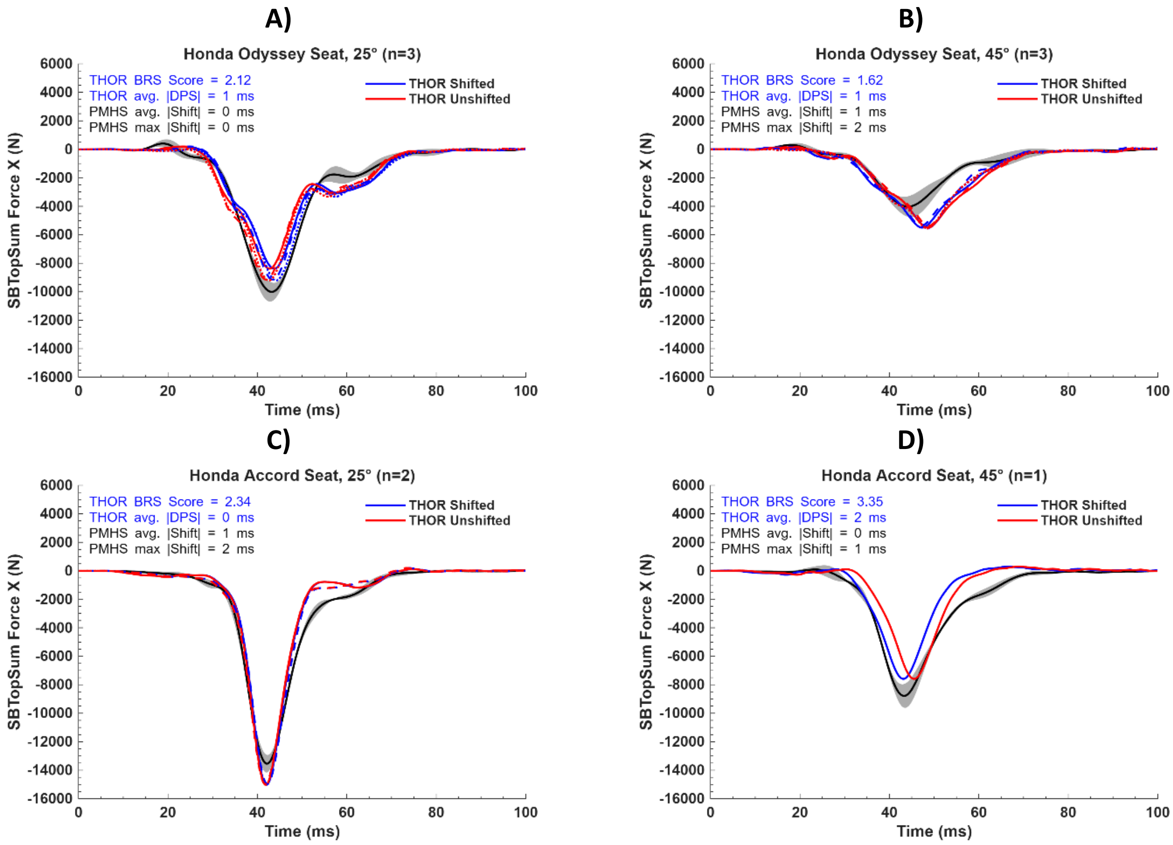

Fig. C24. Comparison of seatback top x-force between the THOR-05F and female PMHS in four conditions: A) ABTS seat at 25° recline; B) ABTS seat at 45° recline; C) FDR seat at 25° recline; and D) FDR seat at 45° recline.

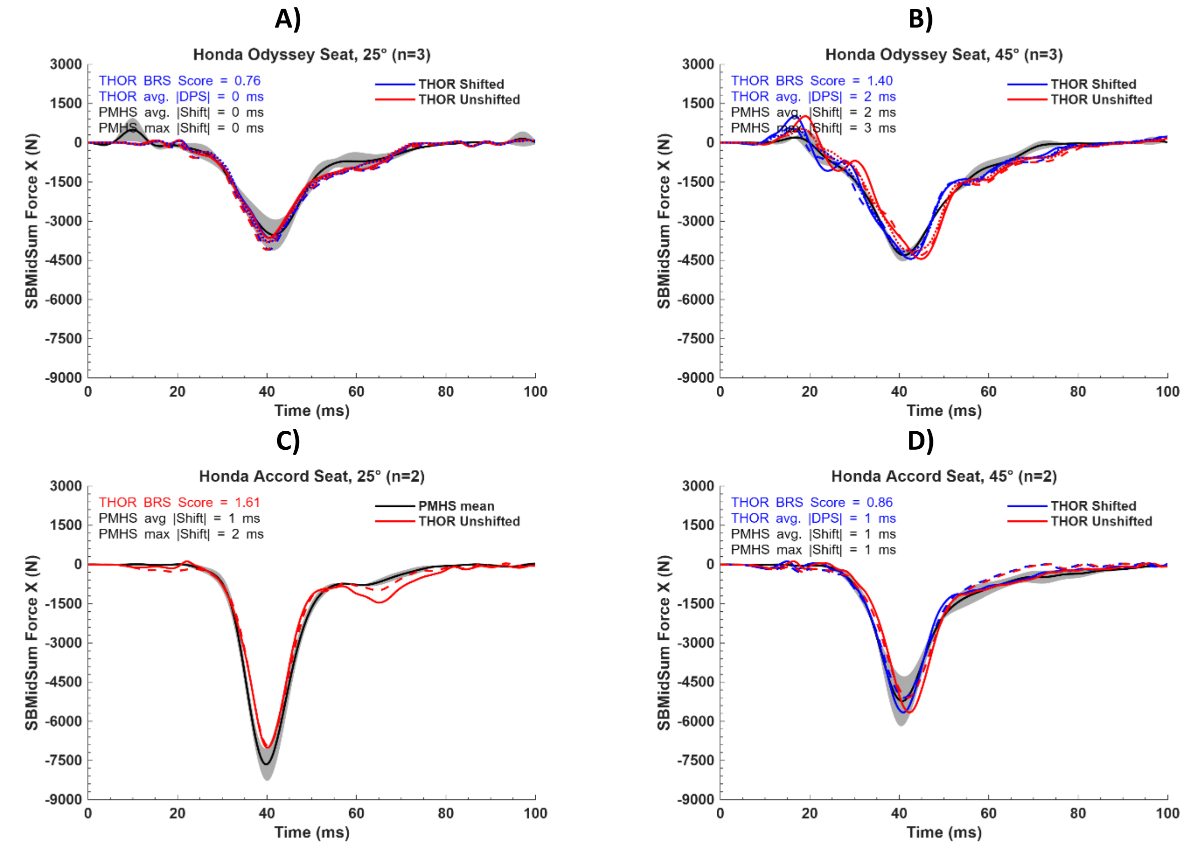

Fig. C25. Comparison of seatback middle x-force between the THOR-05F and female PMHS in four conditions: A) ABTS seat at 25° recline; B) ABTS seat at 45° recline; C) FDR seat at 25° recline; and D) FDR seat at 45° recline.

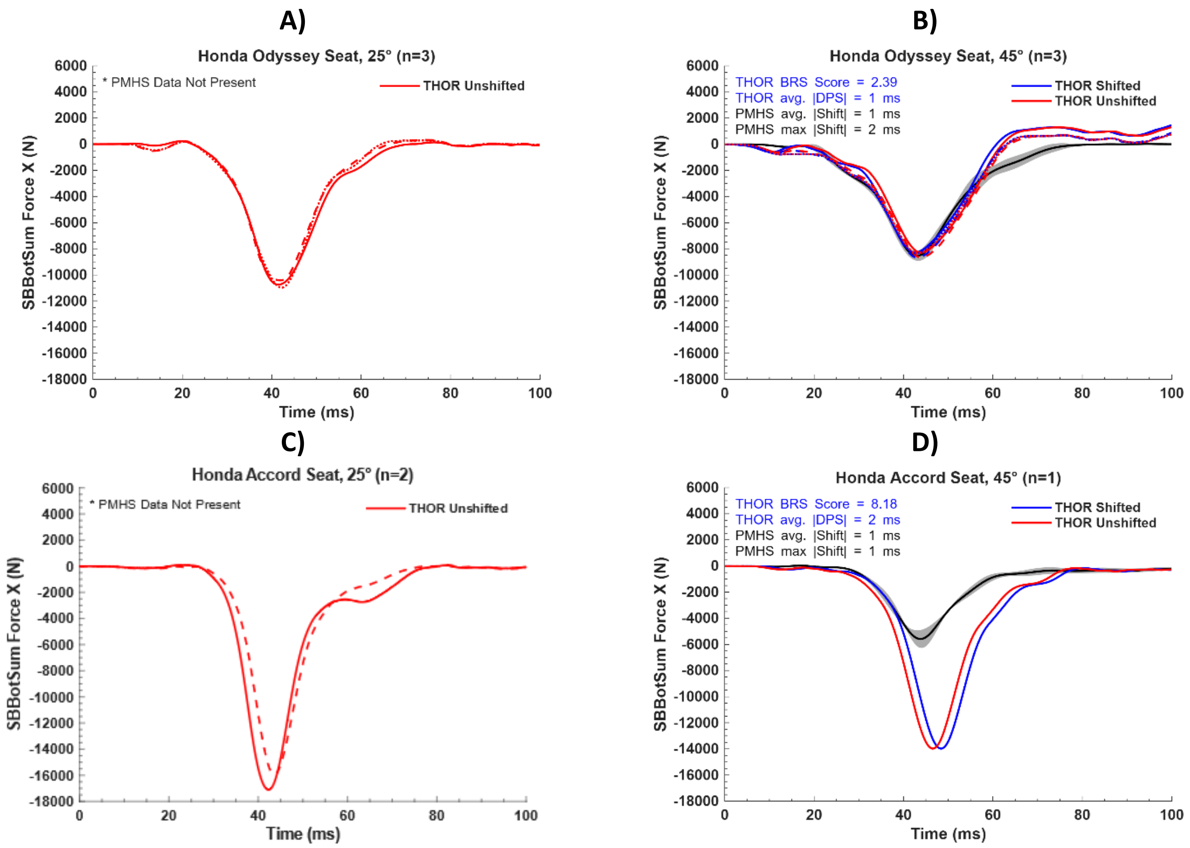

Fig. C26. Comparison of seatback bottom x-force between the THOR-05F and female PMHS in four conditions: A) ABTS seat at 25° recline; B) ABTS seat at 45° recline; C) FDR seat at 25° recline; and D) FDR seat at 45° recline. Note that for both 25° recline conditions, no PMHS corridors were present.

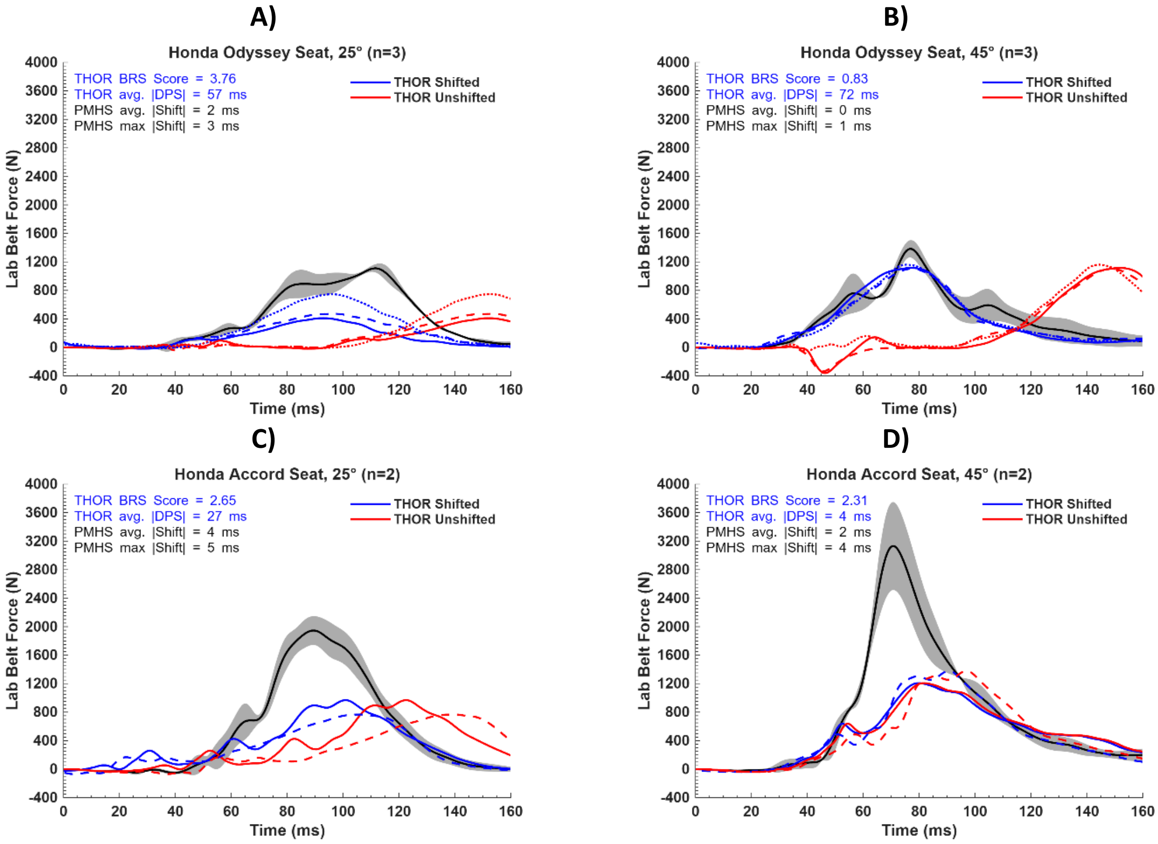

Fig. C27. Comparison of lap-belt force between the THOR-05F and female PMHS in four conditions: A) ABTS seat at 25° recline; B) ABTS seat at 45° recline; C) FDR seat at 25° recline; and D) FDR seat at 45° recline.

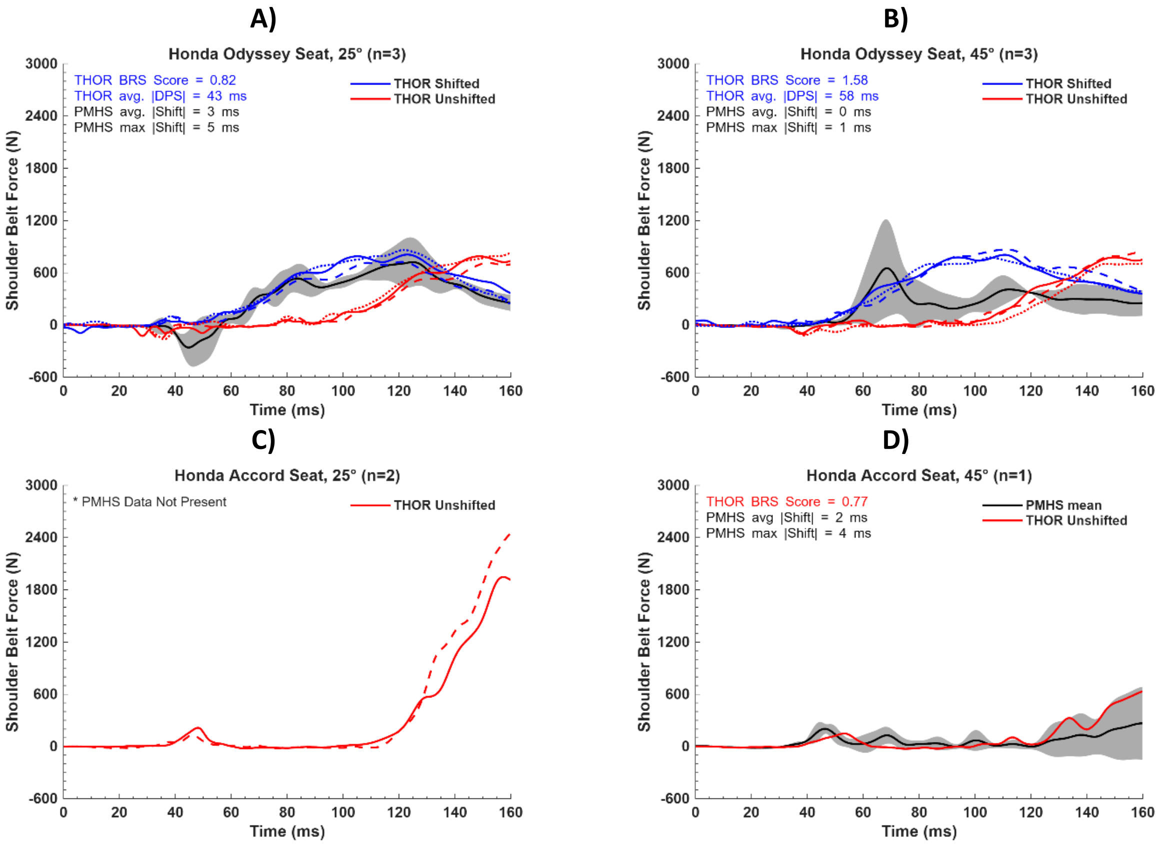

Fig. C28. Comparison of shoulder-belt force between the THOR-05F and female PMHS in four conditions: A) ABTS seat at 25° recline; B) ABTS seat at 45° recline; C) FDR seat at 25° recline; and D) FDR seat at 45° recline. Note that, for the FDR 25° recline condition, no PMHS corridors were present.

Appendix D: Additional THOR-05F and PMHS Comparisons

TABLE DI

COMPARISON OF SEAT LOAD PEAK MAGNITUDES AND TIMING AND KINEMATIC PEAK TIMING FOR 25° TESTS

Location	Measure	ABTS Odyssey		FDR Accord	
		THOR-05F	*PMHS*	*THOR-05F*	*PMHS*
Head Restraint	*Peak Force (kN)*	-10.72	-8.58	-11.57	-8.62
	Peak Force Timing (ms)	46.0	48.4	47.9	47.5
Seatback Top	*Peak Force (kN)*	-8.91	-10.01	-15.00	-13.54
	Peak Force Timing (ms)	42.5	43.2	41.9	42.2
Seatback Middle	*Peak Force (kN)*	-3.85	-3.53	-6.98	-7.65
	Peak Force Timing (ms)	40.1	41.6	40.2	39.9
Seatback Bottom	*Peak Force (kN)*	-10.71	-7.62	-16.53	-7.55
	Peak Force Timing (ms)	42.0	41.6	43.0	43.7
Shoulder Belt	*Peak Force (kN)*	0.78	0.72	2.20	*Not Available*
	Peak Force Timing (ms)	164.8	125.0	160.0	*Not Available*
Lap Belt	*Peak Force (kN)*	0.54	1.11	0.87	1.95
	Peak Force Timing (ms)	152.7	111.6	131.0	89.5
Chestband	*Peak Deflection Timing (ms)*	45.6	44.0	47.2	45.2
Head	*Peak Resultant XZ Displacement Timing (ms)*	47.0	49.2	49.0	48.1
Pelvis	*Peak Resultant XZ Displacement Timing (ms)*	48.8	43.9	68.8	77.0

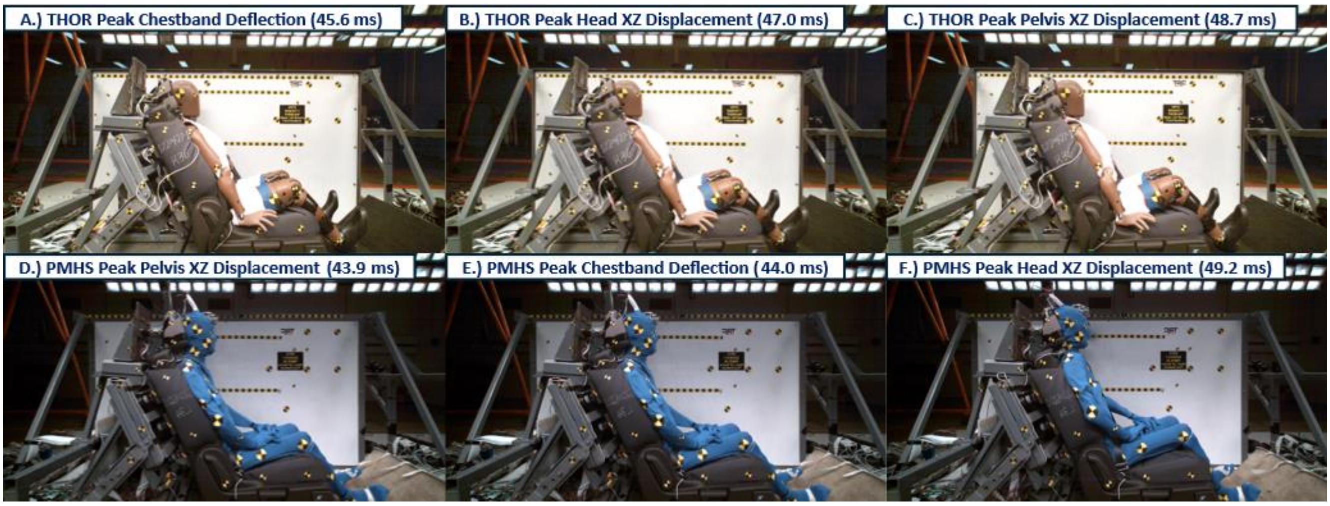

Fig. D1. Kinematic event order comparison at 25° recline in the ABTS seat for the THOR-05F and PMHS. For THOR-05F, the sequence was: A) peak chestband deflection, B) peak head XZ displacement, and then C) peak pelvis XZ displacement. For PMHS, the sequence was: D) peak pelvis XZ displacement, E) peak chestband deflection, and then F) peak head XZ displacement.

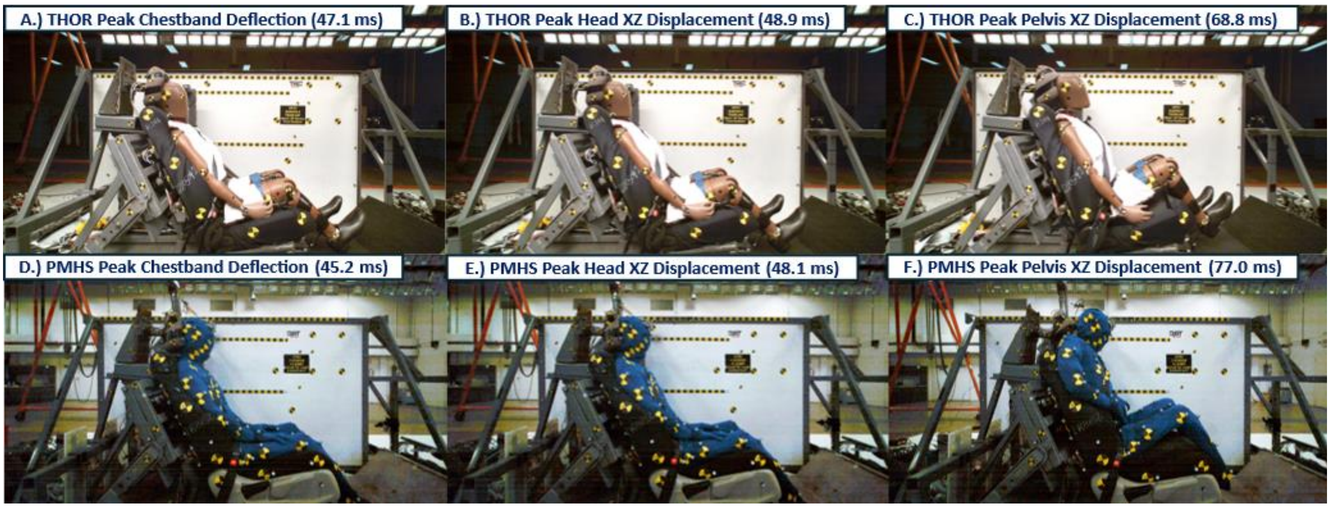

Fig. D2. Kinematic event order comparison at 25° recline in the FDR seat for the THOR-05F and PMHS. For THOR-05F, the sequence was: A) peak chestband deflection, B) peak head XZ displacement, and then C) peak pelvis XZ displacement. For PMHS, the sequence was the same: D) peak chestband deflection, E) peak head XZ displacement, and then F) peak pelvis XZ displacement.

Fig. D3. Comparison of the peak belt loading sequence at 25° recline in the ABTS seat for the THOR-05F and PMHS. Subjects consistently experienced peak lap belt force before peak shoulder belt force. The THOR-05F peaked at 152.7 ms for the lap belt and 164.8 ms for the shoulder belt, while the PMHS peaked at 111.6 ms for the lap belt and 125.0 ms for the shoulder belt.

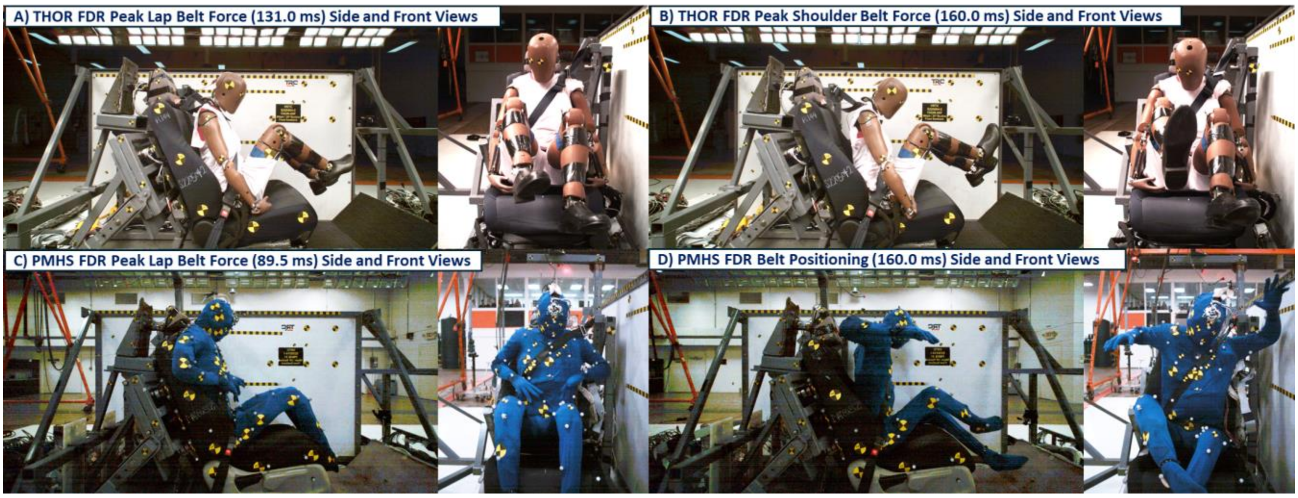

Fig. D4. Comparison of the peak belt loading sequence at 25° recline in the FDR seat for the THOR-05F and PMHS. For THOR-05F, peak lap belt force (131.0 ms) occurred prior to peak shoulder belt force (160.0 ms). For the PMHS, only peak lap belt force data was available, which occurred at 89.5 ms. The PMHS belt positioning at 160.0 ms was included to provide a comparison in the absence of peak shoulder belt data.

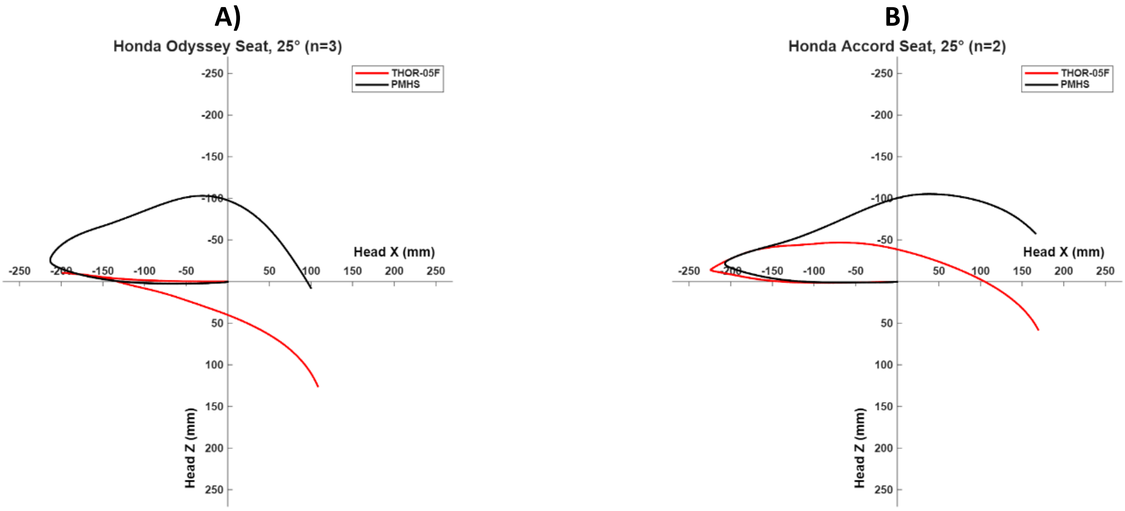

Fig. D5. Average head X-Z trajectories at 25° recline in A) the ABTS Odyssey seat and B) the FDR Accord seat.

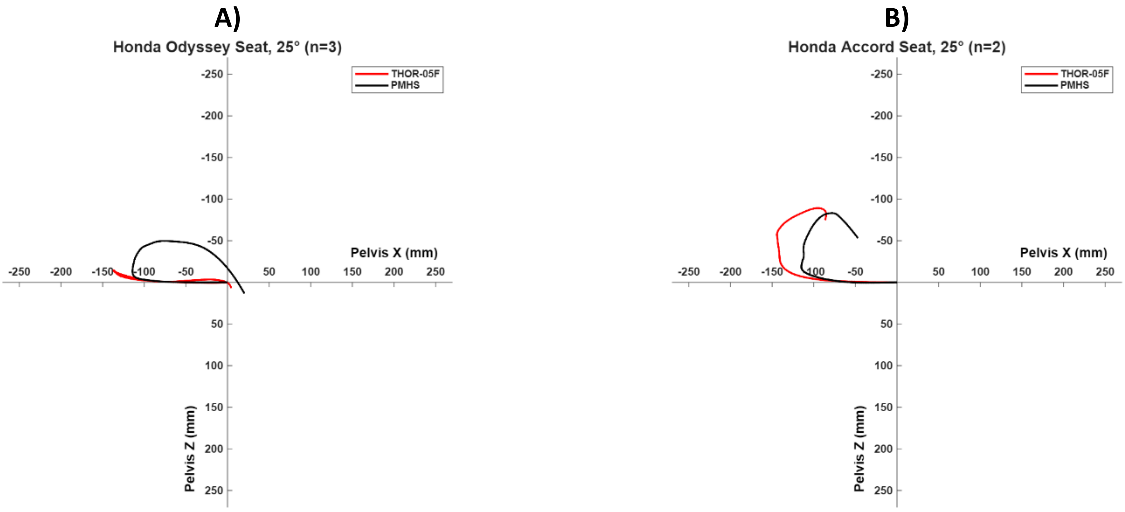

Fig. D6. Average pelvis X-Z trajectories at 25° recline in A) the ABTS Odyssey seat and B) the FDR Accord seat.

TABLE DII

COMPARISON OF SEAT LOAD PEAK MAGNITUDES AND TIMING AND KINEMATIC PEAK TIMING FOR 45° TESTS

Location	Measure	ABTS Odyssey		FDR Accord	
		THOR-05F	*PMHS*	*THOR-05F*	*PMHS*
Head Restraint	*Peak Force (kN)*	-8.98	-5.65	-9.37	-5.37
	Peak Force Timing (ms)	41.5	38.4	42.4	39.1
Seatback Top	*Peak Force (kN)*	-5.47	-4.02	-7.59	-8.78
	Peak Force Timing (ms)	48.6	44.2	45.6	43.4
Seatback Middle	*Peak Force (kN)*	-4.30	-4.30	-5.38	-5.23
	Peak Force Timing (ms)	44.4	41.1	42.1	40.7
Seatback Bottom	*Peak Force (kN)*	-8.44	-8.54	-13.97	-5.58
	Peak Force Timing (ms)	43.7	43.0	46.6	43.9
Shoulder Belt	*Peak Force (kN)*	0.78	0.65	0.75	0.27
	Peak Force Timing (ms)	166.7	68.5	124.3	160.0
Lap Belt	*Peak Force (kN)*	1.13	1.38	1.29	3.13
	Peak Force Timing (ms)	148.3	76.9	89.3	70.8
Chestband	*Peak Deflection Timing (ms)*	41.3	44.9	44.6	45.2
Head	*Peak Resultant XZ Displacement Timing (ms)*	43.5	83.8	111.1	112.4
Pelvis	*Peak Resultant XZ Displacement Timing (ms)*	55.0	60.4	115.5	84.2

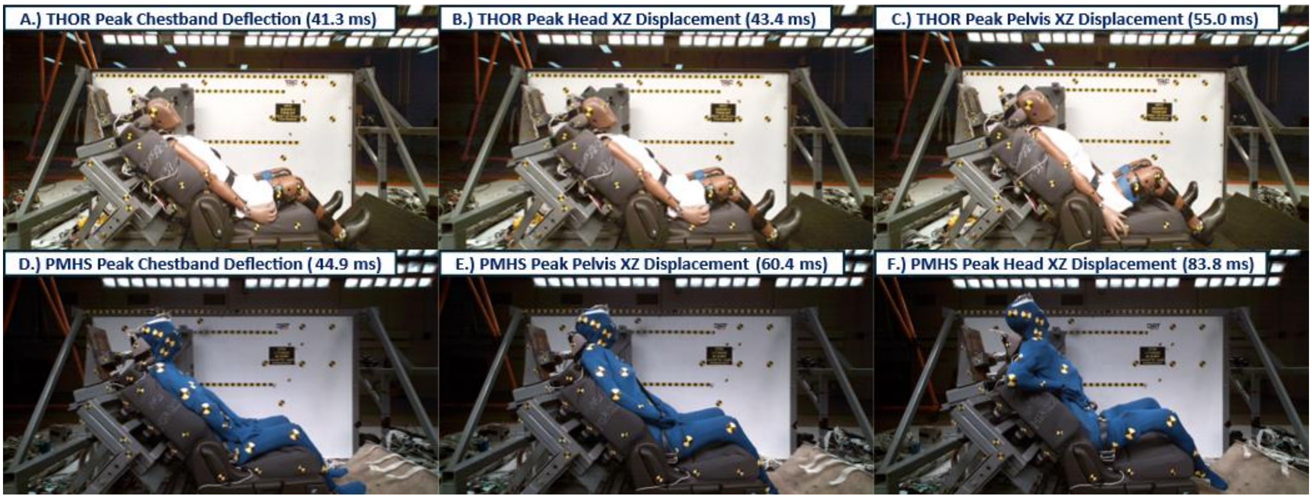

Fig. D7. Kinematic event order comparison at 45° recline in the ABTS seat for the THOR-05F and PMHS. For THOR-05F, the sequence was: A) peak chestband deflection, B) peak head XZ displacement, and then C) peak pelvis XZ displacement. For PMHS, the sequence was: D) peak chestband deflection, E) peak pelvis XZ displacement, and then F) peak head XZ displacement.

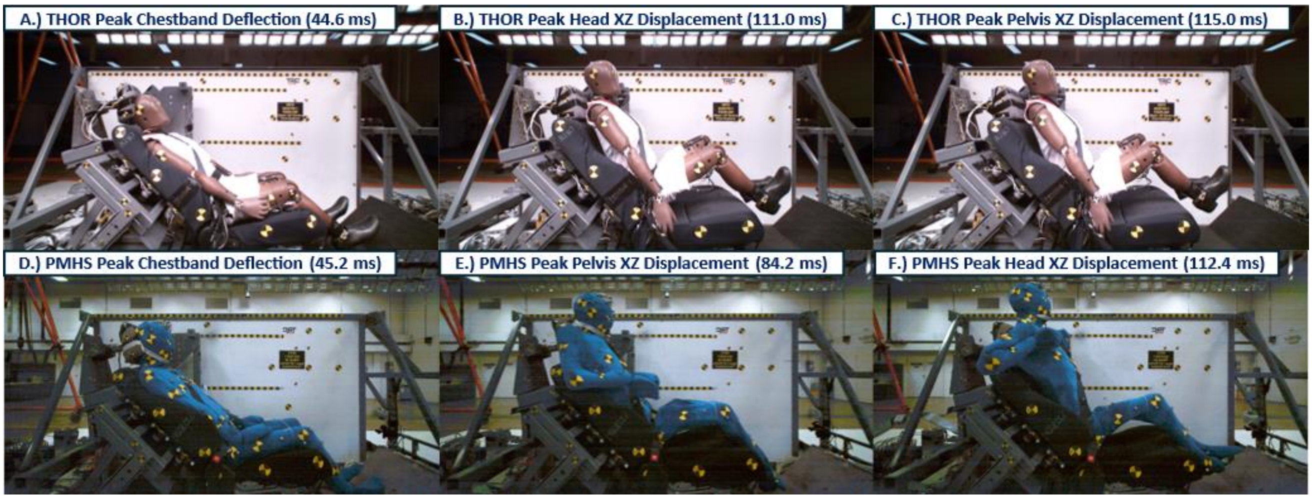

Fig. D8. Kinematic event order comparison at 45° recline in the FDR seat for the THOR-05F and PMHS. For THOR-05F, the sequence was: A) peak chestband deflection, B) peak head XZ displacement, and then C) peak pelvis XZ displacement. For PMHS, the sequence was: D) peak chestband deflection, E) peak pelvis XZ displacement, and then F) peak head XZ displacement.

Fig. D9. Comparison of the peak belt loading sequence at 45° recline in the ABTS seat for the THOR-05F and PMHS. For THOR-05F, peak lap belt force (148.3 ms) occurred prior to peak shoulder belt force (166.7 ms). Conversely, the PMHS experienced peak shoulder belt force (68.5 ms) followed by peak lap belt force (76.9 ms).

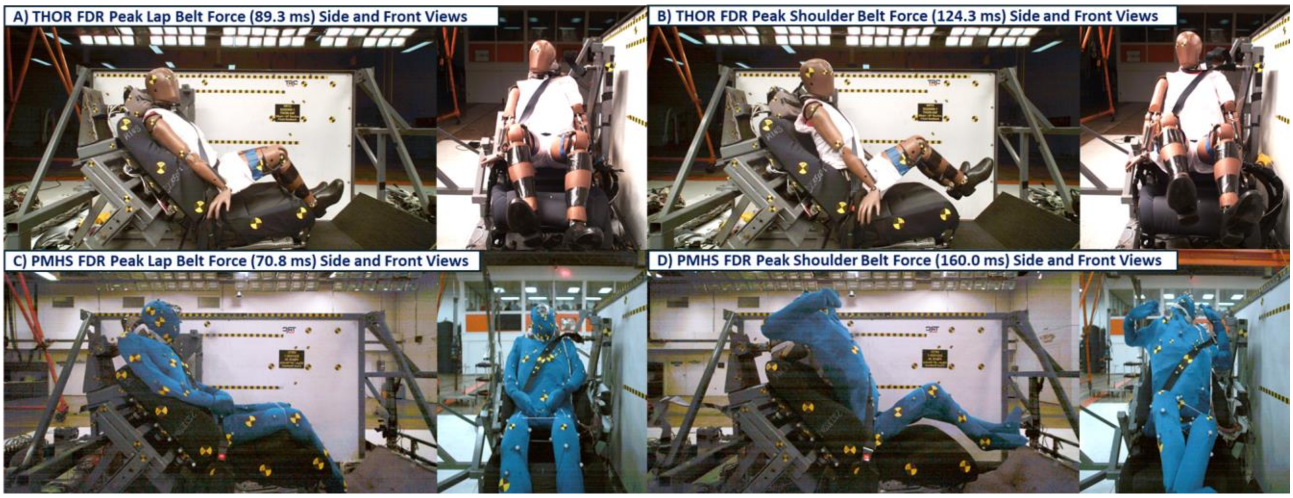

Fig. D10. Comparison of the peak belt loading sequence at 45° recline in the FDR seat for the THOR-05F and PMHS. Subjects consistently experienced peak lap belt force before peak shoulder belt force. The THOR-05F peaked at 89.3 ms for the lap belt and 124.3 ms for the shoulder belt, while the PMHS peaked at 70.8 ms for the lap belt and 160.0 ms for the shoulder belt.

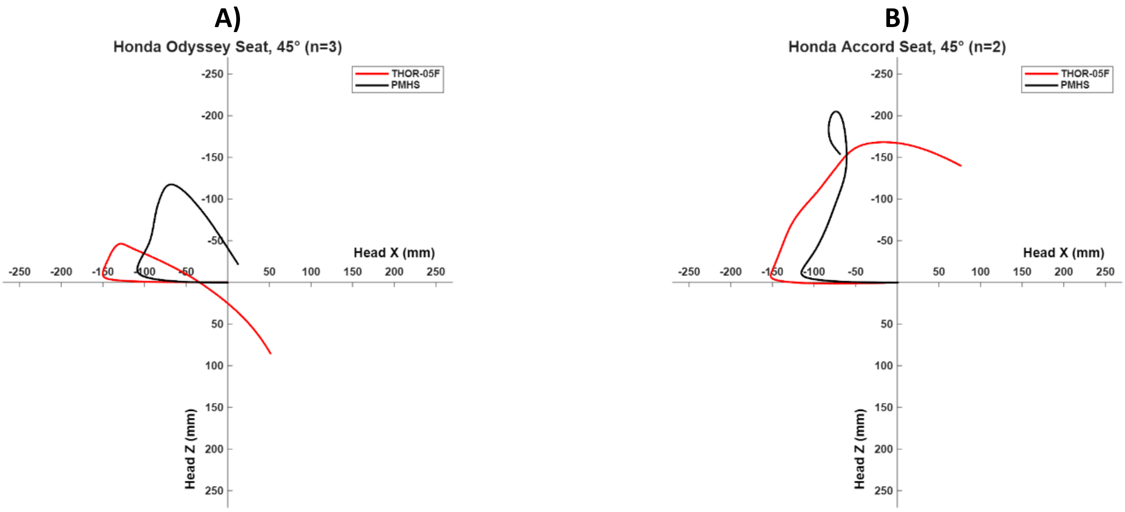

Fig. D11. Average head X-Z trajectories at 25° recline in A) the ABTS Odyssey seat and B) the FDR Accord seat.

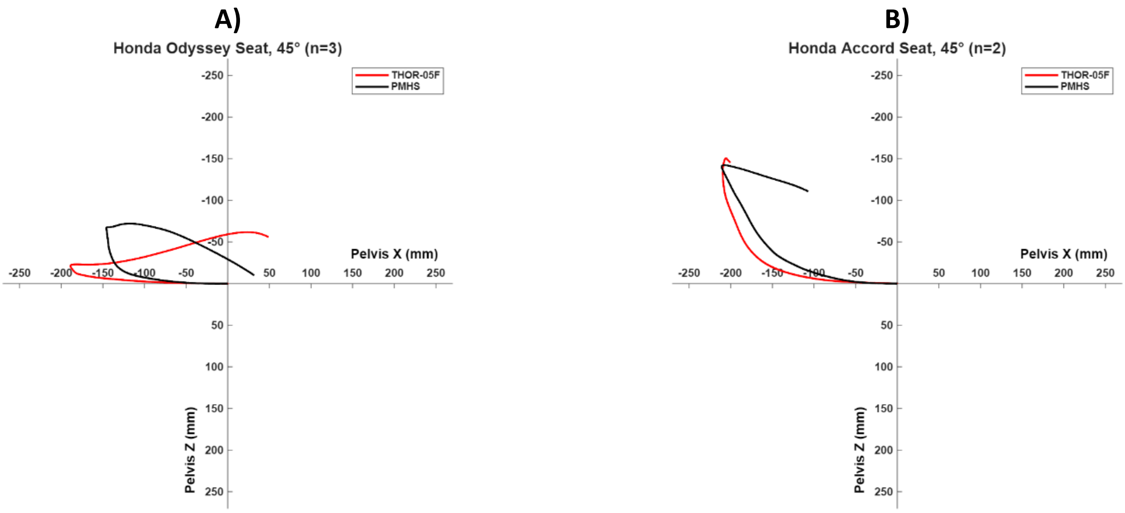

Fig. D12. Average pelvis X-Z trajectories at 45° recline in A) the ABTS Odyssey seat and B) the FDR Accord seat.

TABLE DIII
AVERAGE UNSHIFTED BRS SCORES 25° AND 45° TESTS

Location	*Unshifted BRS Scores*			
	ABTS Odyssey		*FDR Accord*	
	25°	*45°*	*25°*	*45°*
Head Restraint	4.40	2.56	3.02	3.28
Seatback Top	2.27	1.73	2.41	3.38
Seatback Middle	0.78	2.1	1.61	1.12
Seatback Bottom	*Not Calculated*	2.63	*Not Calculated*	8.23
Belt Tensions	4.60	3.17	4.38	2.14
Seat Loading	**3.01**	**2.44**	**2.80**	**3.58**
Head	5.71	1.74	1.38	2.4
Spine	1.58	1.62	2.09	1.23
Thorax	1.04	1.27	1.53	0.80
Pelvis	1.30	1.47	2.03	1.37
Occupant Response	**2.40**	**1.53**	**1.76**	**1.45**